Marine and Coastal

National Environmental Science Program

FINAL REPORT

Project 3.16

Towards the delineation and estimation of the Maugean skate population in Macquarie Harbour, Tasmania

David Moreno, Tzu Nin Kwan, Mark Priest,
Jayson M. Semmens

UNIVERSITY of TASMANIA

IMAS

Institute for Marine and Antarctic Studies

THREATENED SPECIES INITIATIVE

Milestone number: 5
Research Plan number: 3.16

Please address inquiries to: David Moreno or Jayson Semmens, Institute for Marine and Antarctic Studies (IMAS), University of Tasmania, david.moreno@utas.edu.au or jayson.semmens@utas.edu.au;

Preferred citation

Moreno, D., Kwan, T.N., Priest, M. & Semmens, J.M. (2025). Delineation and estimation of the Maugean skate population in Macquarie Harbour, Tasmania. Report to the National Environmental Science Program. Institute for Marine and Antarctic Studies, University of Tasmania.

Copyright

Acknowledgement

This work was undertaken for the Marine and Coastal Hub, a collaborative partnership supported through funding from the Australian Government's National Environmental Science Program (NESP). Thanks to the NCRIS-funded Bioplatforms Australia Threatened Species initiative for sequencing support for the reference genome and population data.
Bathurst harbour tissue samples provided by the Australian Museum (Sydney) and the Australian National Fish collection (CSIRO).
Technical advice and assistance for imaging work provided by Gavin Stevens (Apollo military), Justin Hulls, Peter King and AMC team, and the Defence Science and Technology Group (DSGT).
Technical advice and assistance for molecular work provided by Sophie Mazard, Dodge Tristam, Andrzej Kilian, Toby Patterson, and Pierre Feutry.
We wish to acknowledge contributions to field and laboratory work from Cynthia Awruch, Kay Weltz, Graeme Ewing, Davis Hinton, Start Isles, Peter Coulson, Madeleine Davies-Knight, Erin Woodward, Komeil Razmi, Ehsan Mousavi, and Jawahar Patil
Thanks to Bailee Woolley for final editing.
Thanks to David Ikedife and Carolyn Hogg for their expert comments and suggestions.

NESP Marine and Coastal Hub partners

The Australian Institute of Marine Science, Bioplatforms Australia, Bureau of Meteorology, Charles Darwin University, Central Queensland University, CSIRO, Deakin University, Edith Cowan University, Flinders University, Geoscience Australia, Griffith University, Integrated Marine Observing System, James Cook University, Macquarie University, Murdoch University, Museums Victoria, NSW Department of Planning and Environment, NSW Department of Primary Industries, South Australian Research and Development Institute, University of Tasmania, The University of Adelaide, University of Melbourne, The University of Queensland, University of New South Wales, University of Technology Sydney, The University of Sydney, University of Western Australia and University of Wollongong.

Disclaimer

Cover images: Left: captive Maugean skate (*Zearaja maugeana*. Photo: David Moreno; Centre: Macquarie Harbour. Photo: Kshithij Chandrashekar, Unsplash. Right: Maugean skate adult being released after tagging during population monitoring. Photo: Mark Priest

This report is available on the NESP Marine and Coastal Hub website: www.nespmarinecoastal.edu.au

Contents

List of figures

List of tables

Executive summary

Maugean skate *(Zearaja maugeana*) have one of the most restricted distributions of any extant marine elasmobranch. Recent declines in relative abundance and changes in the demographic structure of the population have coincided with degradation of environmental conditions across their sole remaining habitat, Macquarie Harbour. In light of these events, there is an urgent need for up-to-date information on the structure and dynamics of the population, as well as developing improved tools to complement current monitoring work and help guide recovery actions.

Objectives

This study had two primary aims:

1. To investigate the use of novel imaging technologies as a potential tool to aid in population monitoring of the Maugean skate in Macquarie Harbour. In particular, we explored the use of high-frequency acoustic video for identification and measurement of skate in variable environmental conditions.

   Additionally, we tested various potential deployment configurations and how different operating factors affect the area of sonication and 'image' quality.

2. To investigate fine-scale genetic structuring and demographic history in the Macquarie Harbour Maugean skate population using next generation sequencing techniques.

Key findings

Population monitoring techniques

In-situ deployments of various novel imaging techniques in Macquarie Harbour targeted known skate habitats. Overall, acoustic methods (adaptive resolution imaging sonar – ARIS and synthetic-aperture sonar - SAS) outperformed optical methods (traditional video and light detection and ranging - LiDAR) and were able to reliably capture high quality footage across the halocline and high turbidity conditions. Acoustic video (ARIS) provided the highest resolution in static and dynamic deployments and as a result was chosen at the best potential Maugean skate image-based monitoring tool for use in further trials. Tests in a controlled aquarium setting demonstrated that acoustic video can be reliably used for species identification and measurement.

We present a comparison of various dynamic and static deployment configurations for acoustic video across different habitat types and conditions. ROV born deployments provided the highest stability and image quality, although towed deployments could be optimised further to achieve similar image quality. If so, a towed solution would provide an ideal compromise between low deployment costs and area coverage versus total effort required to perform a representative survey. We present a summary of how different deployment

parameters can be modified to maximise area of sonication and image quality. Further, we present a series of technical and logistical recommendations to consider in the development of an acoustic video-based monitoring program for Maugean skate.

Population genetics and demographic history

We present for the first time a reference quality whole genome and mitochondrial genome for the Maugean skate. Preliminary annotation for both is also presented, although this will be further refined pending transcriptome sequencing of Maugean skate tissues.

Samples from 162 Maugean skate were successfully sequenced using next-generation techniques. Single nucleotide polymorphisms (SNPs) showed that Maugean skate in Macquarie harbour constitute a single homogeneous population. There were relatively low heterozygosity levels across the population (based on SNPs). This pattern was also evident in the whole genome (mean heterozygosity =0.35 per kbp/1 Mbp window). These observations confirm that Maugean skate are genetically depauperate.

Interestingly, inbreeding loading in the population was only moderate based on SNPs (F_H= 0.058). Only 0.42- 2.6% of the genome was estimated to be in ROH>$_{100kb}$, with all runs being relatively short (>2Mb) and widely spread across all scaffolds. This suggests that the species has been genetically stable at low diversity levels. Furthermore, reconstruction of historical demographic patterns suggests that effective population (N_e) size for the species has been historically low for at least 10-20 k years. These characteristics could mean that the historical rarity of the Maugean skate provided a mechanism for purging highly deleterious alleles, possibly providing increased resilience to inbreeding depression. However, given the k selected life history of the species, any changes to genetic structure or diversity caused by the population decline documented between 2014 and 2021 will potentially take a long time to become evident.

We provide a discussion of how these traits are likely to influence recovery scenarios, highlighting the importance of ongoing genetic monitoring and genetic recovery for any conservation strategy for the species going forward.

1. Introduction

Maugean Skate (*Zearaja maugeana*) are the only known estuarine specialist skate species and have one of the most restricted ranges of any extant elasmobranch. The species has been classified as Endangered under the Australian *Environment Protection and Biodiversity Conservation Act (1999)* (EPBC Act) and the *Tasmanian Threatened Species Protection Act (1995)* based on its likely small population size and restricted distribution, it has been observed in only two remote estuarine systems in Tasmania, Bathurst Harbour and Macquarie Harbour on the west coast (Edgar et al., 2010). However, a recently completed NESP funded project found that Maugean skate are now effectively absent from Bathurst Harbour (Moreno et al., 2022), suggesting that most, if not all, of the remaining skate now live in Macquarie Harbour. In 2021, the Maugean skate was included as a priority species under the Australian Government's Threatened Species Action Plan (Threatened Species Action Plan - DCCEEW). These priority species have been selected to help focus the efforts of the Australian Government and partners on threatened species recovery actions.

Macquarie Harbour has a long-documented history of anthropogenic impacts that have resulted in considerable degradation of the environment. Recent work on the Maugean skate in Macquarie Harbour has shown clear signs of population stress and detrimental impacts of the degraded environment (Moreno et al., 2020). These findings highlight the inherent vulnerability of micro-endemic species (range is restricted to one or a few specific locations) and an urgent need to prioritise research and conservation action across what is likely to be the last remaining population for the species, Macquarie Harbour. This project a) furthered the development of novel imaging tools to aid in population monitoring of the species, and b) used next generation genetic sequencing to delineate the Maugean skate population in Macquarie Harbour to inform urgently needed conservation strategies for the species.

Skates have been shown to be inherently more vulnerable to declines caused by habitat disruption and fishing than most other elasmobranchs (sharks and rays), however, a significant number of species remain data deficient (Siskey et al., 2019). One of the biggest challenges to the management of endangered and vulnerable species is the ability to obtain reliable estimates of the size and structure of a population. Unfortunately, methods for population monitoring that are based on the capture, tagging and recapture of individuals require substantial effort (particularly for rare or endangered species), the gear used for capture can often be susceptible to size or sex biases, and the process carries additional risks to the animals (i.e., handling stress, post release mortalities).

Long term (> 12 years) fisheries-independent catch data from research gillnetting has shown a decline in relative abundance and shifts in the size structure of the Maugean skate population in Macquarie Harbour (Moreno et al., 2024). However, due to the cryptic nature of the species and the challenging environmental conditions in the harbour, population size estimates remain highly uncertain, with no current way to provide robust assessments of census levels through time. For species like the Maugean skate, genetic-based abundance estimation tools can be used, however, they require a certain level of genetic diversity to work, which is not supported by current knowledge (Weltz et al., 2018), noting, however, that the genetic portion of this project re-addresses this issue. Additionally, along with inherent

size selectivity for capturing animals greater than 200 mm total length (Moreno et al., 2025), gillnetting catch rates have become more variable since 2023. This is likely to result in biases in any estimates of population size that rely on the skate's capture (i.e., tag and recapture methods, including genetic methods). As such abundance estimation methods not based on capture are required.

Despite being a coastal estuary, the physiochemical profile of Macquarie Harbour results in conditions that more closely resemble deep sea habitats (i.e., low light penetration and low seasonal variability of environmental conditions in waters below 10 m). Visibility in the harbour is severely limited at depths greater than 1 m due to high turbidity and low light penetration, influenced by dissolved humic substance loads in the surface waters. Additionally, the seafloor is largely composed of very fine sediments which are easily disturbed and remain suspended for an extended period (Moreno et al., 2020). These traits restrict the usefulness of traditional video-based survey techniques such as towed video (see Fig 4-5, Appendix A; Moreno et al., 2020), or remote baited underwater cameras (Bicknell et al., 2016).

Technological developments in acoustic imaging (sonar) and real-time 3-D scanning using light detection and ranging (LiDAR, see Filisetti et al., 2018), have resulted in improved sensors that may provide the fine scale detail necessary for identifying organisms reliably (Castillon et al., 2019, Filisetti et al., 2018, Jones et al., 2021). Likewise, advances in deployment platforms such as tow sleds, AUVs and ROVs offer the means to effectively deploy the new sensor technology for the purpose of population monitoring studies. Development of these approaches could result in a cost-effective way to survey at risk and/or data-deficient species, providing a valuable tool for management and conservation.

Both sonar, in particular adaptive resolution imaging sonar (ARIS, see Jones et al., 2021), and LiDAR based methods may offer significant advantages over traditional optical methods in low visibility, high turbidity settings like Macquarie Harbour. Accordingly, adaptive resolution imaging sonar (ARIS, see Jones et al., 2021), synthetic-aperture sonar (SAS, see Hansen, 2011) and LiDAR were all trialled in a 2022 pilot study as potential monitoring/abundance estimation alternatives for Maugean skate. This pilot showed that while LiDAR wasn't suitable, sonar could be effectively used as a biological survey tool in Macquarie Harbour, although the high resolution imagery that ARIS provides was required over that produced by SAS. As such, only the potential of ARIS as a Maugean skate survey tool was assessed in detail in this project.

An important part of using novel imaging tools is their integration into an adequate platform, including the need for additional sensors, as well as optimisation of survey protocols. Furthermore, these devices provide a data rich output that requires the development of pre- and post-processing pipelines to be used effectively. Accordingly, before these tools can be used to estimate relative Maugean skate abundance, there is an important need to undertake this integration, and development stage. This project tackles the survey platform component of these needs by assessing the feasibility of conducting ARIS-based population surveys of Maugean skate in Macquarie Harbour by conducting systematic tests of various deployment platforms for ARIS surveys.

Developing and implementing conservation strategies requires delineation of populations, i.e., investigation of population structuring (e.g., discrete sub-populations within a population). In the Macquarie Harbour Maugean skate population, this was originally attempted with DNA barcodes and microsatellites (Weltz et al., 2018). Both these markers showed that the species has very low genetic diversity; with no diversity detectable in over three thousand base pairs surveyed from the mitochondrial genome, low average microsatellite heterozygosity (an indicator of genetic diversity) and no overall population structure (Weltz et al., 2018). With a view to improving the power of detecting fine-scale population structuring and investigating the evolutionary potential of the Maugean skate to adapt to changing environmental conditions in Macquarie Harbour, we employed a two-pronged approach both of which involve Next Generation Sequencing strategies: 1) whole nuclear (i.e., using DNA from the cell nucleus) genome (the complete set of DNA in an organism) typing and 2) developing a high-resolution dataset of genome-wide single nucleotide (a single DNA building block) polymorphisms (SNPs – pronounced snips), which are the most common type of genetic variation in a species. SNPs derived from Maugean skate tissue samples collected between 2011and 2023 were used to conduct a genome-wide population genetic investigation on the fine-scale genetic structure in the Macquarie Harbour population.

2. Investigating the use of novel underwater-imaging methods for population monitoring of an endangered, cryptic elasmobranch species living in a dynamic, low-visibility coastal environment.

Mark Priest, David Moreno, Jayson Semmens

2.1 Introduction

To date, the only reliable method to monitor Maugean skate (*Zearaja maugeana*) has been the use of fisheries independent gillnet surveys (Lyle et al., 2011). Nets are an effective way to target adult Maugean skate and data from these surveys has yielded crucial insight into trends of relative abundance and changes to the demographic characteristics of this species in Macquarie Harbour (Moreno & Semmens 2023). However, there are some important limitations inherent to the use of nets for monitoring the Maugean skate population:

1. These surveys are resource intensive and time consuming, and the Maugean skate is a naturally rare and cryptic species. Therefore, significant fishing effort has been required to ensure that the surveys are representative (Moreno & Semmens 2023). This has also resulted in limited recaptures, so current population size estimates using traditional tag-recapture techniques have associated uncertainty (Bell et al., 2016).

2. Maugean skate are captured when they become lightly entangled in the nets, either by the rostrum or because of their caudal thorns. Smaller individuals are less likely to become entangled and therefore less likely to be landed. This gear-driven size-selectivity bias has remained consistent through time (mesh size and broad methodology have been kept constant); therefore, it can be accounted for when analysing changes in relative abundance (Moreno & Semmens 2023). However, this also means that the current population monitoring program is somewhat restricted in its ability to detect patterns across juvenile size classes with the same accuracy when compared to adults.

3. Prolonged soak times in nets have been shown to increase the risk of mortality for Maugean skate (Lyle et al., 2011). For example, soak times longer than two hours can significantly increase the risk of depredation from lice (Moreno pers obs.) and may also increase the risk of seal interactions. Accordingly, procedures for the current monitoring program severely restrict the amount of gear used, the total soak times (<1.5 hrs max) and require constant attendance of nets while deployed. While these measures have been highly effective at negating detrimental impacts on skate, they also restrict how much and how long gear is in the water, limiting fishing effort.

Therefore, there is a need to develop alternative sampling methods that can complement or replace traditional net surveys, noting that net surveys also provide data around animal health, reproduction and genetics, that non capture methods cannot.

Macquarie Harbour is a fjord-like coastal estuary on the West coast of Tasmania with distinct bio-geo-chemical characteristics. Oceanic water exchange is restricted by a narrow sill, and there is a large influx of fresh water from the Gordon and King rivers, creating a heavily stratified water column. Maugean skate are found across all depths in the harbour, but they show a strong preference for depths between 7.5 and 12.5 m (Bell et al., 2016, Moreno et al., 2022). Visibility is severely limited at these depths (>1m) due to high turbidity and low light penetration, influenced by dissolved humic substance loads in the surface waters.

Underwater cameras are commonly used tools in marine biological monitoring. However, their usefulness is limited in low light conditions and high turbidity. Underwater cameras are currently used to perform compliance monitoring surveys in Macquarie Harbour with the aid of external light sources. Visibility is largely dependent on external conditions and is often restricted, although occasional Maugean skate sightings have previously been reported (EPA pers comm). However, these compliance camera surveys do not target critical sites and depths where skate are most common, areas which also tend to have even less visibility. Towed video trials in Macquarie Harbour have shown that even when carrying external light sources, visibility is severely restricted due to backscatter (light reflected by suspended particles) caused by turbidity, making this approach inadequate for large scale skate monitoring (Moreno et al., 2020). In contrast, active acoustic survey methods like sonar, are effective in overcoming low visibility conditions. Various sonar technologies have been used to survey marine fish populations by looking at return echoes or more recently acoustic shadows (Ridgeway et al., 2024). However, these methods are limited by low resolution and precision, hindering enumeration and making accurate species identification nearly impossible.

In an in-situ pilot study conducted in November 2022, novel acoustic and optic technologies were investigated as potential tools for Maugean skate monitoring (Appendix A). An autonomous underwater vehicle carrying a sensor array comprising an underwater LiDAR and camera module and a synthetic-aperture sonar were deployed across different known Maugean skate habitats. Both technologies have shown promise for imaging in low light deep-sea environments. For the in-situ trial, Melbourne skate (*Spiniraja whitleyi*) caught as bycatch by commercial fishers were used as a skate surrogate target. Results from this work showed that like other optical methods, LiDAR was severely affected by backscatter caused by high turbidity, and it was not possible to generate any usable data. By contrast, the SAS system performed well regardless of turbidity or position of the vehicle relative to the halocline. The test targets were successfully imaged by the SAS, although they were only identified because the deployment location was known. This study showed that active acoustic methods can be effectively used as a biological survey tool in Macquarie Harbour, although higher resolution imagery than SAS provides would be needed and could be provided by ARIS.

ARIS is an ultra-high frequency multibeam imaging sonar, a type of device commonly referred to as an acoustic camera. These devices use multiple narrow beams in a high frequency range (1.8-3 MHz) to produce video-like high quality images, similar to how medical imaging ultrasounds operate. The high frequency produces very high-resolution images (downrange resolution between 3 and 19 mm) but there is a trade-off with travel distance, resulting in a more limited range (up to 15m @ 1.8 MHz) when compared to other sonar devices. Previous studies have used ARIS to assess biogenic reefs (Griffin et al., 2020), provide fish length estimates (Cook et al., 2019), for mobile surveys of fish passages (Xie et al., 2024), and compare fish assemblages to net-based methods (Egg et al., 2018).

Acoustic cameras show promising performance for biological surveys in dynamic, low-visibility environments. The resolution makes it possible to accurately identify species and reliably estimate sizes. Furthermore, the operating frequency range is above the known hearing range of all fish species, making it non disruptive to fish (Shen et al., 2024). Here, we assess the feasibility of conducting ARIS-based population surveys of Maugean skate in Macquarie Harbour by conducting systematic tests of various deployment platforms for ARIS surveys. These include static deployments using baited remote underwater video surveys (BRUVs), and dynamic deployment via towed deployments (tow fish), and remote operated vehicle (ROV) mounted deployment. We also explore the optimal ARIS orientation metrics (height from benthos and pitch) for future survey designs.

2.2 Methods

2.2.1 Imaging systems

High frequency acoustic imaging camera

The imaging sonar used was an ARIS Explorer 3000 (Sound Metrics, Bellevue, WA, USA). This device operates at two frequencies, a 1.8 MHz mode for increased range and a 3MHz high-resolution identification mode. All observations in this study were conducted using the 3 MHz identification mode, in which the device produces 128 acoustic beams (0.2° horizontal X 15° vertical), resulting in a downrange resolution between 3 and 19 mm. The device is 26 cm x16 cm x14 cm with a mass if 1.55 kg in water (5.12 kg in air) and an 18 Watt average power consumption.

2.2.2 Field and laboratory trials

Laboratory trials

Most studies using acoustic cameras to survey fish have targeted species that swim in the water column or have a higher profile than skate. This means that an acoustic shadow is generated, which can aid in the identification of individuals and in species classification (Shen et al., 2023). To test if dorsoventrally flattened benthic animals can be reliably detected by ARIS, two species of skate (Australian longnose skate, *Dentiraja confusa* and

thornback skate, *Dentiraja lemprieri*) held at the IMAS Taroona research facility were imaged in an aquarium setting.

The ARIS unit was hand-held near the surface of each holding tank, and the skate were imaged (Fig 2.1, left panel). The resulting footage was examined to determine if different species could be identified from the acoustic data. Additionally, echograms of the acoustic video were generated to complement visual scoring of the footage. Visual species identification relied on 2 key morphological differences, rostrum and disk shape. Briefly, thornback skate have a rounded rostrum and oblong disk, whereas Australian longnose process a more angular disk shape and a pronounced pointy rostrum. Note that Maugean skate have similar but more pronounced features to Australian longnose skate.

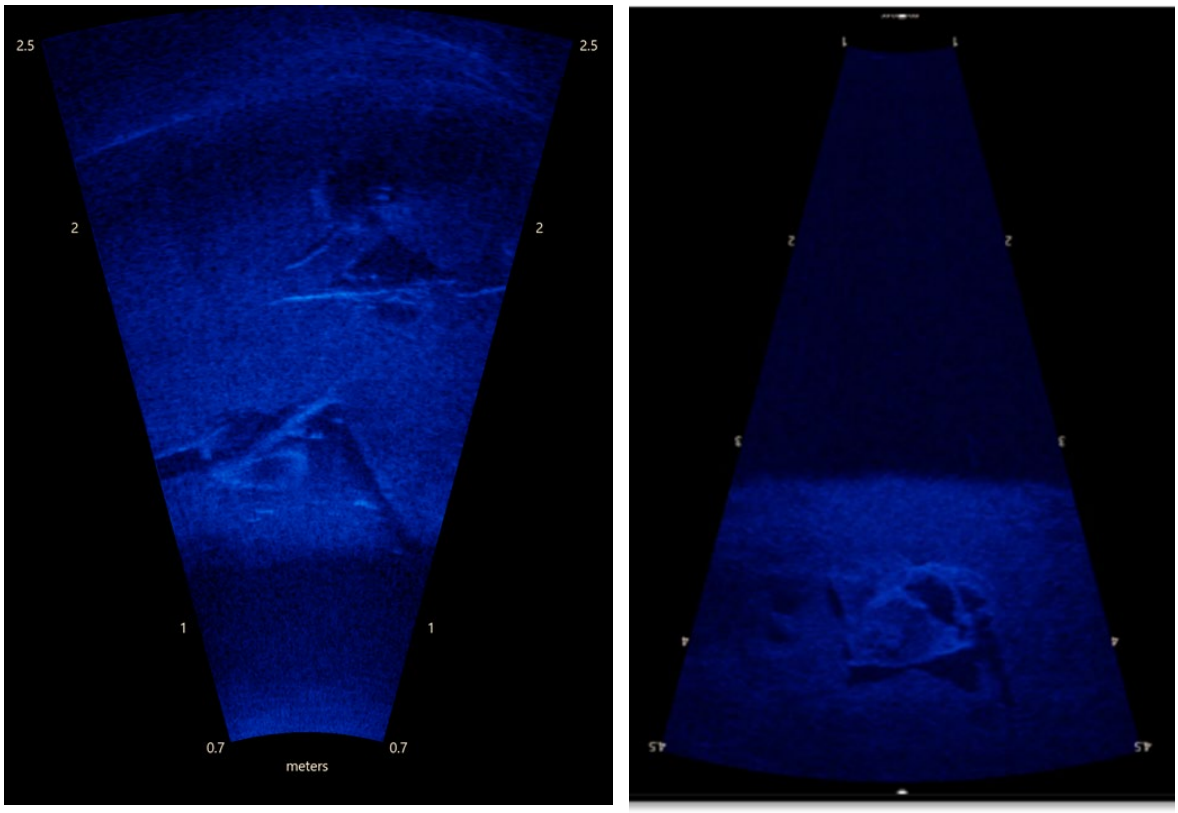

Figure 2-1 Surrogate skate targets used to simulate Maugean skate: (left) ARIS image of one thornback and two Australian long nose skate in an aquarium setting. (right) ARIS image of Maugean skate proxy (Melbourne skate carcass) used for in-situ testing in Macquarie Harbour.

In-situ trial in Macquarie Harbour

Given that Macquarie Harbour is a remote site where it can be logistically challenging and costly to trial equipment, an in-situ trial was conducted to determine if conditions in the Harbour influenced the performance of the acoustic camera.

Multiple diver-held and vessel attached (towed video platform, see details below) deployments of the ARIS acoustic camera were conducted over two days in Macquarie Harbour in June 2022. For diver held deployments, the diver with the ARIS camera had a connected heads-up display that allowed them to see the footage being collected by the acoustic camera in real time. For towed trials, the acoustic camera was fixed to a frame and towed behind the vessel at approximately 1 m from the sea floor at a speed of ~0.5 kt. Each deployment consisted of a transect that intersected a test target (see details below).

Deployments occurred at Table Head and Swan Basin, two known Maugean skate habitats (Bell et al., 2016). The camera was used to image the relevant habitats across a range of depths (1-10 m) to help understand how turbidity and position relative to the halocline affected the image quality. A Melbourne skate carcass (*Spiniraja whitleyi*) collected from fisheries bycatch was used as a surrogate target (Fig 2.1, right panel). The target was weighted and attached to a surface line.

Deployment configuration trials

The ARIS unit can transmit live footage via an umbilical to a top-side monitor, suitable for ROV and towed deployments, and remote deployment, powered and storing footage using an on-board battery and hard-drive, suitable for BRUV surveys. As such deployment configuration trials were conducted using BRUVs, ROVs and a towed configuration.

BRUV deployments were conducted in five locations around Hobart, Australia (Fig. 2.2). The sites chosen comprised differing habitats to assess imaging performance under a variety of conditions. Deployments were conducted during daylight hours with a one-hour soak time.

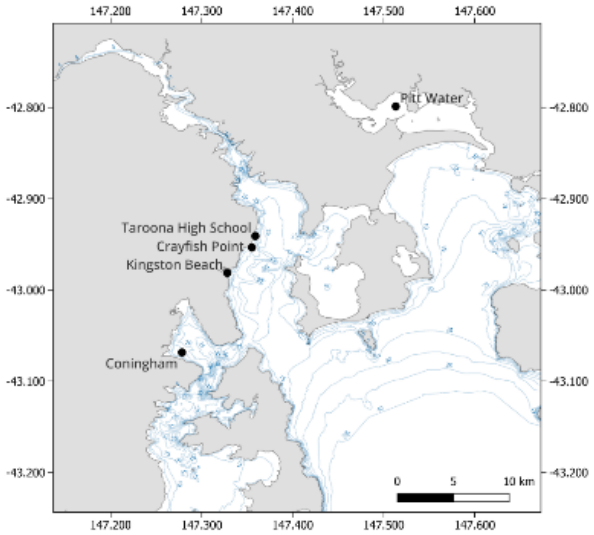

Figure 2-2 Locations of ARIS skate survey tests in South-East Tasmania. BRUV deployments were conducted at Taroona High School, Crayfish Point, and Kingston Breach, ROV deployments were conducted at Pitt water, and towed camera deployments conducted at Conningham.

The ARIS was attached to the BRUV frame directly above a GoPro Hero 10 (GoPro, San Mateo, CA, USA) to allow comparisons with traditional visible-light cameras, validate species identification and ground-truth habitat composition (Fig 2.3C).

Two models of ROV were trialled for ROV deployments. A compact ROV BlueROV2 (Blue Robotics, Torrance, CA, USA) and larger Boxfish ROV (Boxfish Robotics, Remuera, Auckland, New Zealand) (Fig. 2.3A, 2.3B). The ARIS was mounted centrally to the topside of each ROV with custom mounts. Initial tests were conducted in a closed-water pool environment to allow assessments of manoeuvrability and performance of both ROV units and the ARIS in the absence of complicating environmental factors. After mounting the ARIS to each unit, they were both flown over a series of underwater targets designed to resemble juvenile and adult skate (flat circular ceramic tiles of two differing diameters, 40mm and 18mm) (Fig. 2.7). Multiple passes of the targets were made at varying speeds, height off the bottom, and pitch to determine the optimum parameters for benthic surveying. Measurements of the targets were taken using the ARISFish software. Ten distinct frames where the targets were visible were randomly selected from 1.8 and 3 MHz ARIS footage.

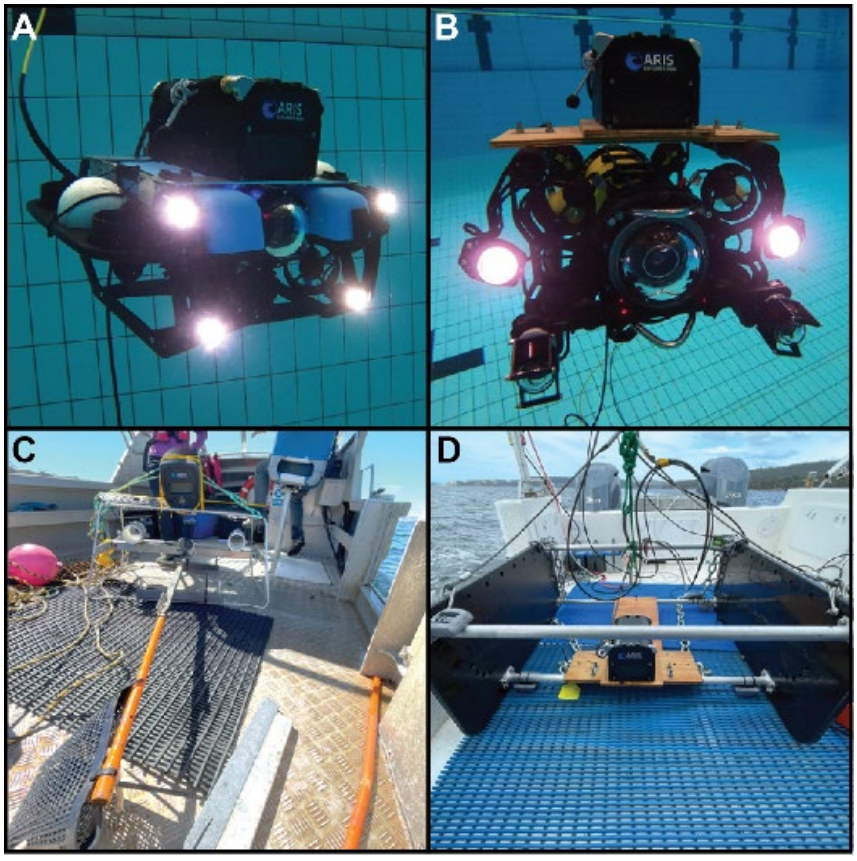

Figure 2-3 ARIS sonar unit mounted to: the topside of the Blue Robotics (A) and Boxfish (B) ROVs during pool tests, a BRUV deployment frame at Kingston Beach (C), and a towed camera frame in the D'Entrecasteaux channel (D).

Average % error and SE deviation were calculated for both target sizes and imaging intensities to assess animal size estimation potential.

The increased control provided by the larger ROV (Boxfish) meant only this unit was used for field trials. ROV field trials were conducted in Pitt Water (Fig. 2.2) and included a variety of habitats and water conditions (reduced visibility and soft benthos) that approximated the different sampling scenarios that may be encountered in Macquarie Harbour. As with the pool trials, underwater targets were used with different flight parameters to assess performance of ARIS imagery with the added complications of open-water weather conditions (waves, tide, wind, etc.) influencing ROV control.

Finally, two towed-video sleds were trialled, predominately to test ARIS imagery at greater speed where control of flight parameters is limited. Initial tests resulted in only the larger towed camera frame (Fig. 2.3 D) being used for field trials as the smaller frame proved to be unstable and difficult to deploy. Field tests were conducted at Conningham (Fig. 2.2), where the soft sediment benthos provided the potential to use the targets to emulate a realistic skate encounter. The towed-video sled was adjusted with weights to alter flying height and was towed behind an IMAS vessel at speeds varying from 0.5 to 3 kt. A live-view camera (TowcamHD, Runaway Bay, QLD, Australia) was also attached to the sled to provide concurrent visible-light footage.

2.2.3 Data analysis

All ARIS imagery was reviewed after the trials and, where appropriate, in conjunction with concurrent visual-light footage (GoPro and ROV). Where possible, target objects (skate

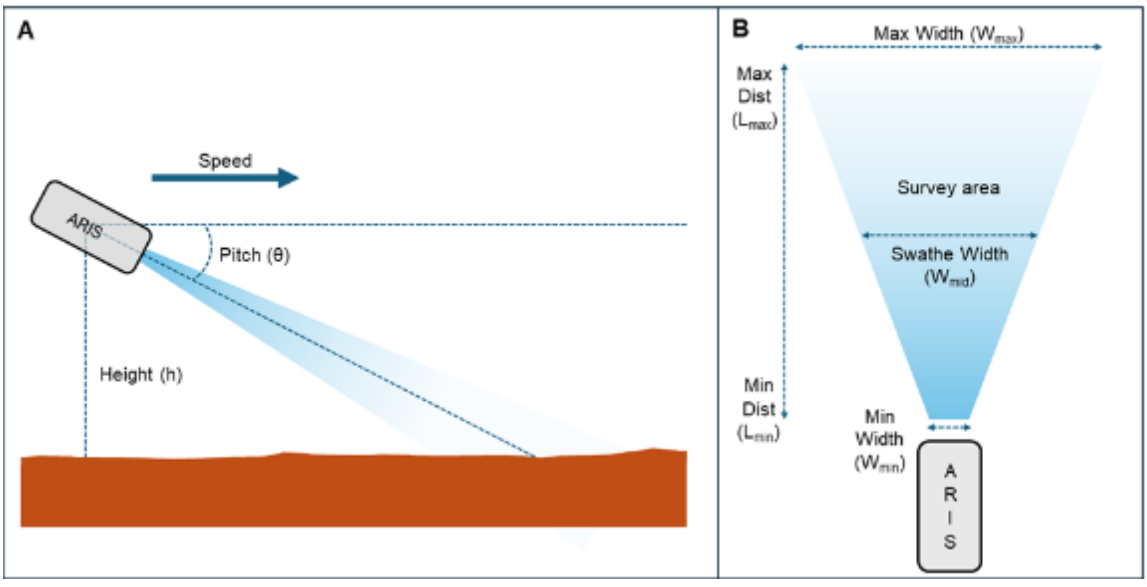

Figure 2-4 Flight metrics of ARIS deployments used to determine optimal survey parameters. A) side-view of dynamic deployments, B) top-view of dynamic deployments displaying derived metrics used for calculating

surrogates) were identified and measured, with identification confirmed via visual-light footage, as were any other serendipitous encounters with other marine organisms.

To obtain an indication of optimal flight parameters for future survey design, we calculated key metrics, survey area and swathe width (width at the mid-point of the survey area) (Fig. 2.4) using basic trigonometry:

$$Survey\ area = \frac{Wmin + Wmax}{2} * (Lmax - Lmin) \quad (1)$$

$$Survey\ area = \frac{Wmin + Wmax}{2} * (Lmax - Lmin) \quad (2)$$

where,

$$Wmin = 2 * Lmin * Tan(15) \quad (3)$$

$$Wmax = 2 * Lmax * Tan(15) \quad (4)$$

$$Lmin\ = height * Tan(82.5 - \theta) \quad (5)$$

$$Lmax\ = height * Tan(97.5 - \theta) \quad (6)$$

These calculations were based on the ARIS field of view specifications provided by the manufacturer, given as 30° horizonal x 15° vertical. Further, nominal effective range, given as 15 m @ 15°C was used as a maximum distance (L_{max}) limit (Sound Metrics, 2024).

Relationships between survey area and swathe width with varying height and pitch were explored along with qualitative assessment of footage, using ARISFish analysis software (Sound metrics, Bellevue, WA, USA), to determine the optimal parameters for designing skate surveys in Macquarie Harbour.

2.3 Results

2.3.1 Laboratory trials

Imaging of captive animals in a controlled aquarium setting showed that ARIS could be successfully used to detect dorsoventrally flattened benthic animals reliably and that resolution was high enough for accurate species identification based on key morphological characteristics despite individuals having a similar size (Fig 2.4). High resolution ARIS footage (3 M Hz) was detailed enough to obtain basic morphometrics from imaged individuals (Fig 2.5)

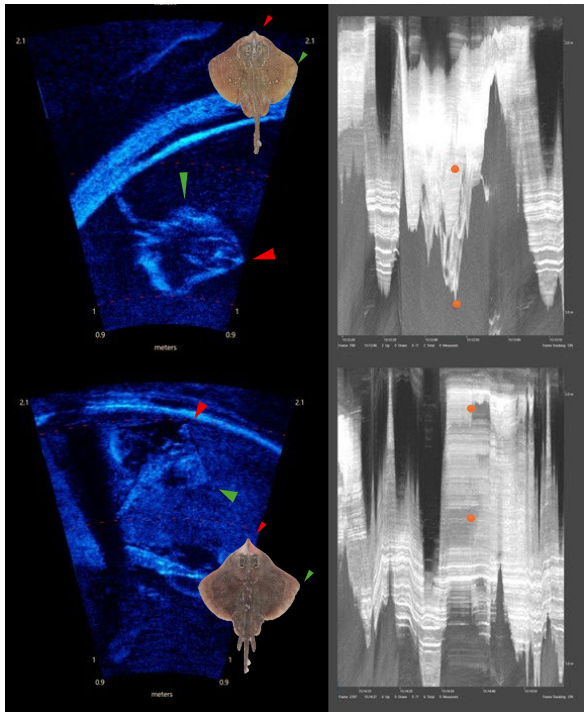

Figure 2-6 Still frames of ARIS footage (left) and the associated echograms (right) showing a thornback skate (top) and Australian longnose skates (bottom) in an aquarium setting (reference photos from CSIRO fish collection). Species were identified using the high-resolution sonar image based on key morphological differences between species (i.e. disk shape -green arrows-, rounded v pointed rostrum -red arrows-). Red circles in the echogram mark the area of interest in the frame shown to the left.

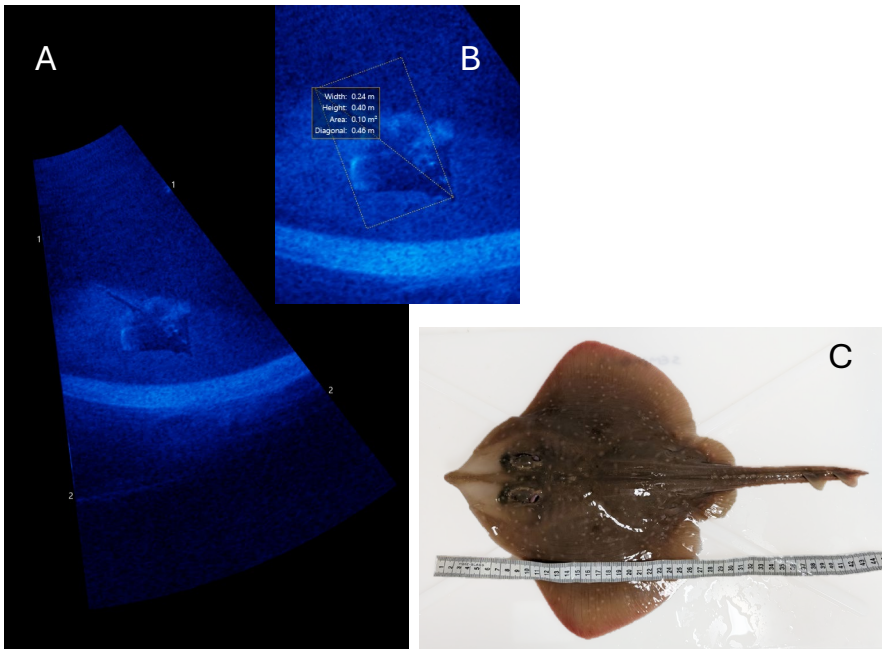

Figure 2-5 (A-B) Acoustic image of a juvenile Australian longnose skate and (C) still frame photography of the same individual. ARIS estimated total length was 45 cm compared with 44 cm actual.

2.3.2 In-situ trials

Macquarie Harbour

Acoustic video footage collected over the Macquarie Harbour trial totalled 40 minutes in diver held deployments and 3 hours in a towed configuration. Melbourne skate targets were successfully imaged using ARIS in a towed configuration (Fig 2.1, left panel). These tests demonstrated that skate can be successfully detected and identified using ARIS imaging in-situ in Macquarie Harbour.

The quality of collected images was not affected by either the halocline or turbidity, in fact for diver held deployments the acoustic video proved to be a better navigation tool than visible light due to the limited visibility. Therefore, all subsequent deployment configuration trials were conducted in more easily accessible sites in Southwest Tasmania.

Deployment configuration trial

Initial ROV-mounted ARIS deployment in the pool environment using the smaller BlueROV2 immediately produced clear identifiable imagery of target objects (including a snorkeler positioning the targets) (Fig. 2.7). However, even within the benign confines of the pool, it was clear that the addition of the ARIS affected ROV stability and manoeuvrability due to the significant negative buoyancy of the ARIS unit. The long length of the ARIS compared to the unit's width meant precise positioning of the ARIS along the fore-aft axis of the ROV was required to prevent rolling. Even then, user-determined roll had to be minimised to prevent toppling. Subsequently, testing was repeated using the larger Boxfish, with the additional power and size of this ROV helping to negate and overcome these balancing issues.

Measurements of skate-surrogate ceramic disc targets (both sizes, i.e. 40mm and 18mm) taken from ARIS imagery in the pool differed from actual measurements by an average of 2.5 % (SE= 0.24 for 40mm and 0.37 for 18 mm respectively). Measurement accuracy was lower in low resolution mode (1.8 M Hz) with an average difference of 5.8 % (SE=0.69) for the 40 mm targets and 7.41% (SE0.92) for the 18 mm targets. However, given the discs were hand-shaped and not perfectly circular, accuracy could be even higher than reported here as orientation varied. Moreover, the claimed image resolution of the ARIS at its highest setting is 3 mm.

BRUV deployments were successfully completed in three locations covering differing habitats, some of which are similar to benthos encountered in Macquarie Harbour. GoPro visible-light footage provided wide, near-field imagery, clearly showing the bait arm and bait bag, while quickly dropping off 1-2 m from the bait bag. In comparison, ARIS imagery provided a narrower field of view starting at the bait bag and extending ~3 m past the bait bag (Fig. 2.6). Results of further testing suggest this could be extended much further with modification of the ARIS orientation, i.e., lower elevation and/or shallower pitch.

Table 2-1 Details of three BRU-AV (acoustic video) deployments using ARIS. Given are deployment depth, angle of the ARIS (pitch), maximum range and survey area of ARIS imagery, and summary of the ecology of each deployment.

Location	Depth (m)	Pitch	Max range (m)	Survey area (m^2)	Ecology
Kingston Beach	15.7	-25°	3.5	3.1	Sandy benthos, draughtboard shark, flathead
Crayfish Point	6.0	-24°	3.2	2.6	Rocky, macroalgal benthos, wrasse
Taroona High School	8.2	-22°	4.8	6.3	Sandy, filamentous algal benthos, sea stars

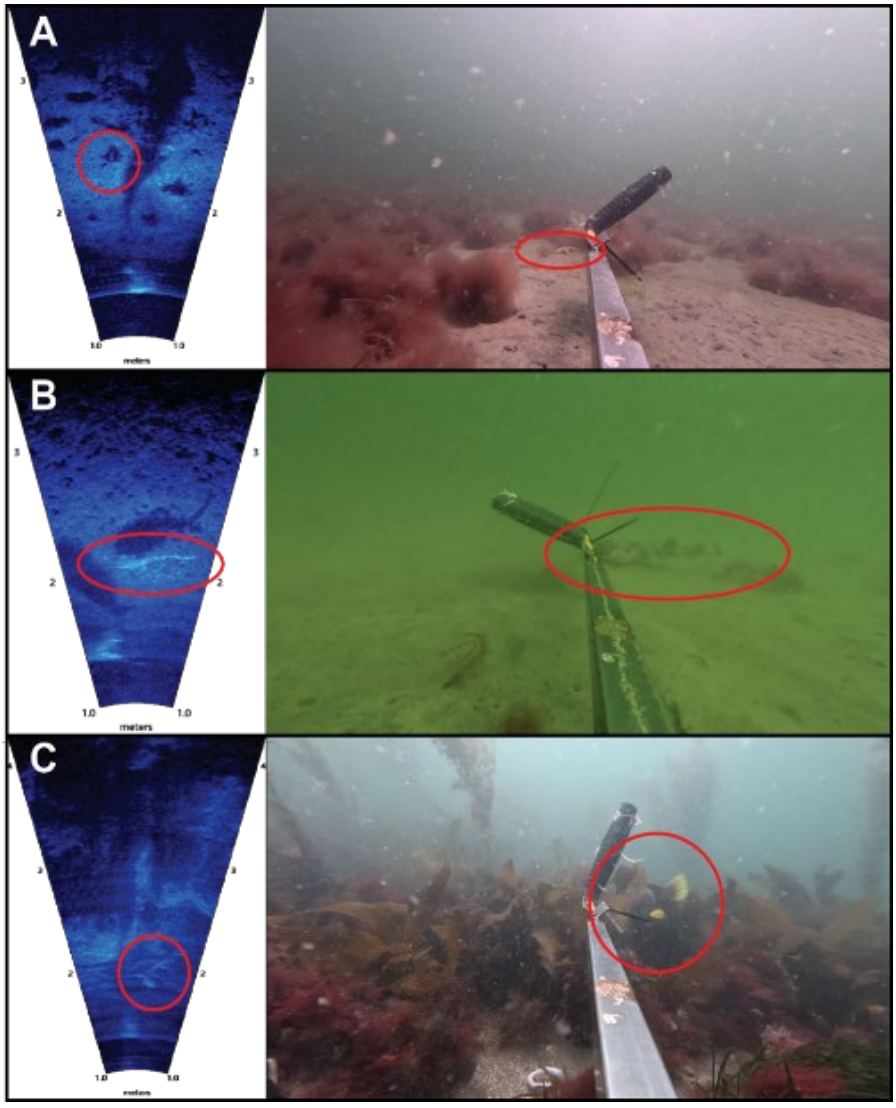

Figure 2-7 Comparisons of Aris (left) and GoPro (right) still images from BRUV deployments in different habitats with subjects of interest circled in red. A) Sand/filamentous algae benthos with sea star at Taroona High School, B) Sand benthos with draughtboard shark at Kingston Beach, C) Algae dominated habitat with wrasse at Crayfish Point.

A variety of organisms were identified in the ARIS footage, examples of which can be seen in Figure 2.6. Confirmation of species identification was provided by the concurrent GoPro footage. Notably, in cases when organisms approached the BRUV head-on, they were seen first in the ARIS imagery before appearing in the GoPro footage. This was especially noticeable in the Kingston Beach deployment when a tide change significantly reduced water clarity in the GoPro footage. Encouragingly, ARIS imagery was stable and clear in all deployments and features were identifiable and matched visible-light video identification, including small features such as invertebrate sand-burrows present in Kingston Beach and Taroona High School deployments.

Field tests conducted in Pitt Water with the larger Boxfish returned footage of sufficient quality to identify ‘skate’ disc targets in a low visibility, sediment-heavy benthos environment (Figure 2.7 B). While conditions during testing were relatively mild, the Boxfish provided ample control to complete multiple transects of varying flight parameters to assess ARIS imagery, detailed below.

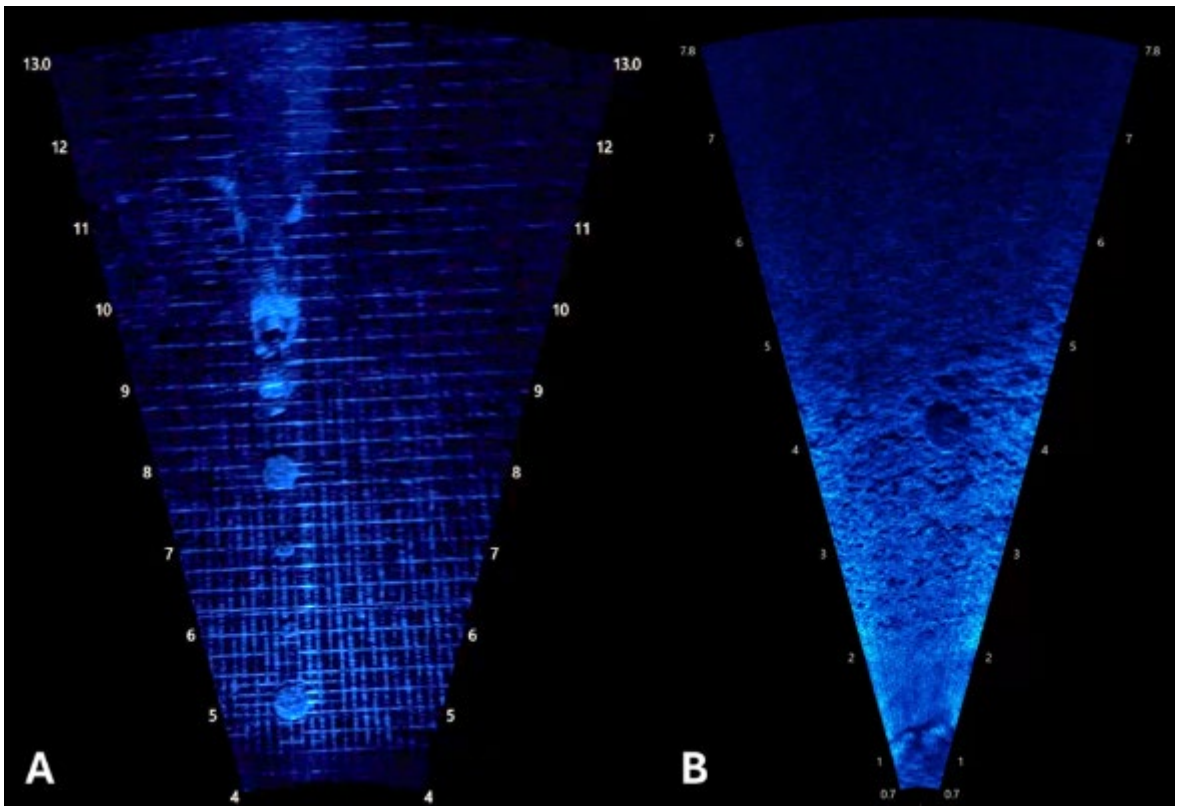

Figure 2-8 Examples of ARIS imagery from ROV deployments A) snorkeler and ceramic disc targets in the closed-water pool environment, B) Ceramic disc target and tether in Pitt Water.

Towed-video deployments proved the hardest of the deployment methods to obtain clear reliable ARIS imagery. The lozenge-shaped dimensions and significant negative buoyance of

the of the ARIS unit meant careful placement was required to balance the towed camera frame and prevent uncontrollable rolling and yaw. Indeed, of the two sleds tested, we were unable to setup the smaller of the two to provide satisfactory video, despite multiple attempts at adjusting ARIS position, frame weighting, and bridle positions. Thus, only the larger of the two frames was used for survey tests, and even then, control of flight parameters proved problematic. As a result, the towed-video camera frame was weighted to fly primarily on, or very close to, the substate and recorded footage was used to test the influence of speed on ARIS imagery.

Extended tows were conducted at survey speeds varying from 0.5 to 3 kt. Review of the resulting footage revealed significant banding and appearance of artifacts at speeds over 1.5 kt, impacting image clarity and consistency. Thus, we anticipate a speed of ~1 kt as a realistic maximum for ARIS surveying, which approximates the speed of towed camera surveys, and suggests that conducting logistically feasible surveys is achievable.

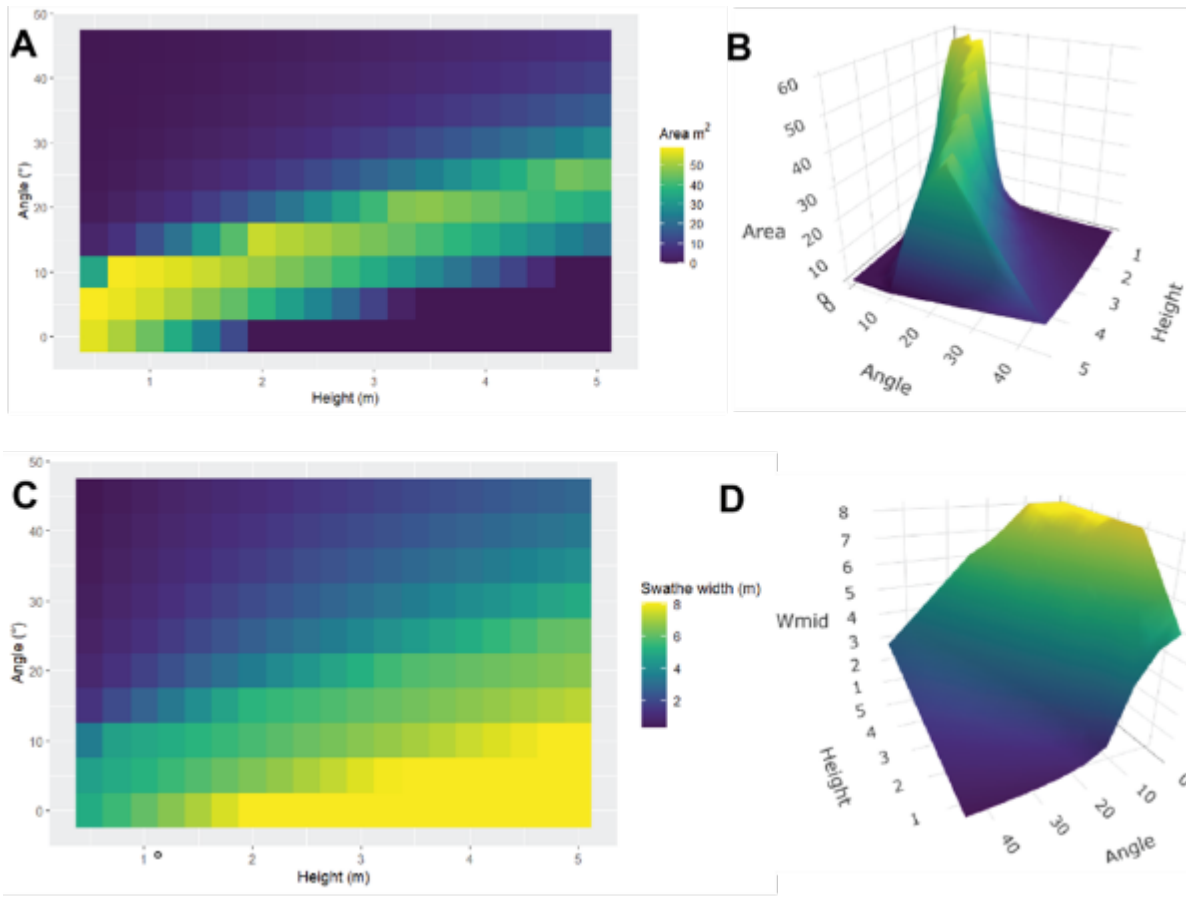

Figure 2-9 Theoretical survey area (A, B) and swathe width (C, D) with varying ARIS height and pitch. The same plots are presented in both 2- and 3-dimensions to aid visualisation.

Plots of the key survey metrics, survey area and swathe width (Fig. 2.8), provide an indication of optimal flight parameters for maximising survey coverage when designing a Maugean skate monitoring program.

Survey area was maximised when the ARIS was at a low height and shallow pitch, decreasing as both height and pitch were increased. While the theoretical maximum area recorded is at the shallowest height and pitch, there was relatively little difference in survey area between this (59.3 m^2 at 0.25 m height and 0° pitch), and slightly greater height and pitch (57.6 m^2 at 1 m height and 10° pitch), the latter being more logistically easier to control in the field. Swathe width was greatest at low pitch and increased with greater height. As height increased the mid-range point, i.e., swathe width, moved closer to the fixed maximum range at 15 m, where maximum swathe width was 8.04 m.

2.4 Discussion

The ability of acoustic cameras to ‘see’ into the depths of Macquarie Harbour’s dark and turbid waters, makes this an ideal tool for surveying environments where traditional methods relying on visible light, such as diver-obtained underwater visual census (UVC) and BRUVs, falter. Here we have demonstrated through in-situ deployments in Macquarie Harbour, that acoustic cameras performance is not affected by low-light, turbidity or when operating across density layers in a segregated water column i.e. haloclines. We showed that skate can be reliably identified on acoustic footage regardless of dynamic or static deployment of the device. Furthermore, we expand on previous proof-of-concept work and assess multiple deployment methods for developing an acoustic camera-based monitoring program for Maugean skate in Macquarie Harbour.

All deployment methods returned imagery that was considered usable in terms of surveying Maugean skate. Static BRUV deployments proved logistically easy and returned the ‘cleanest’ footage, allowing effective organism identification and measurement. The presence of a static background highlights moving subjects, and this can be further enhanced by subtracting the background within the ARISFish software. However, the limitations of this methods for population assessment are well-known and inherent in the design. Namely, bait related issues regarding attraction, survey area, species-specific bait response, and inability to enumerate absolute abundance estimates to avoid repetitive counts of individuals (Harvey et al., 2013). For Maugean skate this final point may prove problematic given the importance of accurate population estimation for such an endangered species. Moreover, one key advantage of BRUVs, their relative low-cost per minutes of footage captured is negated by the sheer cost of the ARIS unit, preventing multiple simultaneous deployments without exorbitant expense.

Dynamic ARIS deployments clearly provide more effective methods for Maugean skate population surveys than static deployments as they offer larger enumerable survey areas while minimising the issue of repeat counting individuals. Differences in imaging between ROV and towed-video ARIS deployments came down primarily to a trade-off between speed

and control. ROV deployments allowed fine-scale immediate on-the-fly adjustments of height and pitch while also providing the ability to revisit and resurvey an area/object of interest, if needed. This resulted in more consistent, higher quality footage with less unidentified objects/features. Whereas towed-video deployments are controlled remotely via tether management and adjustments/feedback suffer from significant time lag making footage less consistent. The advantage of towed-video deployments is that faster survey speeds can be achieved. However, there were clear limits to the speeds at which surveys could be undertaken before image quality suffered, even when post-processing velocity correction is used. Logistically, towed video was easier to deploy than ROVs as; fewer tethers with less management were required, no ROV operator is needed, and there are no battery requirements below water. Yet, towed camera frame deployments required careful and precise setup to fly straight and consistently, minimising yaw, which severely hampered video quality. It should be noted that several of these issues can be diminished or eliminated by designing an acoustic camera specific frame. Furthermore, there are other acoustic cameras available in the market that have comparable performance to ARIS, but in different form factors that may be better suited for specific deployment configurations (e.g. Oculus M-

Table 2-2 Summary of the main pros and cons of different ARIS deployment methods trialled in the study.

Deployment method	**Pros/Cons**
BRUV	✓ Image stability ✓ Easier to identify and measure organisms moving in/out of frame ✓ Quick to deploy/retrieve ✓ Remote deployment ✗ Indeterminate survey area ✗ Only provides a relative abundance estimate (MaxN) ✗ Cost of ARIS unit precluded high numbers of deployments/replication
ROV	✓ High control of flight parameters ✓ Immediate on-the-fly adjustment (can respond to environmental conditions and/or ARIS imaging) ✗ Deployment may be limited by ROV battery life ✗ Possible depth limited by tether length ✗ Logistically challenging deployment (multiple tethers, experienced ROV pilot required)
Towed platform	✓ Increased speeds can survey large areas quickly ✓ Logistically easier than ROV deployments ✗ Hard to control flight parameters consistently (can be improved using dedicated device for ARIS) ✗ Imaging needs correcting for boat velocity and can be degraded at speed ✗ Subjects in fewer imaging frames may hinder positive identification of organisms

series, Blueprint Subsea, UK). A summary of deployment pros and cons is provided in Table 2.2.

In terms of survey design, our exploration of optimal flight parameters revealed two somewhat contrasting trends. Total survey area was maximised by employing a low ARIS height and pitch, whereas swathe width increased with ARIS height for low pitch angles. For traditional UVC methods using divers, wider transects (visibility permitting) would normally be preferred when surveying larger organisms, especially when targeting species with low abundances (Samoilys & Carlos, 2000). However, in the case of video-derived surveys, field-of-view (FOV) is fixed by the camera specifications, and thus swathe/transect width can only be modified by camera orientation (Cappo et al., 2003). The 30° horizontal FOV of the ARIS is much narrower than ~120° human binocular horizontal FOV. Thus, to obtain a swathe of comparable width to many established UVC surveys (~5 m), the ARIS needs to be surveying higher than is optimum for maximising the overall survey area. For UVC, transect area is a somewhat moot point, with water clarity defining visibility and the distance at which organisms can be detected. Moreover, a diver can adjust survey speed, even stopping, in order to identify and/or count cryptic organisms (Pelletier et al., 2011). In contrast, the ARIS video footage has a range limit, independent of visibility and it makes sense to maximise this range as a) swathe width increases with range, and b) when moving at speed, a larger sonicated area will increase the likelihood of detecting an individual in subsequent frames, aiding in identification. This is important given that the frame rate on the ARIS (maximum 15 frames/sec) is much lower than traditional visible-light camera footage (in excess of 120 frames/sec). Finally, the best compromise between surface area and swathe width also needs to consider the logistics of survey deployment and the intrinsic traits of the ARIS footage. For example, surveying close to the benthos runs the risk of inadvertently hitting objects where the benthos is non-uniform. Indeed, in areas of undulating benthos, a low survey height will also create shadows of unsurveyed areas in the ARIS footage behind prominent objects. The ARIS is also sensitive to unwanted motion in yaw and speed, which can create artifacts in the video footage. However, using the mid-range width as the swathe metric gives a degree of ‘buffer’ to account for instability in the video footage, and the extra width at the far-range of the survey area may help identify motile organisms that only come partially into view of the main swath. Taking these points into consideration, it seems the optimal survey height and pitch will likely be ~1.5 m and ~10°, respectively.

Our trials provide promising evidence of the applicability of acoustic cameras as a survey tool for Maugean skate in Macquarie Harbour. Area coverage and species identification using ARIS were comparable to those seen elsewhere with methods that use standard optical cameras for benthic surveys in normal light environments (Thorngren et al., 2017). Accordingly, it is reasonable to assume that the cost of implementing and executing a monitoring program using acoustic video will be comparable to traditional towed video methods (excluding the cost of the device itself), which are commonly considered as a low-cost tool. Furthermore, transect based towed-video survey design is well understood, and the same principles will be directly applicable for building a robust population monitoring program for Maugean skate using acoustic video. Additionally, the novel use of this type of imaging

technology presents an important advancement for the monitoring of cryptic and endangered marine fauna in low visibility environments previously considered hard to survey.

2.5 Conclusion and recommendations

The work presented here demonstrates that acoustic cameras provide a reliable tool to collect high frequency, high-resolution, high-quality data in Macquarie Harbour. ARIS shows promise for static and dynamic deployments, and the data presented here shows how deployment configurations may be altered to optimize data collection and maximize area of sonication depending on survey design and specific research aims. Indeed, as a possible tool to help investigate trends in relative abundance and demographic dynamics of Maugean skate, the acoustic camera would be less disruptive to animals and less prone to underrepresenting smaller individuals than current methods. However, there are some important factors to consider when deciding a survey design, particularly if one of the main aims is to generate accurate population estimates:

a) Any ARIS-based survey design for Maugean skate will require further analysis investigating statistical power and acceptable detectability of change to determine a robust sampling design that fits within the logistical and financial constraints of the program. Maugean skate are not randomly distributed throughout the harbour, so stratified sampling designs among depths or habitat types should be considered (Murphy & Jenkins, 2010). Given the urgent need for updated and ongoing data on the population, we recommend that this work be prioritised.

b) Increased travel speed resulted in increased noise and a decrease in overall image quality. This means that speed will limit area coverage and therefore strongly influence total effort, time and ultimately cost for any given sampling design. It is possible that deployment optimizations and post processing of the data can be used to increase the operating speed of the device. It should be noted that there is some evidence that slow, narrow transects can be beneficial when sampling cryptic fish (Paris & Cabral 2018), so there may be other factors that influence upper deployment speed

c) Using ARIS individual identification is not possible once an individual leaves the frame. Given the increased chance for double counting individuals that exit and re-enter the frame, analysis will have to account for autocorrelation to avoid inflating the probability of type one error. This may be accomplished by incorporating time as a random autoregressive effect in the model and using zero inflated models that can account for overdispersion; or by using methods that can detect trends in data with autocorrelated structures such as time series forecasting (Shahrestani et al., 2017).

d) Prior to implementing ARIS based surveys as a method for population monitoring of Maugean skate it will be necessary to ground truth the technique against concurrent net surveys. Furthermore, net surveys provide access to individuals for sample collection and biological examination (e.g. genetics, reproductive

assessment, health monitoring, etc). Therefore, it is likely that some form of netting will still be needed in the future to inform a more holistic monitoring program.

e) ARIS surveys may be enhanced by complementary use of other survey techniques or technologies resulting in a multi-method design. For example, surveys could be combined with molecular metabarcoding to explore broader community level changes, environmental sensors can be added to the payload to explore environmental drivers of occurrence, and it may be possible to utilize coded active acoustic transmitters that can be 'seen' by the acoustic camera to tag individuals and help understand re-encounter rates.

f) Different ARIS deployment configurations may be used to collect valuable information beyond the primary function of population monitoring. For example, while active deployment options may be ideal for exploring demographic trends, static deployments can be used to investigate key habitats or collect behavioural observations.

g) In our tests, images collected with ARIS had high enough resolution to allow for species identification, measurement and even sex determination (in skate based on claspers). Reliable species identification in acoustic camera images is not always possible in complex habitats. However, this application appears to be optimally suited for use of acoustic video, as Macquarie Harbour has a largely featureless silty bottom and is naturally depauperate. In fact, the Maugean skate is one of only two species of skate that exist in the harbour, the other being the thornback skate which is morphologically distinct, given it has a very short rostrum compared with the Maugean skate's very elongate and triangular rostrum. Therefore, the chances of taxonomic misidentification are very low.

h) While the standard data output of ARIS yielded good results, there are several actions that should be considered to improve analysis: 1) data collection should maximize frames per second (fps) of capture as this has been shown to significantly improve target identification (Shen et al., 2024). 2) construction of a reference library and observer training dataset. 3) developing a post-processing image enhancement pipeline for contrast enhancement, crosstalk reduction and movement correction. ARISFish software and third party solutions like Echo view may be suitable for post processing, although it should be noted that these tools are not designed to deal with platform movement, so some development may be needed 4) While machine learning applications to automate sonar data analysis can be complex, ARIS data can be analysed as video, which should allow leveraging of cheap and accessible tools for machine learning. These tools may be useful to enhance data quality, automate analysis tasks and may even allow for more in-depth analysis (e.g. 3D reconstructions using structure from motion photogrammetry)

i) High resolution, high fps image collection will produce vast amounts of data. Therefore, it is important that any project design account for data storage, management and processing infrastructure

3. Population genetics and demographic history of the Maugean skate in Macquarie Harbour

Tzu Nin Kwan, David Moreno & Jayson M. Semmens

3.1 Introduction

There is an overarching and urgent need to conserve and restore the Maugean skate population. A previous population genetic study of the extant population in Macquarie Harbour has already indicated low genetic diversity typical of a population under a genetic bottleneck (Weltz et al., 2018). However, there is no fine-scale population genetic structuring data to indicate how distinct the remaining population is or if there is adequate genetic diversity to adapt to various environmental changes and/or population decreases, whether natural or human driven. Except for a mitogenome sequence of a Macquarie Harbour specimen, there is no genomic resource available for *Zearaja maugeana*. Furthermore, no nuclear genome of any member of the genus *Zearaja* is sequenced. Therefore, the specific goals of this project were to:

1) Establish a reference genome to serve as a template for population genetic studies and to assess the genomic health (e.g., mutational load and homozygosity runs, etc.).
2) Evaluate the genetic diversity in the Macquarie Harbour population and possibly in the archival Bathurst Harbour samples, which are preserved in formalin, to identify differentiated lineages and adaptive alleles.
3) Inform management strategies to maintain genetic diversity and assess the suitability of subpopulations for restoration and conservation outcomes.

We envision that at the very least, the outcomes of this project will fill the following urgent needs:

- Providing a tool for investigating the evolutionary potential of the Maugean skate to adapt to low population sizes and changing environmental conditions in Macquarie Harbour
- Informing adaptive management strategies, such as captive breeding and translocations of lineages from one geographical region to another, and
- Providing an understanding of how much genetic diversity there is in the Maugean skate population that can be used to assist in the interpretation of the outcomes of genetic-based abundance estimation tools, e.g., close-kin mark-recapture.

3.2 Methods

3.2.1 Reference Genome

Samples

Maugean skate tissue samples were collected non-lethally from a sexually matured female Maugean skate (ID: DMS19) captured in the process of regular population monitoring in Long Bay, Macquarie Harbor in 2021 (Moreno & Semmens 2023). Blood was chosen for genomic DNA (gDNA) extraction as Chondrichthyes' blood is nucleated, making it a relatively simpler material to extract high quantity and intact DNA from. Red blood cells and plasma were separated by spinning 0.2 ml of whole blood at 13000 rpm for four minutes. The samples were then transferred into separate cryovials, and flash frozen in liquid nitrogen.

DNA extraction and sequencing

The blood pellet was washed twice in 1 x Phosphate Buffered Saline (PBS) before extraction. Genomic DNA was extracted following the 2 x CTAB/PCI method (2 % Cetyltrimethyl Ammonium Bromide-Phenol-Chloroform-Isoamyl Alcohol) (as per Porebski et al., 1997). Intactness of the extracted DNA was confirmed using 0.3% agarose gel electrophoresis, purity as checked using NanoDrop, and the total yield quantified using a Qubit broad range assay kit. Genomic DNA was suspended in low Tris-EDTA (TE) buffer (10mM Tris pH8, 0.1mM EDTA).

Genomic DNA was couriered overnight at ambient temperature to the Australian Genome Research Facility, Brisbane (AGRF) for sequencing using PacBio SMRT Revio. Sequencing libraries were constructed using SMRTbell's express template Prep Kit 2.0 (Pacific Biosciences, Menlo Park, CA, USA).

Assembly and scaffolding

Repeated PacBio Hifi sequencing read datasets were combined and used for assembly. GenomeScope 2.0 used k-mer count distribution from Jellyfish v2.2.6 to fit a model that allows for assembly-independent estimation of genome size, heterozygosity and repeat content and ploidy. This information was used in HiFiasm (Cheng et al., 2021) to de-novo assemble the genome using purging settings for homozygous genome. The assembly was then scaffolded into 50 pseudo-chromosomes based on species specific high-throughput chromatin conformation capture (Hi-C) sequencing data (Kwan, Moreno & Semmens *in prep*) using RagTag v2.1.0 (Alonge et al., 2021). Completeness of assembly was assessed using reference independent Merqury (Rhie, 2020) as well as reference-based Benchmarking Universal Single-Copy Orthologs (BUSCO, Waterhouse et al., 2015, BUSCO v 5.4.6, vertebrate_odb10 database, n=3345).

MitoHifi (Uliano-Silva et al., 2023) and MitoFish (Zhu et al., 2023) were used to assemble, annotate and visualise the mitochondrial genome.

Genome annotation

In the absence of fresh tissues to generate RNA transcripts and proteins information necessary for annotation, this study referenced the published transcriptome of the little skate (*L. erinacea*) (GEO; GSE188980 and GSE190730) (Marlétaz et al., 2023). The assembled Maugean skate genome was masked to improve accuracy and efficiency of downstream annotating works. RepeatMasker 4.1.0 (Smit et al., 2013-2015) used known zebrafish repeats and RepeatModeler 2.0.1 (Smit and Hubley, 2008-2015) identified previously unknown repeats in the Maugean skate genome. The masked genome was then mapped with RNA-seq reads of little skate encompassing five bulk embryonic stages and thirteen organs using HISAT2 v2.2.1 (Kim et al., 2019). All sequences of protein-coding genes (n=18,970) predicted from the little skate genome were also mapped using Genome Threader (Gremme at al., 2005). These hint files were used, together with AUGUSTUS species parameter specific to little skate (Marlétaz et al., 2023) to predict genes ab initio in AUGUSTUS (Stanke et al., 2008) and BRAKER2 (Hoff et al., 2015). The resulting annotation was assessed again using BUSCO and the functional of proteins determined using DIAMOND (Buchfink et al., 2015).

Given the lack of available species-specific tissues, this annotation should be considered preliminary and was not used in any subsequent analysis. However, we have chosen to present it here given the urgent need to inform conservation genetics work in this endangered species. Recently, fresh tissue samples of various organs were sampled opportunistically from Maugean skate during the establishment of an ex-situ conservation program (University of Tasmania animal ethics committee (AEC) project A29717). Transcriptome sequencing work for these samples is currently ongoing and once ready, an updated annotation will be presented.

Variant calling, genome-wide heterozygosity and homozygosity

The PacBio HiFi reads were mapped back to the genome assemblies using minimap2 (map-hifi option). Variants were called using GATK version 4 (McKenna et al., 2010) HaplotypeCaller and GenotypeGVCFS with –include-non-variant sites. All variants and invariants were filtered using 0.66 x average depth of coverage (DP) and or 1.5 times greater than the DP. These would have removed hemizygous (0.5x coverage) or duplicated (2x coverage) regions. Filtering using Quality by Depth (QD) < 10 was applied to remove low confidence (i.e QUAL/coverage) and potentially spurious variant. This study calculated heterozygous SNPs in non-overlapping 1 Mb window across all assemblies (>1 Mb) using BEDTools.

Runs of homozygosity (RoH) are genomic regions where identical haplotypes are inherited from each parent. RoH can be provide a useful indication of an individual's demographic past. Longer RoH result from recent inbreeding events, while shorter ones reflect events in the distant past (Silva et al., 2024). RoH calculations can vary depending on the analysis method and parameters used. To account for this, a multi-method approach was used (Silva

et al., 2024), where we analysed the genome using three distinct RoH detection tools a fixed window approach (Dodge et al., 2023), PLINK (Stanhope et al., 2023), and bcftools (Narasimhan et al., 2016).

A fixed window approach to RoH calling was used which targets heterozygous SNPs as detailed in Dodge et al. (2023). Briefly, INDELS were not considered because of possibility of sequencing error (Nurk et al., 2020) which can spuriously inflate heterozygous sites. Heterozygous SNPs were counted in non-overlapping windows containing 10,000 called sites (BEDtools). Run of homozygosity were called by identifying stretches of ≥ 100 consecutive windows, each with fewer than one SNPs per window. Adjacent RoHs were joined if they were separated by a single window, even if this window had > 1 SNPs. For comparison, the GATK variant files were also called for RoH using –homozyg function in PLINK v1.90b6.26 that uses sliding window approach targeting primarily successive homozygous SNPs. The default parameters were used to allow comparison with other elasmobranch genomic studies (e.g. Stanhope et al., 2023). The RoH length parameter –homozyg-kb 1000 was reduced until RoH was detected. The third approach used bcftools RoH Genotypes to call RoH using variants using FreeBayes (min. mapping quality 30; min base quality 20). RoHs were called using non-window Hidden Markov model (HMM) approach to detect autozygosity implemented in bcftools RoH using default settings specifically -GTs-only 30, --AF-dflt 0.4, default HMM options -- *hw-to-az and -- az-to-hw 6.7 x* 10^{-8} *and 5 x* 10^{-9}*,* respectively and without Viterbi training (Narasimhan et al., 2016).

For all three methods, RoH were classified based on length into bins of >0.1, >0.5, >1, >2, >3 and >4 Mbp (when found) to facilitate comparison with inbreeding indices in other studies, where 1Mb is a commonly used threshold considered for signature of recent inbreeding. The proportion of the genome in RoH of respective RoH length class was calculated based on the number of assemblies that were ≥ the RoH length considered.

3.2.2 Genomic population structure

Sample Collection

Tissue samples (fin clips and blood) were collected from Maugean skate in fisheries independent surveys as part of the current monitoring program (2021- ongoing) (as per Moreno & Semmens 2023). Samples were either flash frozen in liquid nitrogen or preserved in a tissue sampling unit (TSU, Allflex), which directly seals a small biopsy punch into a tube containing a proprietary conservation buffer. Tissue from 87 Maugean skate individuals was collected from 2021 to 2023. Additional, blood from four of those individuals was also included as an internal control. This work was approved by the University of Tasmania AEC (Project A23857).

Archival tissue samples (fin clips) were available for 191 individual Maugean skate collected between 2011 and 2015 (Weltz, et al., 2018). Many samples in this collection showed signs

of degradation. Of these 18 samples failed QAQC and were removed from subsequent analysis.

Genomic DNA extraction

As per the recommendation of Diversity Arrays Technology (DArT, Canberra, Australia), 282 samples comprising of 253 fin clip tissues and 29 blood samples were gDNA extracted using DNeasy Blood and Tissue kits and eluted in low TE buffer (10mM Tris pH8, 0,1mM EDTA). Genomic DNA was sent to DArT, restriction enzyme digested using PstI-SphI, and sequenced on NovaseqX system, producing 7.5 million reads per library. The reads were processed for sequencing, genome complexity reduction and SNP calling using DArT proprietary pipeline and the resultant SNPs were mapped using reference genome of blonde ray (*Raja brachyura*, GCA_963514005.1).

Filtering

The R package 'dartR' v2.7.1 (Gruber et al., 2018) was used to process and analyse DArTseq SNP data. The data was checked for accidental replicates (e.g. recapture of lost tag individual, accidental duplication during lab processing) using the replicate function. SNPs were filtered to remove monomorphic loci, and to retain loci of repeatability >95%, individual and loci call rates of >60% and 80% respectively. Default read depth (i.e. lower = 5, upper = 50), and minor allele frequency (minor allele count MAC = 2) filtering were applied. Loci that are sex linked, as well as those that reside within a fragment (secondaries) or those with too similar trimmed sequence tags were removed (threshold=0.2, rs=5, tag length=69). Loci that are in linkage disequilibrium (LD) were filtered out at threshold = 0.2. This resulted in 4,667 SNPs and 162 individuals. Mapping of these filtered SNPs onto the reference genome of *Raja brachyura* demonstrated uniform scattering across the 48 chromosomes thus ensuring genomic representation (Appendix B, Fig 4_6).Of the individuals removed during the filtering stage 83 belonged to the archival collection (2012-2014) and 19 to the recent population monitoring program (2020-2023).

Genetic diversity, population structure and relatedness

To investigate spatial and temporal fine-scale population structure of Maugean skate within Macquarie Harbour, filtered samples were grouped by capture location and collection date. Overall and group specific population diversity was calculated (F_{st}) and pairwise group differences were estimated using the method outlined by Weir and Cockerham (1984) with 99% confidence intervals estimated through bootstrapping 1000 times. Population differences were visualized through principal coordinate analysis (PCoA) and phylogenetic trees using neighbour-joining. This was confirmed by discriminant analysis of principal components (DAPC) to identify optimal clustering based on genetic differentiation between groups while accounting for within group variation (Jombart et al., 2010). Model fit was assessed using Bayesian Information Criterion (BIC).

Population and group specific coefficients were estimated using the dartR package (i.e. inbreeding coefficients (F_{IS}, F_H, and F_{iii}), observed (H_O) and expected heterozygosity (H_E)). To account for missing data, individual-level standardised heterozygosity (H_S) was calculated using the genhet package (Coulon, 2010). Individual inbreeding coefficients (F_H, and F_{iii}) were calculated using the functions –ibc and –het implemented in PLINK. F_H emphasizes observed versus expected homozygosity (Keller et al., 2011) whereas F_{III} is focused on identifying excess homozygosity by assessing correlation of uniting gametes (Yang et al., 2011). Individuals less inbred than population average will have negative F values, and vice versa (Yang et al., 2011). Mean and SE values for the population were calculated for both indices based on the individual values.

A multi-method approach was used to investigate relatedness and identify sibships within and between the two sampling cohorts. As a first step, the gl.grm function (implemented in R using the function A.mat from package rrBLUP, Endelman and Jannink, 2012) was used, which quantifies the Identity-by-State (IBS) relatedness based on observed alleles regardless of their ancestry. From the relatedness score, kinship then can be determined by considering the probability that an individual pair inherit a particular allele from a common ancestor (Wang, 2022). This study follows kinship values and their 95% confidence interval (CI), and relatedness threshold as specified in Speed and Balding (2015, see Appendix B).

Multiple algorithms exist that are commonly used to estimate relatedness based on genomic coancestry. The program COANCESTRY was used to implement 4 algorithms (TrioML, WNag, LynchRt and DyadML) to estimate pairwise relatedness across the population (Wang, 2011). Finaly, sibship and parentage inference were refined using the COLONY software. Unlike the approaches mentioned above, this program infers parentage and sibships jointly with likelihood over the entre genomic pedigree configuration rather than of pairs of individuals, providing a more robust approach (Jones and Wang, 2010). The analysis assumed the potential for inbreeding (based on the small, inferred population size and recent declines), polygamous female and male mating (based on field observations -Awruch et al., 2021-, and preliminary genomic analysis of captive individuals -Moreno, pers comm-), and dioecious reproduction.

Demographic history

Effective population size (N_e) is the hypothetical number of breeding individuals that would result in the inbreeding load and gene frequency variance observed in a population under idealised Wright-Fisher conditions (i.e. a baseline population with discrete generations and no overlapping cohorts which observes random mating and has no genetic pressure due to selection, mutation and migration (Wange et al., 2016). This study utilised both PacBio HiFi sequencing reads of a single Maugean skate genome as well as the population SNPs to reconstruct the species recent and distant demographic history.

The filtered 4667 SNPs were analysed for recent historical effective population size using two methods: Estimating Population sizes EPOS (Lynch et al., 2020) and GONE (NOVO et

al., 2023). However, implementation of GONE was unsuccessful, as it requires higher SNPs density (in the range of tens of thousands per chromosome), than was available in the reduced representation DArT SNPs for this study. The EPOS bases its analysis on site frequency spectrum (SFS) that describes the distribution of allele frequencies at heterozygous SNPs capturing present and historical mutation and democracy events such as decline or expansion. Analysis assumed that L= $2.6x10^{8}$ as the total sequence sampled in Maugean skate, mutation rate 2.5 $x10^{-9}$ (see below), and used 10,000 bootstraps to generate confidence interval.

To explore more distant demographic history of the species, the filtered GATK variants files from the single individual were analysed using Pairwise sequential Markovian coalescent (PSMC, Li & Durbin et al., 2011). The program seqtk was used to phase haplotype assemblies to produce diploid consensus genome. PSMC was run with 25 iterations with the default time segment parameters N25 -t15 -r5 -p "4+25*2+4+6" (as also used in other elasmobranch species (Sanhope et al., 2023)). A total of 100 bootstrap replicates were performed to evaluate variance in N_e estimates. PSMC plots were rescaled based on the generation time of g = 6 years for Maugean skate (Awruch et al., 2021). Mutation rates could not be empirically derived, so values of $\mu = 2.5 \times 10^{-9}$ and $\mu = 2.5 \times 10^{-10}$ per site per generation were used based on estimates in other elasmobranch species (Sendell- Price et al., 2023, Stanhope et al., 2023).

3.2.3 Initial genetic investigation of preserved specimens from Bathurst Harbour

The earliest known record of Maugean skate in Bathurst Harbour is from 1988. After this, five other individuals (including an egg with a developing embryo) were recorded from 1988 to 1992. Despite various dedicated surveys in the intervening years, there have been no subsequent records of the species in the area, and so, investigating the genetic structure of this population and how it may differ from Macquarie Harbour has not been possible so far (Moreno et al., 2022). Four of the original five specimens were collected from Bathurst Harbour, preserved (formalin fixed), and are currently held in the Australian Museum collection (ID I.40748-001) and the Australian National Fish Collection (IDs GT15307_H1987_01, GT15308_H5544_01 and GT16538_H3576_01). A muscle biopsy was collected from each of the specimens for genetic analysis.

Long-term storage in formalin compromises DNA and results in low-quality fragmented DNA, precluding the use of various genomic technologies. Therefore, this study focused on detecting nucleotide variation on the mitochondrial genome (mito-genome). This is because the mito-genome is present in multiple copies therefore improving the ability to reconstruct sequence compared with nuclear sequence. Noting that mitochondrial DNA has a much slower mutation rate than nuclear DNA and so differences can be difficult to detect.

Extraction required a specialized protocol to account for DNA degradation in the formalin fixed sample that used QiAamp FFPE kit and library construction using the IDT xGen cfDNA and FFPE Library. Sequencing was completed by AGRF using 150 PE Illumina NovaSeq.

The Illumina reads were trimmed for adapters and poor reads using Trimmomatic (Bolger et al., 2014), quality checked using FastQC iteratively. The reads were aligned, and variant sequence called using NOVOPlasty (Dierckxsens et al., 2017-2020). The results were also compared with manual alignment using Burrow-Wheeler Aligner (BWA, Li and Durbin, 2019) against a reference mito-genome of a Macquarie Harbour specimen constructed in this study (i.e individual DMS19), and the alignment and variants inspected on IGV 2.17.4. The detected variant sequences were confirmed by aligning against raw PacBio Hifi reads of individual DMS19. A minor allele frequency (MAF) of 0.05 was applied.

3.3 Results

3.3.1 Genome assembly, annotation and patterns of genome-wide heterozygosity

The Maugean skate genome assembly represented the first sequenced genome to date for this micro endemic and threatened species. The genome size was 2.57 Gbp based on

Table 3-1 De-novo assembly metrics of PacBio Hifi reads using Hifiasm assembler.

Continuity	Total contigs	6,769
	Max contig	12 Mbp
	Contig NG50	1 Mbp
	Gaps	0.00%
	Cumulative length	3 Gbp
Base accuracy	Base pair QV (Q)	57.7
	k-mer completeness	97.80%
	False duplication	0.00
Haplotype phasing		Primary assembly
Functional completeness	BUSCO genes (v 5.4.6)	90.50%
	Transcript mapability	97%

Table 3-2 Annotation completeness of genome using BUSCO v 5.5.0 in protein mode against vertebrata_odb10 database.

Predicted genes	34,559
BUSCO completeness	88.00%
BUSCO fragmented	6.60%
BUSCO Missing	5.40%

GenomeScope, a k-mer approach that is assembly and reference genome independent (Fig. 3-1 left). This was concordant with 2.48 Gbp worth of contigs scaffolded using the 2.2 Gbp reference genome of little skate (Fig. 3-1 right). The de-novo assembled contigs achieved BUSCO v 5.4.6 completeness of 90.50% (see Appendix B for QUAST assembly metrics) and scaffolding did not improve this. Assembly metrics exceeded those outlined by the Vertebrate Genome Project for quality of a reference genome (Rhie et al., 2021). A total of 34,559 genes (with BUSCO v5.5.0 completeness 88%) were predicted and annotated on the assembly. The gene content for this assembly was thus relatively complete in the absence of species-specific transcripts.

Based on GenomeScope, the skate genome had a gross estimated level of heterozygosity of 0.6% consistent with the near unimodal distribution. Calling and filtering of variants using GATK provided a slightly lower estimate of 3.8 million heterozygous sites ranging between 0-7.5 sites per kb per Mb window. Mean heterozygosity per kb was 0.353 (SD=0.5) based on 1435 1 Mb windows (Fig.3.2).

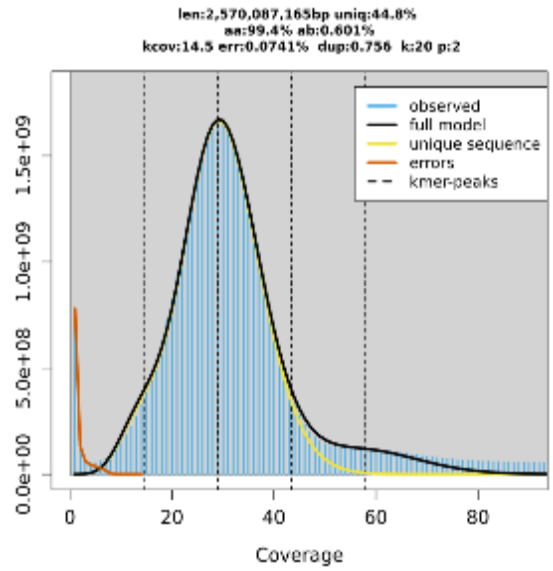

Genome size (Gbp)	2.57
Pseudo-chromosome scaffolds	50
Total contigs	6769
Placed contig (Gbp)	2.48
Placed sequences	3181
Unplaced contig	3615
Unplaced base pairs (Gbp)	0.48
Gap length (Mbp)	0.3
Functional Completeness (BUSCO v 5.4.6)	90.50%

Figure 3-1 (Left) GenomeScope plot showing k-mer spectrum and fitted model for Maugean skate. Note that diploid plot has two peaks at 14 x and 28 x coverage indicating a diploid genome. (Right) Scaffolding of *de-novo* contigs to 50 pseudo-chromosomes using RagTag against the reference genome of little skate (*Leucoraja erinacea*, RefSeq GCF_028641065.1)

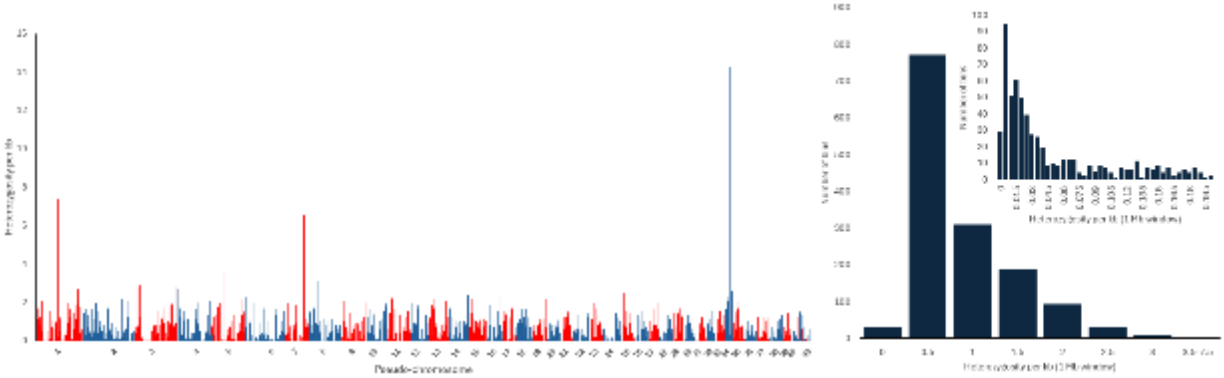

Figure 3-2 (left) Genome heterozygosity per kb of a Maugean skate (DM19) plotted for each scaffold (pseudo-chromosomes) at non overlapping 1Mb windows. (right) Size frequency histograms of per window heterozygosity.

The assembled mitochondrial genome of 16,968 bp in size. The mito-genome has the expected 37 genes, comprised of 13 protein-coding genes, 2 rRNAs and 22 tRNAs (see Fig. 3.3).

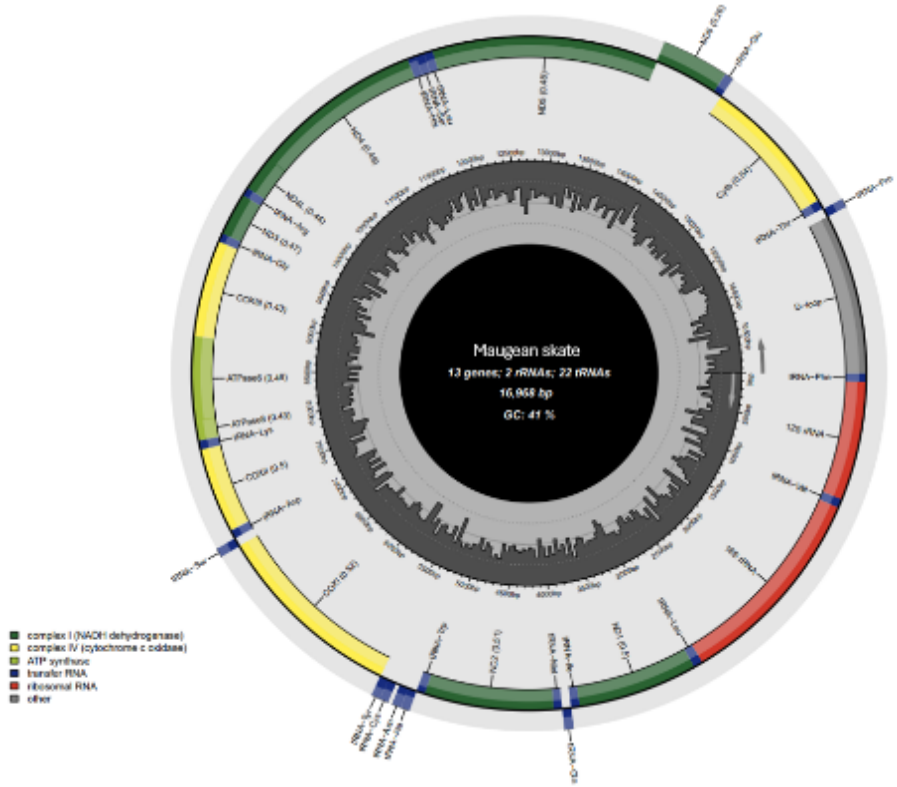

Figure 3-3 CIRCOS map of a complete and annotated mitochondrial genome of a Maugean skate sampled from Long Bay, Macquarie Harbour in 2021. Inner circle histogram represents GC content.

3.3.2 Run of homozygosity

This study used 3 methods to call RoH in the skate genome because different algorithm and parameters can affect RoH discovery. All three methods produced consistent results, indicating low F_{ROH} estimates and failing to detect long RoHs.

Firstly, the fixed window method described in Dodge et al., (2023) was applied using stringent criteria, where no heterozygous SNPs per 10 kbp window were allowed. There were 54 $RoH_{>1\ Mbp}$ (equivalent of 0.07 Gbp), covering 1.8 Gbp of genome ($F_{RoH>1Mbp}$ = 3.7%).

Secondly, the same variants were called for RoH using the function –homozgy in PLINK, which employs a sliding window to target contiguity of homozygous SNPs. No $RoH_{>1\ Mbp}$ were detected despite 1) relaxing the sliding window constraint (---homozyg-window-snp-100 (default 50, increasing SNPs number in each sliding window), --homozyg-window-missing 10 (default 5, allowing more missing genotypes in each window), –homozyg-window-het

2(default 1, allowing more heterozygous SNP in each window)), 2) reducing stringency on SNP density (homozyg-density 10 (default 50, allowing fewer SNPs per kb), 3) increasing gaps between SNPs (--homozyg-gap 5000 (default 1000 kbp, allow bigger gaps between homozygous SNPs)), and 4) reducing minimum SNPs in a RoH (–homozyg-snp 10 (default 50, require few SNPs for a Roh)). Rather, the minimum RoH length had to be reduced from default 1000 to 100 kbp for RoH to be detected (Table 3.3). A total of 29 $RoH_{>0.1\ Mbp}$ were found, giving an estimated $F_{RoH>0.1Mbp}$ = 1.3%.

Thirdly, a non-window hidden Markov model (HMM) approach implemented in bcftools was used. As with PLINK, this method detected no $RoH_{>1\ Mbp}$. The maximum RoH was no larger than 0.3 Mbp and $F_{RoH>0.1Mbp}$ was comparably low at 0.4% (see Appendix B details on the distribution of $RoH_{>0.1\ Mbp}$ across the genome).

Table 3-3 Genome runs of homozygosity (RoH) calculated using 3 different methods. RoH are classified into size classes (Mbp). Details on the distribution of RoH can be found in Appendix B

	Fixed window (Dodge et al., 2023)				PLINK --homozyg				bcftools RoH			
RoH (Mbp)	N	RoH length (bp)	Contig > RoH	RoH (%)	N	RoH length (bp)	Contig > RoH	RoH (%)	N	RoH length (bp)	Contig > RoH	RoH (%)
>0.1	67	7.55E+07	2.82E+09	2.67	29	3.68E+06	2.82E+09	1.30	87	1.17E+07	2.82E+09	0.42
>0.5	59	7.38E+07	2.30E+09	3.21	3	7.54E+05	2.66E+09	0.28	8	1.88E+06	2.66E+09	0.07
>1	54	6.94E+07	1.85E+09	3.76	0	0.00E+00	2.52E+09	0	0	0	2.52E+09	0
>2	3	6.98E+06	1.17E+09	0.60								

3.3.3 Population structure and diversity

Based on the 4,667 DArTseq SNPs of 162 individuals organised into 3 broad sampling locations in Macquarie Harbour, observed heterozygosity (H_O) and expected heterozygosity (H_E, i.e. heterozygosity under Hardy-Weinberg equilibrium) ranged from 0.272 to 0.286, and 0.286 to 0.291 respectively. As expected, based on the ratio of H_o:H_e, group-level inbreeding coefficients (F_{IS}) were low (0.027 to 0.092). Standardised heterozygosity (H_S) and individual

Table 3-4 Estimated observed heterozygosity (H_O), expected heterozygosity (H_E), standardised heterozygosity (H_s), population inbreeding coefficient (F_{IS}) and individual inbreeding coefficient (F_H) with its respective standard error (SE) and 95% confidence intervals (CI) for each location as well as all combined locations as a single population of Macquarie Harbour

Location	N	H_o (±SE)	H_E (±SE)	H_s (±SE)	F_{IS} (95% CI)	F_H (95% CI)
Lower basin	50	0.273 (0.002)	0.289 (0.002)	0.986 (0.017)	0.092 (-0.093-0.021)	0.062 (0.030-0.093)
Table Head /Liberty Point	87	0.272 (0.002)	0.291 (0.002)	0.995 (0.008)	0.087 (0.107-0.174)	0.067 (0.048-0.086)
World Heritage area	25	0.286 (0.002)	0.286 (0.002)	1.023 (0.022)	0.027(-0.068-0.059)	0.017 (-0.029-.0650)
Macquarie Harbour	162	0.27 (0.002)	0.291 (0.002)	0.997 (0.008)	0.089 (-0.014-0.005)	0.058 (0.043–0.074)

breeding coefficient (F_H) ranged from 0.986 to 1.023 and 0.017 to 0.067 respectively (Table 3-4).

Pairwise F_{st} (fixation index) showed that genetic differentiation of individuals between sampling locations was very low at less than 0.01 and not statistically distinct (Table 3.5) (Values below 0.05 indicates little to no genetic differentiation, whilst F_{ST} above 0.25 to 1 indicates increasingly higher differentiation). Therefore, pooling all 162 individuals as one harbour population (Table 3.4) yielded H_O = 0.276 (± SE=0.002), H_E = 0.291 (± SE=0.002), Hs = 0.997 (± SE = 0.008), F_{IS} = 0.089 (with 95% CI encompassing zero) and F_H = 0.058 (95% CI = 0.043-0.074).

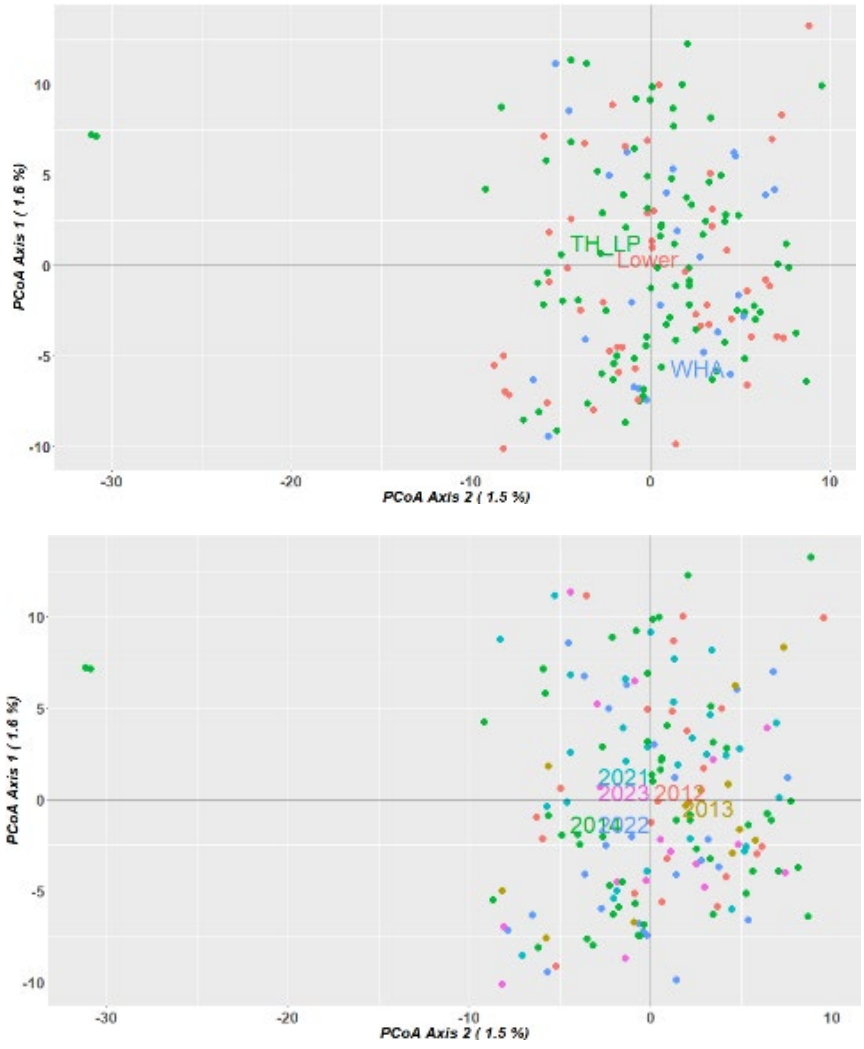

Figure 3-4 Principal coordinate analysis of individual Maugean skate SNP genotypes identified based on sampling a) location and b) year of sampling.

Table 3-5 Pairwise estimate of genetic differentiation (Fst) between sampling locations using filtered SNPs (top)

	WHA	TH	LB
World Heritage area (WHA)	-	-	-
Table Head – Liberty point (TH)	0.000177		
Lower Basin (LB)	0.000237	0.0000997	-

All p values > 0.5

The lack of genetic differentiation across all samples was evident in principal coordinate analysis (PCoA). The first two principal components explained very little (2.5%) of the variance in the dataset and did not result in any significant clustering (Fig. 3.4). Homogenous mixing of individuals was evident regardless of sampling location and year (Fig. 3.3a and 3.3b). Further phylogenetic analysis and discriminant analysis of principal components (DACP) confirmed no evidence of fine scale structure within the population (see Appendix B).

3.3.4 Relatedness and inbreeding coefficients

Despite the low genome-wide heterozygosity, the absence of long RoH (specifically $F_{RoH>1\ Mbp}$) on the reference genome low inbreeding loads for that individual (DMS19 sampled in 2021). To provide insight into population-wide patterns, SNP data was used to determine relatedness and inbreeding extent for all 162 individuals.

Estimates of relatedness derived using multiple methods in COANCESTRY were used to estimate individual inbreeding coefficients across the two sampling cohorts. The resulting values were consistently low (<0.1) across all methods (Appendix B). To account for potential biases introduced by inbreeding in a small population, two further methods were implemented using PLINK (F_H and F_{III}), which are specifically designed to detect excess homozygosity due to inbreeding. Population averages were consistent with previous analysis indicating similar and low inbreeding loads for both cohorts (Fig 3.7 (Top)). Notably, unlike the other methods, F_{III} found a small number of individuals (n=16) with coefficients above 0.3 (Fig 3.6).

To validate the relationship between genome wide ROH and SNP based inbreeding coefficients, SNP data from DMS19 was analysed. F_H and F_{III} were calculated as 0.02 and 0.06 respectively. This was comparable with results from COANCESTRY, where all methods resulted in estimates below 0.03 (across Ritland, LynchRd, TrioML and DyadML estimator). This suggests that SNP data accurately represent genome wide inbreeding loads. Furthermore, the overall consistency between methods increases our confidence in the results and suggests that Maugean skate exhibit low inbreeding loads across the population.

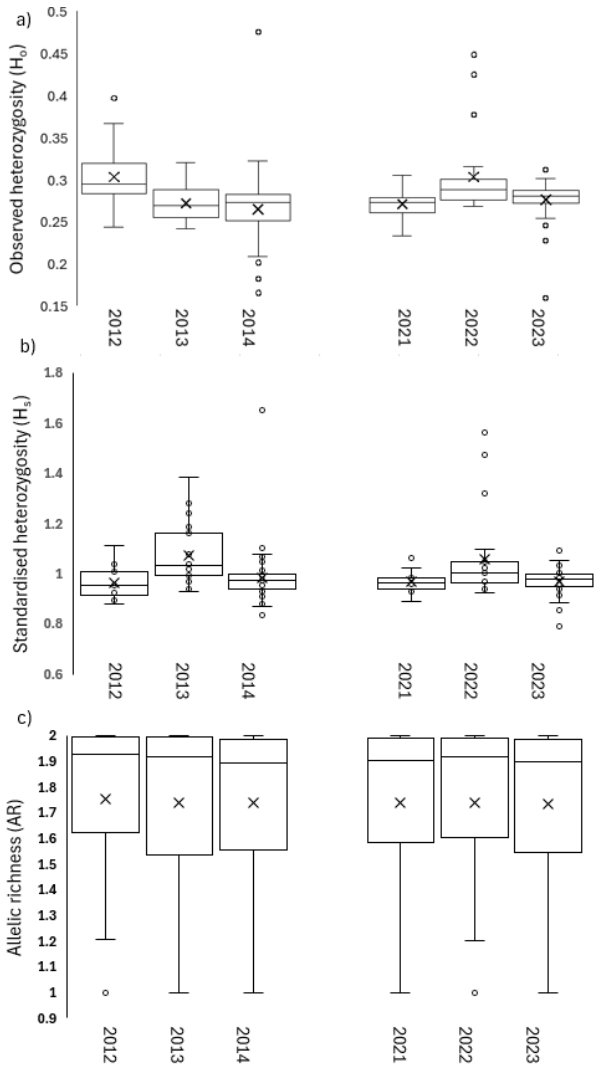

Figure 3-5 Genomic diversity of Maugean skates presented as boxplot of a) individual heterozygosity (H_o) for the 162 individuals, standardised heterozygosity (H_S) and c) allelic richness (AR) for the 4,667 loci across each of the 6 years (Note, year groups are based on time of sampling, not individual age, so they contain various overlapping generations).

Relatedness analyses using a comprehensive range of estimators (COANCESTRY) did not detect many closely related individuals in the sampled population. Sibship analyses were conducted using COLONY. Two full sibling pairs were detected in the 2012/2014 cohort, but none in the 2021-2023 cohort. Further, 6 and 5 half-sibling pairs were detected respectively in each cohort (Fig 3.6). The number of sibships detected by COLONY matched the number of clusters based on relatedness in COANCESTRY (Appendix B).

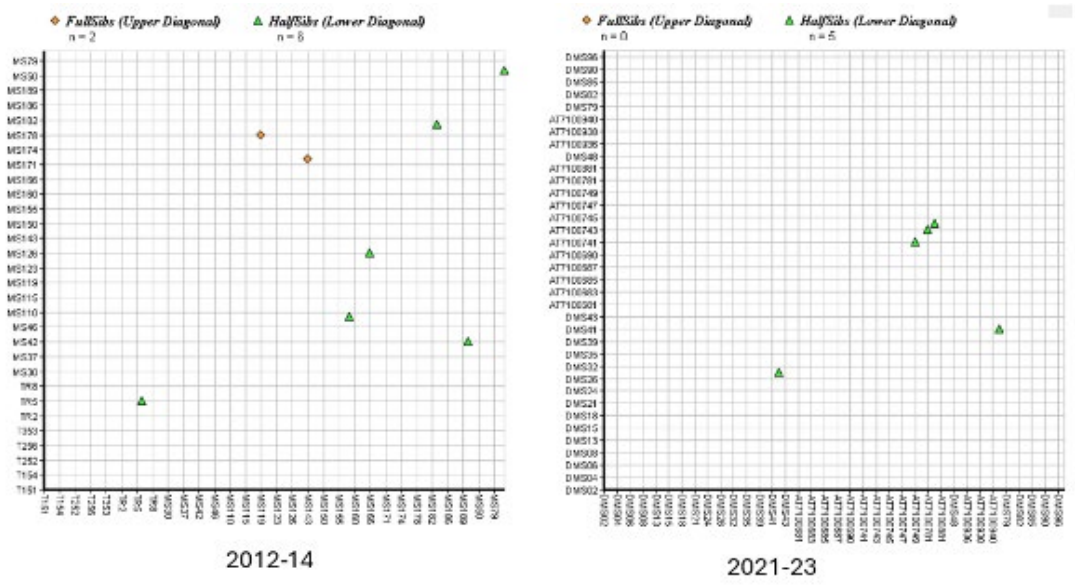

Figure 3-7 Full and half sibling assignment of 162 Maugean skates organised into 2012-2014 and 2021-2023 cohort using COLONY.

Cohort	F_{IS}	F_H	F_{III}
2012-2014	-0.00961 (0.003)	0.0724 (0.0117)	0.130 (0.032)
2021-2023	-0.0141 (0.02)	0.0418 (0.009)	0.0555 (0.008)

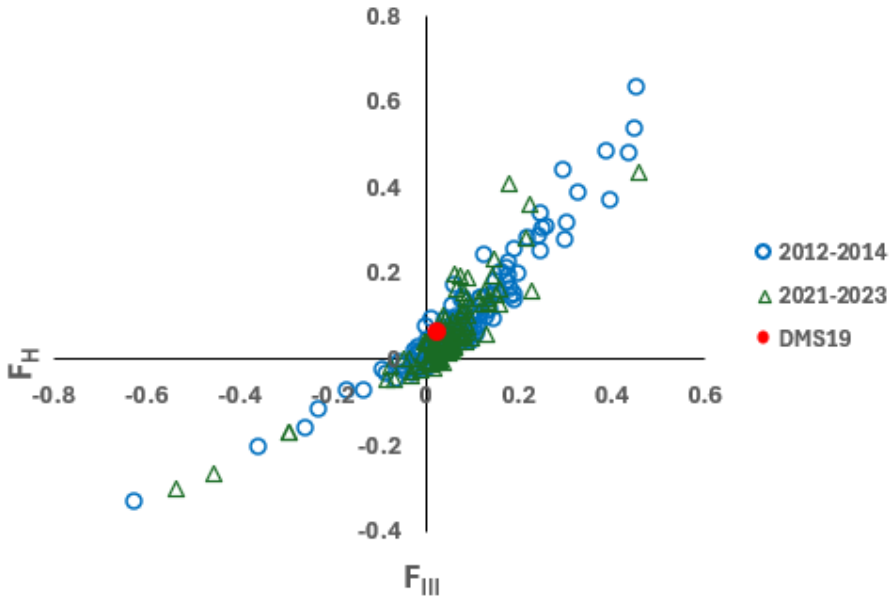

Figure 3-6 (bottom) Individual inbreeding coefficients (F_H and F_{III} implemented in PLINK) for 162 Maugean skates identified by sampling cohorts, and individual DMS19 (reference genome). (top) Mean population inbreeding coefficients based on SNP panels.

3.3.5 Demographic history

To gain insights into the historical factors influencing the observed genetic diversity patterns, this study inferred historical effective population size (N_e) from the variants contained in the diploid genome of Maugean skate by employing the Pairwise Sequentially Markovian Coalescent (PSMC) method. Regardless of the mutation rate used, the analysis showed that the species has persisted at low population sizes since at least the last glacial maxima (~20K ya), when they are believed to have colonised Macquarie Harbour. Before this event, the population showed an ancestral steep decline, followed by a period of gradual, steady decline 100K to 1M ya (Fig 3.7). PSMC inferences become upwardly biased towards the present (Patton et al., 2019), so estimates below 10K ya were not included. At 10K ya, the estimated N_E population was 0.303×10^4 (95% CI $0.295–0.310 \times 10^4$) and 0.605×10^4 (95% CI $0.597–0.614 \times 10^4$) based on $\mu = 2.5 \times 10^{-9}$ and $\mu = 2.5 \times 10^{-10}$ per site per generation respectively (Fig 3.8).

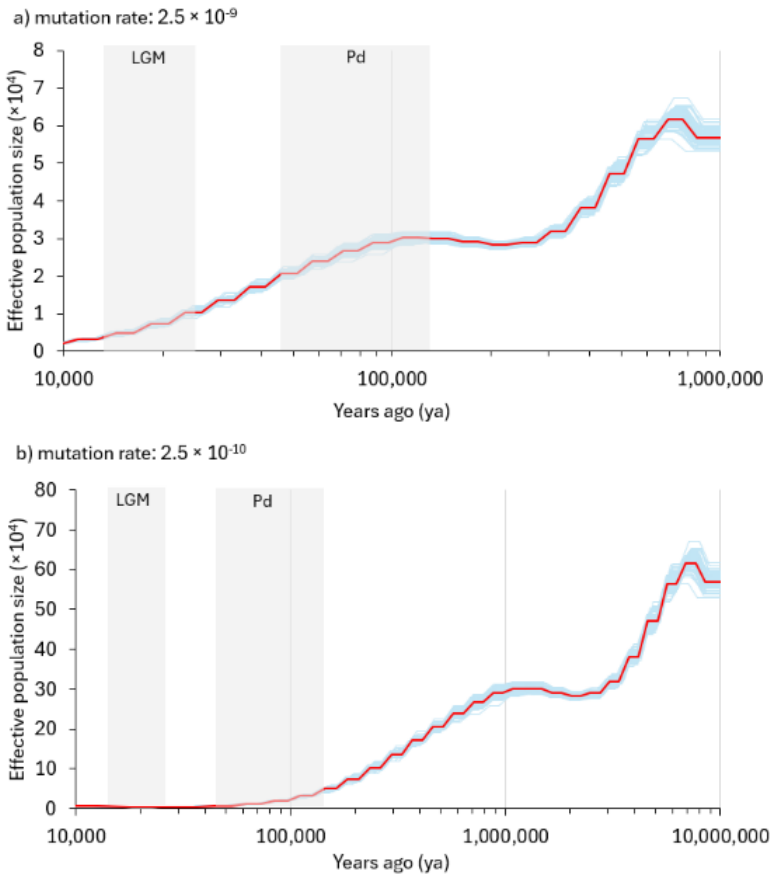

Figure 3-8 Historical effective population size (Ne) inferred from a single individual diploid genome of Maugean skate (DMS19) by employing the PSMC method. The blue line denotes 100 bootstraps, with the red line representing mean Ne. PSMC plot is scaled with generation time (g = 6) and mutation rate per site per generation of a) 2.5×10^{-9} and b) 2.5×10^{-10}. Shaded area indicates key climatic events: penultimate deglaciation (Pd, 135-43 kybp) and Last Glacial Maximum (LGM, 25-14 kybp).

To explore more recent demographic events, EPOS analysis of SNPs was used (note that GONE analysis could not be implemented, see methods). Results showed that the population remained at a stable low level from approximately 7.5K ya (the authors of the method suggest that the algorithm is unable to reliably detect very recent demographic changes, Lynch et al., 2020). The inferred population size over this period is consistent with the PSMC results.

3.3.6 Bathurst Harbour

The protocol used here resulted in successful mtDNA extraction from formalin preserved samples. The mitogenome of the Bathurst specimens were compared against the reference mitogenome from Macquarie Harbour. Preliminary results have shown the presence of several variant sequences (MAF > 5%) absent in Macquarie Harbour (see Appendix B). This study detected SNPs in D-loop, ND1 and cytochrome oxidase 1 that separate the individuals from Bathurst Harbour from the Macquarie Harbour reference mitogenome (see example of SNP in ND1, Appendix B). The SNPs were also confirmed by aligning against the raw reads that produced the reference mito-genome to ensure haplotype sequence is genuinely unique. The implication of SNPs on protein coding is not investigated here.

While these results should be considered preliminary, they suggest that mitogenome differences may have existed between the Macquarie and Bathurst Harbour populations. If substantial differences are found, this data could provide valuable insight into the evolutionary past of the species. Furthermore, development of the species transcriptome and re-annotation of the genome may provide insight into the function of identified variant regions. This could prove valuable for current conservation efforts and might help improve our understanding of why the Maugean skate appears to have been able to persist in Macquarie Harbour and not Bathurst Harbour.

3.4 Discussion

Here we present for the first time a reference-quality genome and mitogenome for the Maugean skate with preliminary annotation. Furthermore, we provide an assessment of population structure of the species that expands on previous work (Weltz et al., 2018) by incorporating the use of next-generation sequencing techniques and SNPs, allowing for the assessment of fine-scale structure. These results contribute to our limited understanding of population genetics and demographic history of the Maugean skate. Considering the growing evidence of environmental changes across its sole remaining habitat, Macquarie Harbour (Ross et al., 2020), and documented changes in the population (Moreno and Semmens 2023; Moreno et al., 2024, 2025), the information and tools presented here will be fundamental to inform conservation and population management efforts of this unique micro-endemic species.

3.4.1 Population structure, diversity and demographic history

Previous work looking at genetic structuring in this species using microsatellites and mtDNA (Weltz et al., 2018) concluded that Maugean skate in Macquarie Harbour was likely to be a single population, although the authors cautioned that due to limitations in number of microsatellites found, further work was needed to corroborate this interpretation and investigate if fine scale-structuring was present. Single nucleotide polymorphism (SNP) has been demonstrated to have a greater ability to detect fine-scale structuring in elasmobranchs (Rodrigues Domingues et al., 2018). In this study, phylogenetic trees, PCoA, and DAPC on SNPs showed no evidence of genetic structure amongst Maugean skate in Macquarie Harbour. This analysis indicated nearly complete overlap between individuals across capture locations, suggesting very high genetic flow across the whole harbour. This was further supported by F_{st} values, a commonly used metric to measure differences between populations based on genetic structure. There were no significant pairwise differences between locations, and clustering analysis resulted in the delineation of no significant groupings. Our results provide further support to the hypothesis that Maugean skate in Macquarie Harbour belong to a single highly homogeneous population and should be managed accordingly.

Regardless of the sequencing technique used, one important consideration in population genetics is that representative sample sizes are crucial to form meaningful conclusions and reduce uncertainty (Wright et al., 2020). Here tissue from 264 individuals was sequenced and the final filtered dataset comprised 162 individuals. The final filtered dataset represented a wide array of sizes, habitats and capture locations across the entire known range of the species inside the harbour. This represents a large number when compared to genomic studies in other endangered fauna (e.g. Hu et al., 2020, Morin et al., 2020). Our sample corresponds to a significant proportion of the estimated population (see below), increasing confidence that the patterns described here are truly representative of the population.

Acoustic tracking (Moreno et al., 2020) showed that Maugean skate tend to display fine-scale long-term site attachment, resulting in limited home ranges (<10 km^2). Further, Maugean skate show clear affinity towards a small number of sites and a narrow range of depths across the harbour (Bell et al., 2016). Accordingly, it had been proposed that fine scale population structuring should exist within the Harbour due to the spatial ecology of the species (Weltz et al., 2018). However, some individuals will occasionally display a change in behaviour and become highly mobile. During these events, individuals can move across the whole area of the harbour within a few days (Bell et al., 2016). These events are relatively uncommon (once or twice a year) and they only last a short time (1 day to 2 weeks) after which regular home ranging behaviour is resumed, and it is not uncommon for individuals (10-15% of acoustically tracked individuals -Bell et al., 2016; Moreno et al., 2020-) to resettle at a different site. The timing of these changes in behaviour is largely independent between individuals and does not appear to correlate with sex, size, seasonality or time of the year, although some concurrent movements were observed that correspond to fluctuations in environmental conditions (Moreno et al., 2020). Further work is required to help understand

the potential drivers behind these relocation events. Nonetheless, it is likely that this is an important mechanism for maintaining genetic flow across the population and may help explain the complete absence of fine scale population structuring.

Both SNPs and whole-genome diversity metrics showed that Maugean skate in Macquarie Harbour have low genetic diversity. Average genome wide heterozygosity per kb of Maugean skate was 0.353, derived from the 50 pseudo-chromosomes. To our knowledge, this is the lowest value reported for any elasmobranch species, including species listed by the International Union for Conservation of Nature (IUCN, https://www.iucnredlist.org/) as endangered and critically endangered like whale (*Rhincodon typus*) and great hammerhead (*Sphyrna mokarran*) sharks (Stanhope et al., 2023), respectively, although it should be noted that only a few species currently have full sequenced genomes (fewer than 1% of extant species). Across marine predators from other taxa (i.e. teleost fishes, cetaceans and pinnipeds), the only species with similar or lower reported heterozygosity are Orca (*Orcinus orca*; IUCN listing: Data deficient) and the critically endangered (IUCN) vaquita (*Phocoena sinus*) (Robinson et al., 2022). These results are consistent with previous estimates of diversity for the species based on mtDNA and 8 microsatellite markers (Weltz et al., 2018). Only a small number of studies to date have used genotyping methods to investigate patterns of genetic diversity in rajids ((Delaval et al., 2021, Nelson et al., 2022). Interestingly, SNP derived diversity levels were similar to those reported for the critically endangered (IUCN) blue skate (*D. batis,* H_o=0.27; Delaval et al., 2021) and the clearnose skate (*R. elegantaria*; IUCN listing: Least concern*;* H_o=0.146 - 0.24; Nelson et al., 2022). Although endangered avian and terrestrial mammal species like orange belly parrots (*Neophema chrysogaster)* and Tasmanian devils (*Sarcophilus harrisii*) have lower genetic diversity (or lower total number of SNPs) (Morrison et al., 2020; Patton et al., 2019), Maugean skate are genetically depauperate when compared to other critically endangered marine elasmobranchs and marine predators.

It is unclear how N_e correlates to census counts in most elasmobranch species (N_e/N_c), and due to the conservative life histories of these species, demographic events could require multiple generations to be reflected (Chapman et al., 2011). Furthermore, this analysis was based on samples collected over multiple three-year periods and include individuals from various overlapping generations. Therefore, these values are unlikely to reflect recent population declines (Moreno et al., 2023) and should be therefore not be interpreted as contemporary estimates of population size. We recommended that a more useful approach to investigate recent events and inform conservation and recovery actions, would be to use age and growth data to divide existing and future samples into cohorts to investigate relative changes in effective number of breeders (N_b) through time (Davenport et al., 2020).

Reconstruction of the species demographic history based on a single genome showed that Maugean skate has persisted at a small effective population size (N_e 3030-6050) for at least 20k years (based on current estimates of generation length and mutation rate). It is important to note that for long term demographic reconstruction we used mutation rates derived from other elasmobranch species. Mutation rates in elasmobranchs are lower than other taxa but

remain poorly understood (Sender price et al., 2013). Changes to the mutation rate will not affect the general shape and pattern of the PSMC but will change the placement along the x and y axes. Therefore, the overall trajectory of the PSMC curves presented here is likely to be accurate, but the scaling should be considered approximate. DArT SNPs derived EPOS inferences were consistent with the findings of the PSMC analysis and suggests that these patterns are broadly true for the whole population. Together, these findings suggest that the recently observed declines are not the result of a long natural decline, and the species has been able to remain viable at continuous low population sizes. Demographic reconstruction of genomic data provides a very valuable insight into the historical processes that shaped the current genetic structure of a species as well as provide insight into their evolution. Although beyond the scope of this work, whole genome sequencing from multiple Maugean skate could greatly improve accuracy and expand the temporal coverage of future investigations of demographic history of the species.

The demographic history of the species is consistent with the hypothesis that Maugean skate colonised Macquarie Harbour during the last glacial maxima (Weltz et al., 2018). Interestingly, before this potential founding event, even at peak levels, the estimated range of population sizes was relatively small when compared to levels reported for endangered, pelagic elasmobranchs such as shortfin mako (*Isurus oxyrinchus*; IUCN listing: Endangered) and great hammerhead sharks, which ranged in the 10,000s (Stanhope et al., 2023). The low population sizes of the skate likely occur because in contrast with those wide-ranging pelagic species, the Maugean skate has the most limited range of any known elasmobranch (Bell et al, 2016). This is reflected in the species physiology, biology and movement ecology, which appear to be highly specialised to the conditions in this unusual estuary (Morash et al, 2020, Moreno et al, 2020). Paleo analysis of sediment cores from the harbour showed that this system has consistently been oxygen restricted and depauperate (Ross et al., 2020). Therefore, it is possible that the low historical N_e reflects a limited persistent carrying capacity in the system. These observations highlight a fundamental link between environmental conditions in Macquarie Harbour and the Maugean skate population and the species ability to persist through past demographic events.

Despite the low genetic diversity, there was no evidence of significant inbreeding loading (i.e. accumulation of recessive deleterious alleles which may be exposed by inbreeding and result in inbreeding depression (Caballero et al., 2017)) in the population. Observed and expected heterozygosity levels did not differ significantly (0.27 and 0.29 respectively), resulting in an F_H=0.07 (F_{IS} of 0.089, F_{III}=0.05) and indicating that the population does not deviate markedly from Hardy–Weinberg equilibrium. Similarly, we found that across the whole genome, the total cumulative fraction in long runs of homozygosity ($ROH_{>100kb}$) was 0.4-2.6%, resulting in a low average inbreeding coefficient of $F_{ROH>100kb}$= 0.026. By contrast, the recently published genome of the endangered great hammerhead shark (*S. mokarran*) showed the total cumulative fraction of $ROH_{>100kb}$ was 74.4% (Stanhope et al., 2023). Interestingly, ROH runs in the Maugean skate are not only comparatively rare, but those that exist are evenly distributed across the genome, which suggests that despite the low diversity the species is genetically stable (Ceballos et al., 2018). ROH were also relatively short, with a maximum

recorded length of 2 Mbp despite 521 contigs being over 1 Mbp. ROH patterns for the reference genome show no evidence of recent demographic processes in this individual, however, whole genome sequencing data from more individuals will be necessary to corroborate if these observations occur across the whole population.

It had previously been reported based on microsatellite markers that Maugean skate exhibit a significant deviation from the expected L-shape in allelic frequency distribution, thus suggesting a potential recent bottleneck (Weltz et al., 2018). However, it has been shown that in species with low genetic diversity like the Maugean skate, microsatellite-based markers are not a feasible way to measure inbreeding accurately, and genomic tools like SNP panels and whole-genome sequencing provide a much more robust way to estimate inbreeding directly (Taylor et al., 2015). Considering the low inbreeding loadings in the modern population estimated from the SNP panel data, our findings suggests that the decline in diversity from the observed potential founding event was either not severe enough to result in a detectable genetic bottleneck signal, or that the population has successfully recovered since.

Kinship analysis found evidence of a low number of consanguineous individuals across the sample (only 2 and 11 pairs of individuals out of 162 skates are full and half-siblings respectively). Sperm storage, multiple paternity (Garcia-Salinas 2021) and mechanisms of cryptic female choice (Lyons et al., 2021) have been reported for other elasmobranch species. Such mechanisms could help explain how an isolated species like the Maugean skate has been able to maintain what appears to be a panmictic population despite historically low population sizes and long-term isolation. The genetic tools developed in this study and the recent establishment of an ex-situ conservation program for the species provides an ideal opportunity to refine our understanding of mating systems in the species.

Generally, when species experience catastrophic population declines that results in loss of genetic diversity, recovery tends to be hindered by high inbreeding depression, loss of adaptive potential and accumulation of deleterious mutations (Hellmair et al., 2014). However, there are a growing number of examples of species that have remained viable in the long term despite low genetic diversity such as Island foxes (*U. littoralis*), Apennine brown bears (*Ursus actos marsicanus*), the kākāpō *(S. habroptilus*) and the Vaquita (*P. sinus*) (Benazzo et al., 2017, Robinson et al., 2018, Dussex et al., 2021, Robinson et al., 2022). Recently, genomic analysis has shown that historical populations of these species have been naturally stable at low sizes in the long term. Species with long term small populations may be naturally more resilient to inbreeding because the higher homozygosity results in strongly deleterious alleles being exposed to selection more commonly (Kyriazis et al, 2020) and purging mechanisms may therefore counter drift by decreasing the total number of deleterious variants (Benazzo et al., 2017, Dahasque et al., 2024). Results from SNPs and whole genome analyses suggest that despite a small population size and low genetic diversity, Maugean skate show no evidence of recent genetic bottlenecks or severe inbreeding. However, further whole-genome sequencing from multiple individuals will be necessary to better understand population level patterns of deleterious allele accumulation

and potential long-term stability, as well as strengthening demographic history reconstruction. Our findings suggests that the Maugean skate could have a high potential for successful recovery if a) no further population declines occur, b) the mechanisms responsible for habitat deterioration are addressed, and c) environmental remediation occurs in a timely fashion. This is the first time that an in-depth genomic assessment of a small population, micro-endemic elasmobranch species have been reported, so the tools developed here will be of great interest for evolutionary and developmental research of sharks and rays, but also vertebrate fauna in general (Pearce et al., 2021).

Our analysis of population heterozygosity and allelic richness through time suggests that genetic diversity in the population has remained consistent since 2012. However, a grave concern for the Maugean is that if further population declines occur, a critical threshold will be reached that results in lowered genetic fitness due to inevitable inbreeding loadings in any recovery scenario, as seen in species like Tasmanian devils (*S harrisii*) (Bruniche-Olsen et al., 2014) and Mexican grey wolves (*C. lupus baileyi*) (Taron et al., 2021). Additional whole genome data for multiple individuals will be important in understanding patterns of genetic fitness in the species and inform what these critical demographic thresholds are. Further, Maugean skate exhibit k-selected life history traits (Awruch et al., 2021). This means that impact driven changes to the genetic structure of the population are likely to take many generations to become evident. Because of this, effects of the recent population changes may not yet be apparent, and contemporary N_e estimates presented will not reflect current effective population size accurately (Chapman et al., 2011). Therefore, ongoing genetic monitoring of the wild population will be a crucial resource to inform recovery. Furthermore, developing additional whole genome sequences would allow the assessment of genetic fitness, erosion and population level diversity.

One critical limitation of this study is that due to size selectivity bias in the nets used to obtain samples, the youngest age classes are underrepresented. If breeding between consanguineous animals results in a loss of fitness that causes early mortality in their offspring, such individuals will be largely absent from our sample. This is important because there is evidence of compromised recruitment coinciding with population declines after 2014. Namely changes in the demographic structure of the population (Moreno and Semmens 2023) and a report of decreased egg viability rates in the wild (Moreno, unpublished). Observations of a recent successful recruitment event following improved oxygen conditions in 2021 (Moreno, et al., 2024) and high hatching success rates reported from ex-situ holding (Semmens pers comm) suggest that environmental conditions during rearing may play a significant role in hatching success. Nevertheless, the mechanisms responsible are not well understood and require urgent analysis. We recommend that the genomic resources presented here be further examined to investigate detrimental allele loadings and mutation rates in the species. Likewise, genetic analysis of the captive population can help fill critical knowledge gaps regarding the effects that these may have on embryos and early life juveniles. This will be crucial to improving our understanding of genetic fitness of the species and how that may affect extinction risk, particularly in the context of recovery from recent declines and management of future threats.

High quality, single individual genomic resources like the ones presented here provide a valuable initial step that can help inform conservation and identify key research avenues. However, in the future, whole genome-sequencing of more individuals would provide population wide estimates, provide insight into genetic fitness and deleterious allele accumulation, enable the empirical derivation of mutation rates for the species, and help improve certainty of historical population estimates, as well as enable the use of analysis like GONE, which can improve recent demographic history estimates.

4. Conclusion

Maugean skate in Macquarie Harbour constitute a single homogeneous population. Their high genomic homogeneity and lack of population structure do not support the suggestion that possible connectivity or external provisioning from a previously undiscovered remnant population exists. Results in this work suggest that Maugean skate populations in Macquarie and Bathurst Harbours had genetically distinct features. Further analysis of Bathurst Harbour preserved individuals and novel approaches such as the use of sedimentary ancient DNA (*sed*aDNA) may be able to provide additional insight on the genetic connectivity and history between these two populations.

In Macquarie Harbour, the species appears to have existed at a small population size during the last 20 k years, although further analysis is required to improve recent demographic history estimates. There is evidence that in that time they survived significant periods of environmental change based on paleo-environmental records (Ross et al, 2022). As previously conjectured, the species exhibits low genetic diversity. Despite this, only moderate or low levels of inbreeding loading were found. This suggests that the natural rarity of the Maugean skate may play a role in limiting their vulnerability to inbreeding loading. Therefore, despite low genetic diversity and low numbers, the Maugean skate may not be condemned to extinction if appropriate conservation actions to remediate their habitat are implemented on time.

However, low genetic diversity could also mean that the species has restricted adaptive potential and may be particularly vulnerable to disease outbreaks and rapid environmental changes (Pearce et al., 2021). Recently, anthropogenic impacts have resulted in high magnitude environmental degradation of the conditions in the system that occurred over a short time scale. The impacts of these changes are likely to be compounded by historical stressors (e.g. legacy mining waste) and broad scale ongoing issues like climate change. It is not clear how recent and future declines in the population may affect their genetic fitness. Therefore, we may be at a critical opportunity window for conservation.

DArT sequencing produced high quality SNPs that allowed for analysis of kinship structures. This means that although the low level of diversity in the species may present technical challenges, SNPs may be suitable to develop close kin population models in this species. This study highlights the importance of incorporating genetic and genomic monitoring in management and recovery strategies of endangered species. The whole genome, mitogenome and SNP information provided here will be of significant value to modelling potential recovery scenarios, understanding the effects of management interventions, managing ex-situ conservation efforts, and informing re-introduction strategies. Furthermore, with fewer than 1% of extant elasmobranch species having a sequenced genome (Pearce et al, 2021), our results will be of broader interest for future investigations of evolutionary biology and conservation genetics.

5. References

ALONGE, M., LEBEIGLE, L., KIRSCHE, M., JENIKE, K., OU, S., AGANEZOV, S., WANG, X., LIPPMAN, Z. B., SCHATZ, M. C. & SOYK, S. 2022. Automated assembly scaffolding using RagTag elevates a new tomato system for high-throughput genome editing. *Genome biology,* 23**,** 258.

ALVES, F., BANKS, S. C., EDWORTHY, M., STOJANOVIC, D., LANGMORE, N. E. & HEINSOHN, R. 2023. Using conservation genetics to prioritise management options for an endangered songbird. *Heredity,* 130**,** 289-301.

AWRUCH, C. A., BELL, J. D., SEMMENS, J. M. & LYLE, J. M. 2021. Life history traits and conservation actions for the Maugean skate (*Zearaja maugeana*), an endangered species occupying an anthropogenically impacted estuary. *Aquatic Conservation: Marine and Freshwater Ecosystems,* 31**,** 2178-2192.

BELL, J., LYLE, J., SEMMENS, J., AWRUCH, C., MORENO, D., CURRIE, S., MORASH, A., ROSS, D. & BARRETT, N. 2016. Movement, habitat utilisation and population status of the endangered Maugean skate and implications for fishing and aquaculture operations in Macquarie Harbour.

BELL, J. D. & LYLE, J. M. 2016. Post-capture survival and implications for by-catch in a multi-species coastal gillnet fishery. *PLoS One,* 11**,** e0166632.

BENAZZO, A., TRUCCHI, E., CAHILL, J. A., MAISANO DELSER, P., MONA, S., FUMAGALLI, M., BUNNEFELD, L., CORNETTI, L., GHIROTTO, S. & GIRARDI, M. 2017. Survival and divergence in a small group: The extraordinary genomic history of the endangered Apennine brown bear stragglers. *Proceedings of the National Academy of Sciences,* 114**,** E9589-E9597.

BICKNELL, A.W., GODLEY, B.J., SHEEHAN, E.V., VOTIER, S.C. AND WITT, M.J. 2016. Camera technology for monitoring marine biodiversity and human impact. *Frontiers in Ecology and the Environment*, *14*(8), pp.424-432.

BRÜNICHE-OLSEN, A., JONES, M. E., AUSTIN, J. J., BURRIDGE, C. P. & HOLLAND, B. R. 2014. Extensive population decline in the Tasmanian devil predates European settlement and devil facial tumour disease. *Biology letters,* 10**,** 20140619.

BUCHFINK, B., XIE, C. & HUSON, D. H. 2015. Fast and sensitive protein alignment using DIAMOND. *Nature methods,* 12**,** 59-60.

CABALLERO, A., BRAVO, I. AND WANG, J., 2017. Inbreeding load and purging: implications for the short-term survival and the conservation management of small populations. *Heredity*, *118*(2), pp.177-185.

CAPPO, M., HARVEY, E., MALCOLM, H. & SPEARE, P. 2003. Potential of video techniques to monitor diversity, abundance and size of fish in studies of marine protected areas. *Aquatic Protected Areas-what works best and how do we know,* 1**,** 455-64.

CASTILLÓN, M., PALOMER, A., FOREST, J. & RIDAO, P. 2019. State of the art of underwater active optical 3D scanners. *Sensors,* 19**,** 5161.

CEBALLOS, F. C., JOSHI, P. K., CLARK, D. W., RAMSAY, M. & WILSON, J. F. 2018. Runs of homozygosity: windows into population history and trait architecture. *Nature Reviews Genetics,* 19**,** 220-234.

CHAPMAN, D. D., SIMPFENDORFER, C. A., WILEY, T. R., POULAKIS, G. R., CURTIS, C., TRINGALI, M., CARLSON, J. K. & FELDHEIM, K. A. 2011. Genetic diversity despite population collapse in a critically endangered marine fish: the smalltooth sawfish (*Pristis pectinata*). *Journal of Heredity,* 102**,** 643-652.

CHENG, H., CONCEPCION, G. T., FENG, X., ZHANG, H. & LI, H. 2021. Haplotype-resolved de novo assembly using phased assembly graphs with hifiasm. *Nature methods,* 18**,** 170-175.

CONNOLLY, R., JINKS, K., SHAND, A., TAYLOR, M., GASTON, T., BECKER, A. & JINKS, E. 2023. Out of the shadows: automatic fish detection from acoustic cameras. *Aquatic Ecology,* 57**,** 833-844.

COOK, D., MIDDLEMISS, K., JAKSONS, P., DAVISON, W. & JERRETT, A. 2019. Validation of fish length estimations from a high frequency multi-beam sonar (ARIS) and its utilisation as a field-based measurement technique. *Fisheries Research,* 218**,** 59-68.

COULON, A. 2010. genhet: an easy-to-use R function to estimate individual heterozygosity. *Molecular Ecology Resources*, 10, 167-169.

DAVENPORT, D., BUTCHER, P., ANDREOTTI, S., MATTHEE, C., JONES, A. & OVENDEN, J. 2021. Effective number of white shark (*Carcharodon carcharias*, Linnaeus) breeders is stable over four successive years in the population adjacent to eastern Australia and New Zealand. *Ecology and Evolution,* 11**,** 186-198.

DEHASQUE, M., MORALES, H. E., DÍEZ-DEL-MOLINO, D., PEČNEROVÁ, P., CHACÓN-DUQUE, J. C., KANELLIDOU, F., MULLER, H., PLOTNIKOV, V., PROTOPOPOV, A. & TIKHONOV, A. 2024. Temporal dynamics of woolly mammoth genome erosion prior to extinction. *Cell,* 187**,** 3531-3540. e13.

DELAVAL, A., FROST, M., BENDALL, V., HETHERINGTON, S. J., STIRLING, D., HOARAU, G., JONES, C. S. & NOBLE, L. R. 2022. Population and seascape genomics of a critically endangered benthic elasmobranch, the blue skate *Dipturus batis*. *Evolutionary Applications,* 15**,** 78-94.

DELAVAL, A. N. 2021. Population genomics of a critically endangered data-deficient elasmobranch, the blue skate *Dipturus batis*.

DODGE, T. O., FARQUHARSON, K. A., FORD, C., CAVANAGH, L., SCHUBERT, K., SCHUMER, M., BELOV, K. & HOGG, C. J. 2023. Genomes of two Extinct-in-the-Wild reptiles from Christmas Island reveal distinct evolutionary histories and conservation insights. *Molecular Ecology Resources*, 00, 1-17.

DOMINGUES, R. R., HILSDORF, A. W. S. & GADIG, O. B. F. 2018. The importance of considering genetic diversity in shark and ray conservation policies. *Conservation genetics,* 19**,** 501-525.

DUSSEX, N., VAN DER VALK, T., MORALES, H. E., WHEAT, C. W., DÍEZ-DEL-MOLINO, D., VON SETH, J., FOSTER, Y., KUTSCHERA, V. E., GUSCHANSKI, K. & RHIE, A. 2021. Population genomics of the critically endangered kākāpō. *Cell Genomics,* 1.

EDGAR, G. J., LAST, P. R., BARRETT, N. S., GOWLETT-HOLMES, K., DRIESSEN, M. & MOONEY, P. 2010. Conservation of natural wilderness values in the Port Davey marine and estuarine protected area, south-western Tasmania. *Aquatic Conservation: Marine and Freshwater Ecosystems,* 20**,** 297-311.

EGG, L., PANDER, J., MUELLER, M. & GEIST, J. 2018. Comparison of sonar-, camera-and net-based methods in detecting riverine fish-movement patterns. *Marine and Freshwater Research,* 69**,** 1905-1912.

ENDELMAN, J. B. & JANNINK, J.-L. 2012. Shrinkage estimation of the realized relationship matrix. *G3 Genes, Genomes, Genetics,,* 2**,** 1405-1413.

FILISETTI, A., MAROUCHOS, A., MARTINI, A., MARTIN, T. & COLLINGS, S. Developments and applications of underwater LiDAR systems in support of marine science. OCEANS 2018 MTS/IEEE Charleston, 2018. IEEE, 1-10.

GARCÍA-SALINAS, P., GALLEGO, V. & ASTURIANO, J. F. 2021. Reproductive Anatomy of Chondrichthyans: Notes on Specimen Handling and Sperm Extraction. I. Rays and Skates. *Animals,* 11**,** 1888.

GOUDET, J. 2005. Hierfstat, a package for R to compute and test hierarchical F-statistics. *Molecular Ecology Notes,* 5**,** 184-186.

GREMME, G., BRENDEL, V., SPARKS, M. E. & KURTZ, S. 2005. Engineering a software tool for gene structure prediction in higher organisms. *Information and Software Technology,* 47**,** 965-978.

GRIFFIN, R. A., JONES, R. E., LOUGH, N. E., LINDENBAUM, C. P., ALVAREZ, M. C., CLARK, K. A., GRIFFITHS, J. D. & CLABBURN, P. A. 2020. Effectiveness of acoustic cameras as tools for assessing biogenic structures formed by Sabellaria in highly turbid environments. *Aquatic Conservation: Marine and Freshwater Ecosystems,* 30**,** 1121-1136.

GRUBER, B., UNMACK, P. J., BERRY, O. F. & GEORGES, A. 2018. dartr: An r package to facilitate analysis of SNP data generated from reduced representation genome sequencing. *MolecularE Resources,* 18**,** 691-699.

GUREVICH, A., SAVELIEV, V., VYAHHI, N. AND TESLER, G., 2013. QUAST: quality assessment tool for genome assemblies. *Bioinformatics*, *29*(8), pp.1072-1075.

HANSEN, R. E. 2011. Introduction to Synthetic Aperture Sonar, *Sonar Systems*, Kolev, N. Z. (Ed.), ISBN: 978-953-307-345-3.

HARVEY, E., MCLEAN, D., FRUSHER, S., HAYWOOD, M., NEWMAN, S. & WILLIAMS, A. 2013. The use of BRUVs as a tool for assessing marine fisheries and ecosystems: a review of the hurdles and potential. *University of Western Australia,* 20.

HELLMAIR, M. & KINZIGER, A. P. 2014. Increased extinction potential of insular fish populations with reduced life history variation and low genetic diversity. *PLoS One,* 9**,** e113139.

HOFF, K. J., LANGE, S., LOMSADZE, A., BORODOVSKY, M. & STANKE, M. 2016. BRAKER1: unsupervised RNA-Seq-based genome annotation with GeneMark-ET and AUGUSTUS. *Bioinformatics,* 32**,** 767-769.

HU, J.-Y., HAO, Z.-Q., FRANTZ, L., WU, S.-F., CHEN, W., JIANG, Y.-F., WU, H., KUANG, W.-M., LI, H. & ZHANG, Y.-P. 2020. Genomic consequences of population decline in critically endangered pangolins and their demographic histories. *National Science Review,* 7**,** 798-814.

JOMBART, T., DEVILLARD, S. & BALLOUX, F. 2010. Discriminant analysis of principal components: a new method for the analysis of genetically structured populations. *BMC genetics,* 11**,** 1-15.

JONES, O.R. AND WANG, J., 2010. COLONY: a program for parentage and sibship inference from multilocus genotype data. *Molecular ecology resources*, *10*(3), pp.551-555.

JONES, R. E., GRIFFIN, R. A. & UNSWORTH, R. K. 2021. Adaptive Resolution Imaging Sonar (ARIS) as a tool for marine fish identification. *Fisheries Research,* 243**,** 106092.

KELLER, M. C., VISSCHER, P. M. & GODDARD, M. E. 2011. Quantification of Inbreeding Due to Distant Ancestors and Its Detection Using Dense Single Nucleotide Polymorphism Data. *Genetics*, 189, 237-249.

KIM, D., PAGGI, J. M., PARK, C., BENNETT, C. & SALZBERG, S. L. 2019. Graph-based genome alignment and genotyping with HISAT2 and HISAT-genotype. *Nature Biotechnology,* 37**,** 907-915.

KYRIAZIS, C. C., ROBINSON, J. A., NIGENDA-MORALES, S. F., BEICHMAN, A. C., ROJAS-BRACHO, L., ROBERTSON, K. M., FONTAINE, M. C., WAYNE, R. K., TAYLOR, B. L. & LOHMUELLER, K. E. 2023. Models based on best-available information support a low inbreeding load and potential for recovery in the vaquita. *Heredity,* 130**,** 183-187.

KYRIAZIS, C. C., WAYNE, R. K. & LOHMUELLER, K. E. 2019. High genetic diversity can contribute to extinction in small populations. *BioRxiv,* 31**,** 940-1012.

LANKOWICZ, K. M., BI, H., LIANG, D. & FAN, C. 2020. Sonar imaging surveys fill data gaps in forage fish populations in shallow estuarine tributaries. *Fisheries Research,* 226**,** 105520.

LI, H. & DURBIN, R. 2010. Fast and accurate long-read alignment with Burrows–Wheeler transform. *Bioinformatics,* 26**,** 589-595.

LIU, S. & HANSEN, M. M. 2017. PSMC (pairwise sequentially Markovian coalescent) analysis of RAD (restriction site associated DNA) sequencing data. *Molecular Ecology Resources,* 17**,** 631-641.

LYLE, J. M., BELL, J. D., CHUWEN, B. M., BARRETT, N., TRACEY, S. R. & BUXTON, C. D. 2014. *Assessing the impacts of gillnetting in Tasmania: implications for by-catch and biodiversity*, Citeseer.

LYNCH, M., HAUBOLD, B., PFAFFELHUBER, P. & MARUKI, T. 2020. Inference of historical population-size changes with allele-frequency data. *G3: Genes, Genomes, Genetics,* 10**,** 211-223.

LYONS, K., KACEV, D. & MULL, C. G. 2021. An inconvenient tooth: Evaluating female choice in multiple paternity using an evolutionarily and ecologically important vertebrate clade. *Molecular Ecology,* 30**,** 1574-1593.

MARLÉTAZ, F., DE LA CALLE-MUSTIENES, E., ACEMEL, R. D., PALIOU, C., NARANJO, S., MARTÍNEZ-GARCÍA, P. M., CASES, I., SLEIGHT, V. A., HIRSCHBERGER, C. & MARCET-HOUBEN, M. 2023. The little skate genome and the evolutionary emergence of wing-like fins. *Nature,* 616**,** 495-503.

MIJANGOS, J. L., GRUBER, B., BERRY, O., PACIONI, C. & GEORGES, A. 2022. dartR v2: An accessible genetic analysis platform for conservation, ecology and agriculture. *Methods in Ecology and Evolution,* 13**,** 2150-2158.

MORASH, A. J., LYLE, J. M., CURRIE, S., BELL, J. D., STEHFEST, K. M. & SEMMENS, J. M. 2020. The endemic and endangered Maugean Skate (*Zearaja maugeana*) exhibits short-term severe hypoxia tolerance. *Conservation Physiology,* 8**,** coz105.

MORENO, D., LYLE, J., SEMMENS, J., MORASH, A., STEHFEST, K., MCALLISTER, J., BOWEN, B. & BARRETT, N. 2020. Vulnerability of the endangered Maugean Skate population to degraded environmental conditions in Macquarie Harbour.

MORENO, D., PATIL, J., DEAGLE, B. & SEMMENS, J. M. 2022. Application of environmental DNA to survey Bathurst Harbour (Tasmania) for the Endangered Maugean Skate (*Zearaja maugeana*).

MORENO, D. & SEMMENS, J. M. 2023. Interim report – Macquarie Harbour Maugean skate population monitoring. Hobart, Tasmania. Institute for Marine and Antarctic Studies, University of Tasmania, Hobart, Tasmania, Australia.

MORENO, D., TRACEY, S. & SEMMENS, J. M. 2024. Interim Report Number 2 - Macquarie Harbour Maugean skate population status and monitoring Hobart, Tasmania. Institute for Marine and Antarctic Studies, University of Tasmania, Hobart, Tasmania, Australia.

MORENO, D., TRACEY, S. & WOOLLEY, B., SEMMENS, J. M. 2025. 2014-2024 Macquarie Harbour Maugean skate population status and monitoring report. Institute for Marine and Antarctic Studies, University of Tasmania, Hobart, Tasmania, Australia.

MORIN, P. A., ARCHER, F. I., AVILA, C. D., BALACCO, J. R., BUKHMAN, Y. V., CHOW, W., FEDRIGO, O., FORMENTI, G., FRONCZEK, J. A. & FUNGTAMMASAN, A. 2021. Reference genome and demographic history of the most endangered marine mammal, the vaquita. *Molecular Ecology Resources,* 21**,** 1008-1020.

MORRISON, C.E., HOGG, C.J., GALES, R., JOHNSON, R.N. AND GRUEBER, C.E., 2020. Low innate immune-gene diversity in the critically endangered orange-bellied parrot (Neophema chrysogaster). *Emu-Austral Ornithology*, *120*(1), pp.56-64.

MURPHY, H. M. & JENKINS, G. P. 2010. Observational methods used in marine spatial monitoring of fishes and associated habitats: a review. *Marine and Freshwater Research,* 61**,** 236-252.

NARASIMHAN, V., DANECEK, P., SCALLY, A., XUE, Y., TYLER-SMITH, C. & DURBIN, R. 2016. BCFtools/RoH: a hidden Markov model approach for detecting autozygosity from next-generation sequencing data. *Bioinformatics,* 32**,** 1749-1751.

NELSON, L. N., JONES, C. M. & MCDOWELL, J. R. 2022. Rangewide Population Structure of the Clearnose Skate. *Transactions of the American Fisheries Society,* 151**,** 356-372.

NOVO, I., PÉREZ-PEREIRA, N., SANTIAGO, E., QUESADA, H. & CABALLERO, A. 2023. An empirical test of the estimation of historical effective population size using Drosophila melanogaster. *Molecular Ecology Resources,* 23**,** 1632-1640.

NURK, S., WALENZ, B. P., RHIE, A., VOLLGER, M. R., LOGSDON, G. A., GROTHE, R., MIGA, K. H., EICHLER, E. E., PHILLIPPY, A. M. & KOREN, S. 2020. HiCanu: accurate assembly of segmental duplications, satellites, and allelic variants from high-fidelity long reads. *Genome Research*, 30, 1291-1305.

PATTON, A. H., MARGRES, M. J., STAHLKE, A. R., HENDRICKS, S., LEWALLEN, K., HAMEDE, R. K., RUIZ-ARAVENA, M., RYDER, O., MCCALLUM, H. I. & JONES, M. E. 2019. Contemporary demographic reconstruction methods are robust to genome assembly quality: a case study in Tasmanian devils. *Molecular biology and evolution,* 36**,** 2906-2921.

PEARCE, J., FRASER, M. W., SEQUEIRA, A. M. & KAUR, P. 2021. State of shark and ray genomics in an era of extinction. *Frontiers in Marine Science,* 8**,** 744986.

PELLETIER, D., LELEU, K., MOU-THAM, G., GUILLEMOT, N. & CHABANET, P. 2011. Comparison of visual census and high definition video transects for monitoring coral reef fish assemblages. *Fisheries Research,* 107**,** 84-93.

POREBSKI, S., BAILEY, L. G. & BAUM, B. R. 1997. Modification of a CTAB DNA extraction protocol for plants containing high polysaccharide and polyphenol components. *Plant Molecular Biology Reporter,* 15**,** 8-15.

RHIE, A., WALENZ, B. P., KOREN, S. & PHILLIPPY, A. M. 2020. Merqury: reference-free quality, completeness, and phasing assessment for genome assemblies. *Genome Biology,* 21**,** 1-27.

RIDGWAY, J. L., MADSEN, J. A., FISCHER, J. R., CALFEE, R. D., ACRE, M. R. & KAZYAK, D. C. 2024. Side-scan sonar as a tool for measuring fish populations: Current state of the science and future directions. *Fisheries* 49.10 (2024): 454-462.

ROBINSON, J. A., BROWN, C., KIM, B. Y., LOHMUELLER, K. E. & WAYNE, R. K. 2018. Purging of strongly deleterious mutations explains long-term persistence and absence of inbreeding depression in island foxes. *Current Biology,* 28**,** 3487-3494. e4.

ROBINSON, J. A., KYRIAZIS, C. C., NIGENDA-MORALES, S. F., BEICHMAN, A. C., ROJAS-BRACHO, L., ROBERTSON, K. M., FONTAINE, M. C., WAYNE, R. K., LOHMUELLER, K. E. & TAYLOR, B. L. 2022. The critically endangered vaquita is not doomed to extinction by inbreeding depression. *Science,* 376**,** 635-639.

ROBINSON, J. A., RÄIKKÖNEN, J., VUCETICH, L. M., VUCETICH, J. A., PETERSON, R. O., LOHMUELLER, K. E. & WAYNE, R. K. 2019. Genomic signatures of extensive inbreeding in Isle Royale wolves, a population on the threshold of extinction. *Science Advances,* 5**,** eaau0757.

ROSS, D., MORENO, D., BELL, J., MARDONES, J. & BEARD, J. 2022. Assessment of the Macquarie Harbour Broadscale Environmental Monitoring Program (BEMP) data from 2011-2020.

SAMOILYS, M. A. & CARLOS, G. 2000. Determining methods of underwater visual census for estimating the abundance of coral reef fishes. *Environmental Biology of Fishes,* 57**,** 289-304.

SHAHRESTANI, S., BI, H., LYUBCHICH, V. & BOSWELL, K. M. 2017. Detecting a nearshore fish parade using the adaptive resolution imaging sonar (ARIS): An automated procedure for data analysis. *Fisheries Research,* 191**,** 190-199.

SHEN, W., PENG, Z. & ZHANG, J. 2024. Identification and counting of fish targets using adaptive resolution imaging sonar. *Journal of Fish Biology,* 104**,** 422-432.

SILVA, G. A. A., HARDER, A. M., KIRKSEY, K. B., MATHUR, S. & WILLOUGHBY, J. R. 2024. Detectability of runs of homozygosity is influenced by analysis parameters and population-specific demographic history. *PLOS Computational Biology,* 20**,** e1012566.

SIMÃO, F. A., WATERHOUSE, R. M., IOANNIDIS, P., KRIVENTSEVA, E. V. & ZDOBNOV, E. M. 2015. BUSCO: assessing genome assembly and annotation completeness with single-copy orthologs. *Bioinformatics,* 31**,** 3210-3212.

SISKEY, M. R., SHIPLEY, O. N. & FRISK, M. G. 2019. Skating on thin ice: Identifying the need for species-specific data and defined migration ecology of Rajidae spp. *Fish and Fisheries,* 20**,** 286-302.

SPEED, D. & BALDING, D. J. 2015. Relatedness in the post-genomic era: is it still useful? *Nature Reviews Genetics,* 16**,** 33-44.

STANHOPE, M. J., CERES, K. M., SUN, Q., WANG, M., ZEHR, J. D., MARRA, N. J., WILDER, A. P., ZOU, C., BERNARD, A. M. & PAVINSKI-BITAR, P. 2023. Genomes of endangered great hammerhead and shortfin mako sharks reveal historic population declines and high levels of inbreeding in great hammerhead. *Iscience,* 26.

STANKE, M., KELLER, O., GUNDUZ, I., HAYES, A., WAACK, S. & MORGENSTERN, B. 2006. AUGUSTUS: ab initio prediction of alternative transcripts. *Nucleic Acids Research,* 34**,** W435-W439.

TAYLOR, H. R., KARDOS, M. D., RAMSTAD, K. M. & ALLENDORF, F. W. 2015. Valid estimates of individual inbreeding coefficients from marker-based pedigrees are not feasible in wild populations with low allelic diversity. *Conservation Genetics,* 16**,** 901-913.

ULIANO-SILVA, M., FERREIRA, J. G. R., KRASHENINNIKOVA, K., FORMENTI, G., ABUEG, L., TORRANCE, J., MYERS, E. W., DURBIN, R. & BLAXTER, M. 2023. MitoHiFi: a python pipeline for mitochondrial genome assembly from PacBio high fidelity reads. *BMC Bioinformatics,* 24**,** 288.

WANG, J. (2011). COANCESTRY: A program for simulating, estimating and analysing relatedness and inbreeding coefficients. Molecular Ecology Resources, 11(1), 141–145.

WANG, J., SANTIAGO, E. & CABALLERO, A. 2016. Prediction and estimation of effective population size. *Heredity,* 117**,** 193-206.

WANG, J. (2022). A joint likelihood estimator of relatedness and allele frequencies from a small sample of individuals. Methods Ecol Evol. 2022;00:1–20.

WELTZ, K., LYLE, J. M., SEMMENS, J. M. & OVENDEN, J. R. 2018. Population genetics of the endangered Maugean skate (*Zearaja maugeana)* in Macquarie Harbour, Tasmania. *Conservation Genetics,* 19**,** 1505-1512.

WEIR BS, COCKERHAM CC. 1984. Estimating F-statistics for the analysis of population structure. Evolution 38:1358–70

WRIGHT, B. R., FARQUHARSON, K. A., MCLENNAN, E. A., BELOV, K., HOGG, C. J. & GRUEBER, C. E. 2020. A demonstration of conservation genomics for threatened species management. *Molecular Ecology Resources,* 20**,** 1526-1541.

XIE, Y., HORNSBY, R. L., HANOT, W. H., BARTEL-SAWATZKY, M. & NELITZ, J. L. 2024. Identifying fish and estimating abundance and swim velocities of migrating Pacific

salmon using adaptive resolution imaging sonar in mobile surveys. *ICES Journal of Marine Science,* 81**,** 1295-1306.

YANG, J., LEE, S. H., GODDARD, M. E. & VISSCHER, P. M. 2011. GCTA: A tool for genome-wide complex trait analysis. *AJHG*, 88, 76-82.

ZHU, T., SATO, Y., SADO, T., MIYA, M. & IWASAKI, W. 2023. MitoFish, MitoAnnotator, and MiFish Pipeline: updates in 10 years. *Molecular Biology and Evolution,* 40**,** msad035.

Appendix A

Macquarie Harbour in situ tests for optical video, ARIS, LiDAR and SAS

Trials using traditional towed video and external illumination were conducted in 2019 (Moreno et al, 2020). As seen in figure 4-4, visibility was severely limited when targeting key skate habitats and depths (7.5-15 m). The high volume of suspended particulate matter resulted in backscatter, which restricted the effectiveness of external lights. As a result, the sea floor could not be imaged reliably and in some cases could not be seen at all even when the device was static and sitting on the bottom (e.g. Figure 4-8 Left). When visibility was better, the towed camera had to be flown very close to the substrate to produce usable footage, which restricted the total visible area to < 0.5 m^2. This means that skate would have to be in very close proximity to the device to be recorded, making identification and measurement unlikely (Figure 4-5).

In situ ARIS trials in Macquarie Harbour were conducted in June 2022 using towed and diver held deployments (Figure 4-1). In situ trials for optical modules (LiDAR and camera) and synthetic aperture sonar were conducted in October 2022 (Figure 4-3).

Sites were chosen based on known Maugean Sites were chosen based on known Maugean skate distribution. Deployments aimed to test image quality when operating above, below and across the halocline (5-12 m). Melbourne skate carcases purchased from commercial fishers were deployed for use as proxy targets, juvenile Melbourne skate are similar in size to Maugean skate (Figure 4-2 Left).

The LiDAR sensor encountered similar issues to traditional optics (Figure 4-4). The large amount of backscatter created by suspended matter meant that the sensor could not accurately resolve an image of the seafloor. By contrast, the SAS module deployed alongside was able to produce a reliable image under the same conditions. Both ARIS and SAS deployments demonstrate that acoustic methods were not adversely affected by turbidity, density differences or operating through the halocline. SAS data was georeferenced and used to look at the known deployment site for the proxy skate targets. The targets can be clearly identified; however, image resolution was not high enough to allow measurement and species identification. Furthermore, if the location of the targets was not known in advance, it is likely that the skates would not have been correctly located (Figure 4-3). By contrast, ARIS footage had a narrower area of sonication but had sufficient resolution to allow accurate and reliable species identification (Figure 4-10).

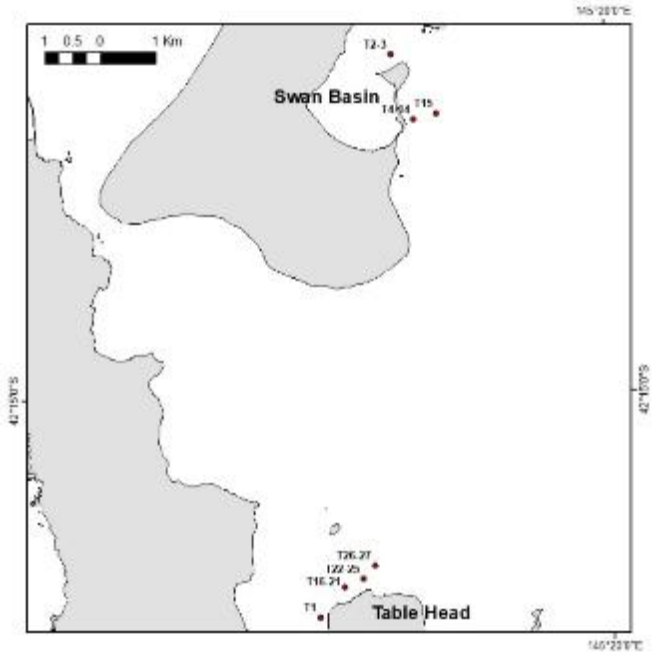

Figure 4-1 Map of deployment sites for dive and tow acoustic video trials in Macquarie Harbour

Figure 4-2 (Left) Proxy targets used to simulate Maugean skate across all equipment trials. (Right) REMUS autonomous vehicle with LiDAR and SAS sensor arrays used in Macquarie Harbour for in-situ trials

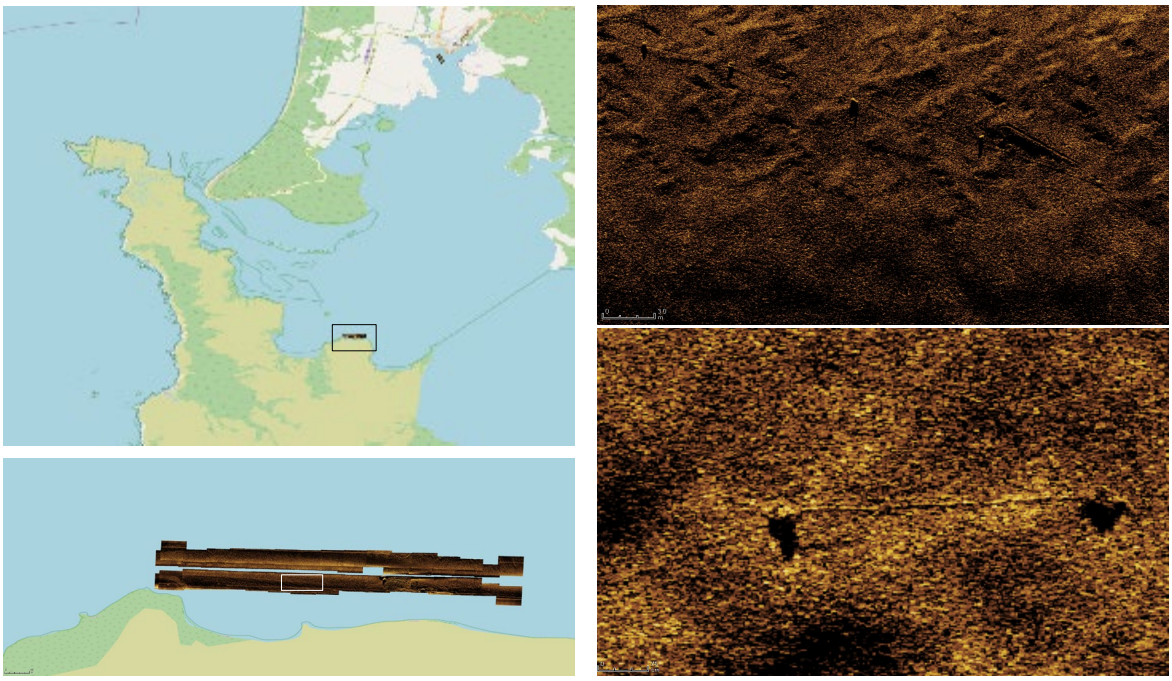

Figure 4-3 (Top left) Overlay of georeferenced SAS scan data collected in Macquarie Harbour. (Bottom left) SAS transect in Table Head targeting a known habitat of high importance for the Maugean skate (Moreno et al, 2020). (Top right) Close up of the surveyed area showing various Melbourne skate targets attached by a rope. (Bottom right) Close up of two skate targets showing the resolution of SAS data.

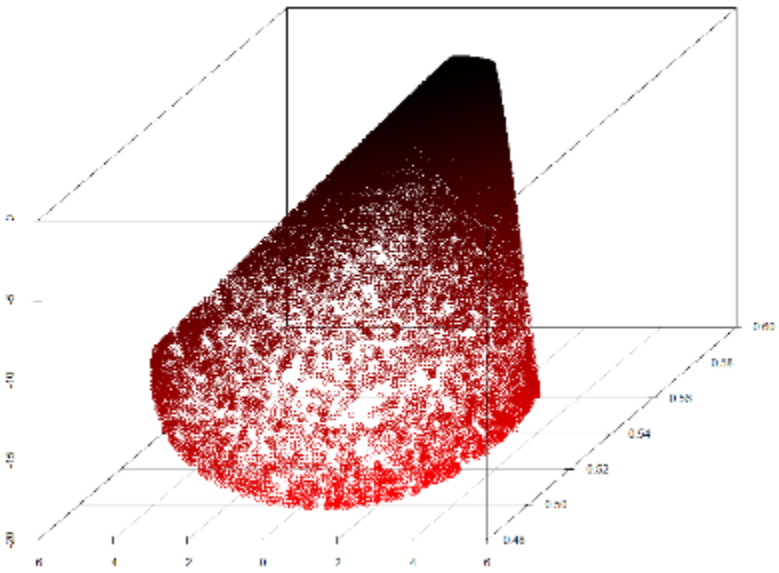

Figure 4-4 Example raw LiDAR capture data cloud (not georeferenced) showing significant backscatter along the water column that made resolving the seafloor not possible during the in-situ trial.

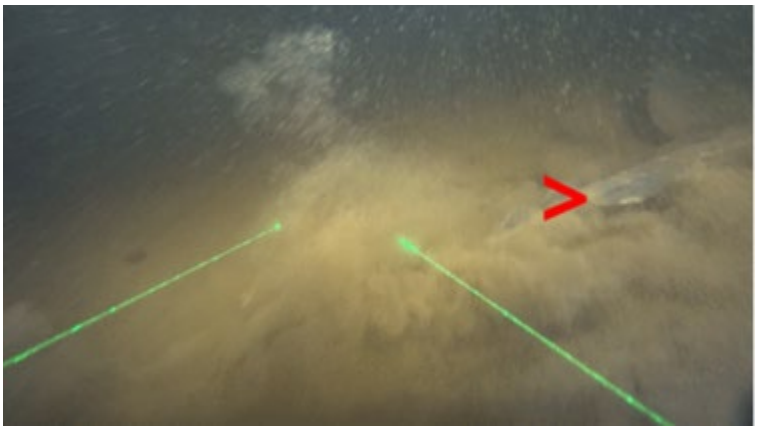

Figure 4-5 Example still frame from traditional towed video trials using external lights in Pine cove Macquarie Harbour at ~12 m depth. A skate can be seen, although due to the small visible area (~0.25 m^2) it is not possible to identify the species. Distance between lasers = 20cm

Deployment configuration trials for ARIS

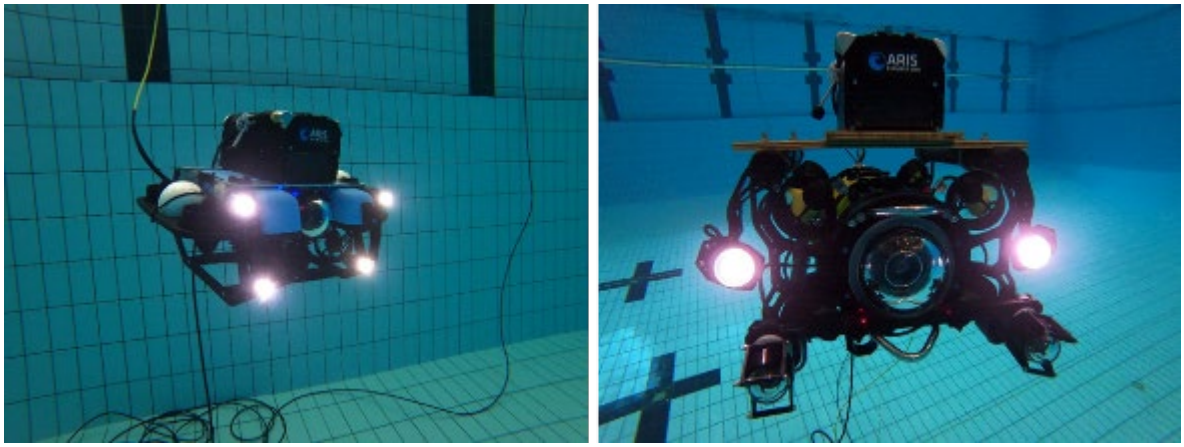

Figure 4-6 Pictures of ARIS deployment using blue ROV with heavy light kit and additional buoyancy (left) and boxfish (right) vehicles.

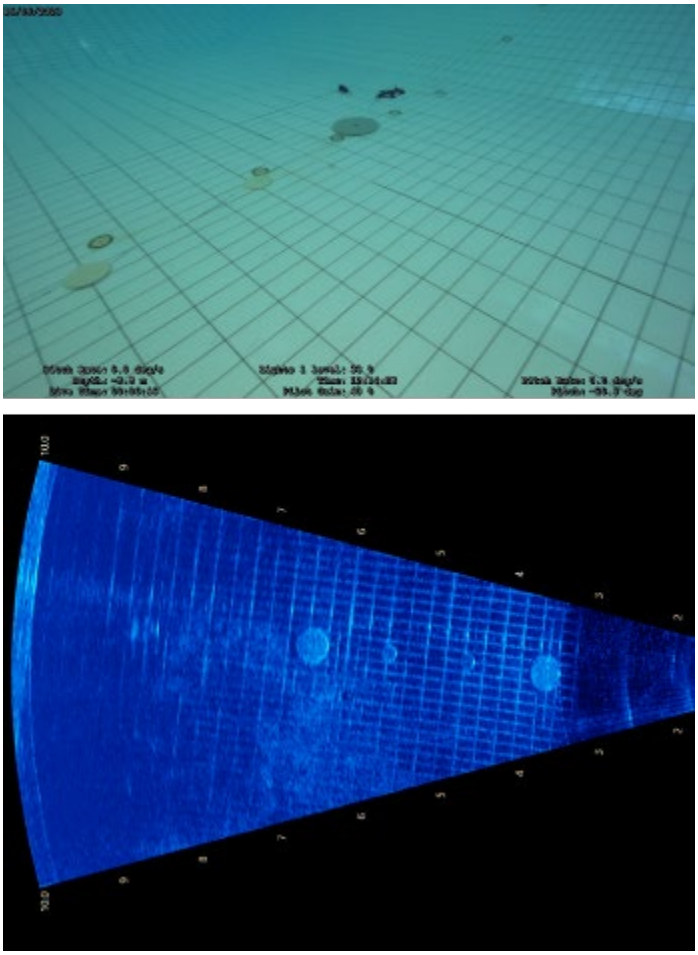

Figure 4-7 Optical and acoustic video comparison of ceramic disk targets in a controlled environment.

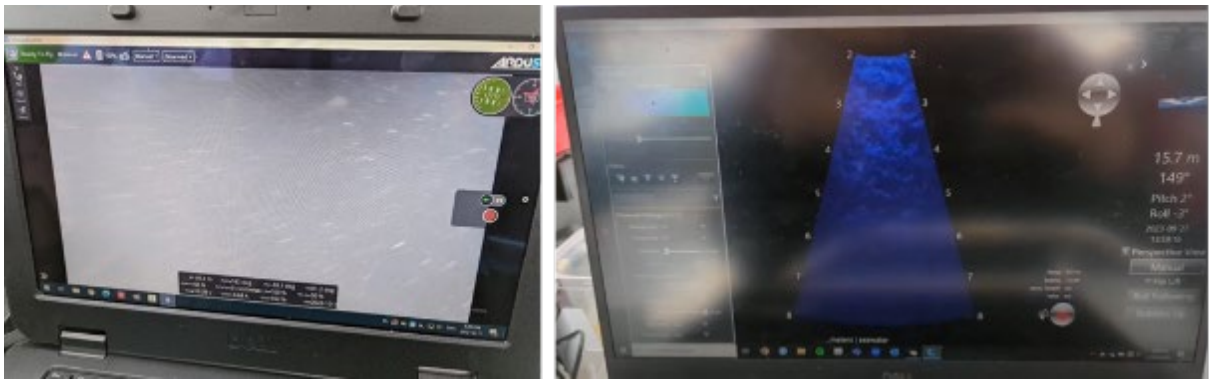

Figure 4-8 Live capture of optical and acoustic video during deployment trials in a high turbidity environment using a towed configuration

Aquarium ARIS test

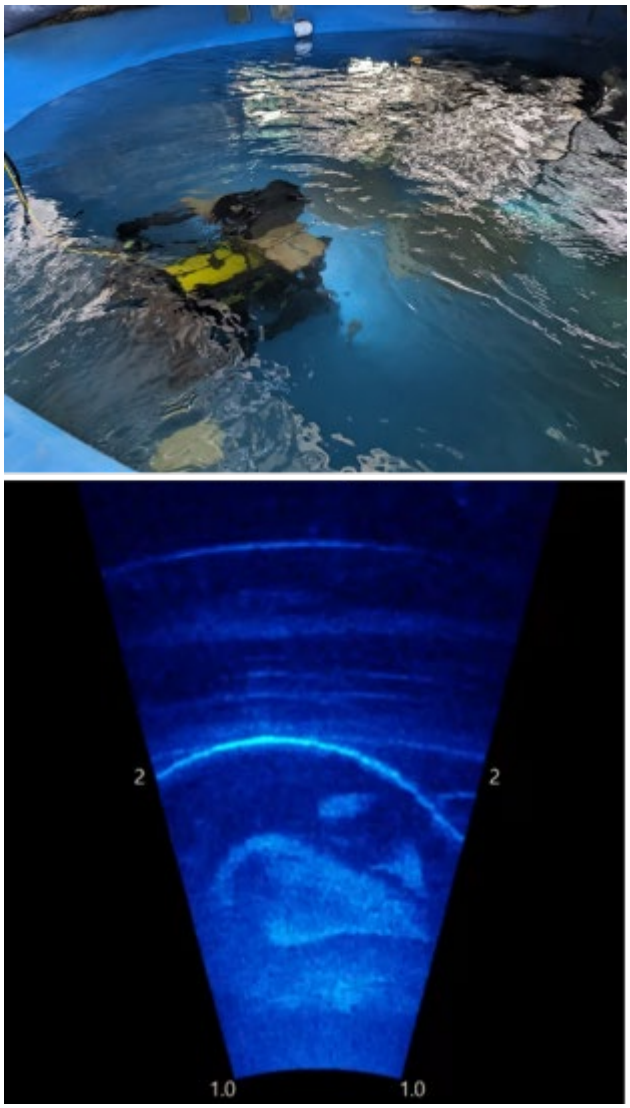

Figure 4-9 Aquarium testing of ARIS for species identification and measuring. The image shows a live adult Melbourne skate (female)

Appendix B

Genome assembly

Table 5-1 QUAST (Gurevich et al., 2013) summary report of Maugean skate HiFiasm genome assembly.

	GFA_to_FASTA_on_data_66__Fasta_file
# contigs (>= 0 bp)	6796
# contigs (>= 1000 bp)	6796
Total length (>= 0 bp)	2963505672
Total length (>= 1000 bp)	2963505672
# contigs	6796
Largest contig	10658139
Total length	2963505672
GC (%)	44.48
N50	1478264
N75	572093
L50	521
L75	1320
# N's per 100 kbp	0.00

SNP calling and filtering.

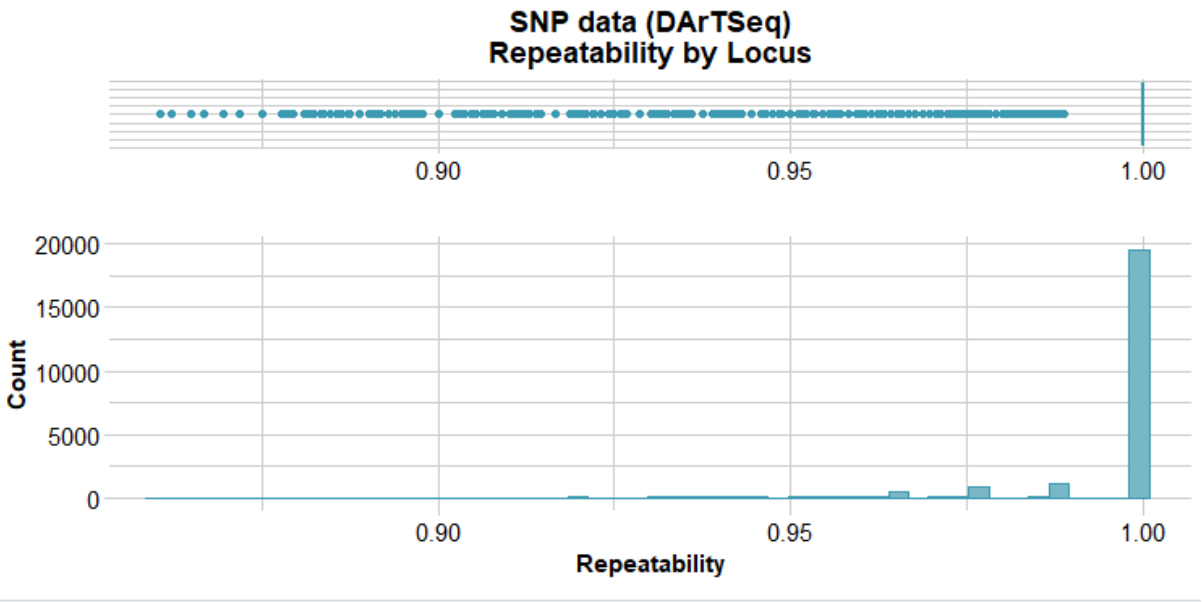

Figure 5-10 Technical repeatability of SNP loci.

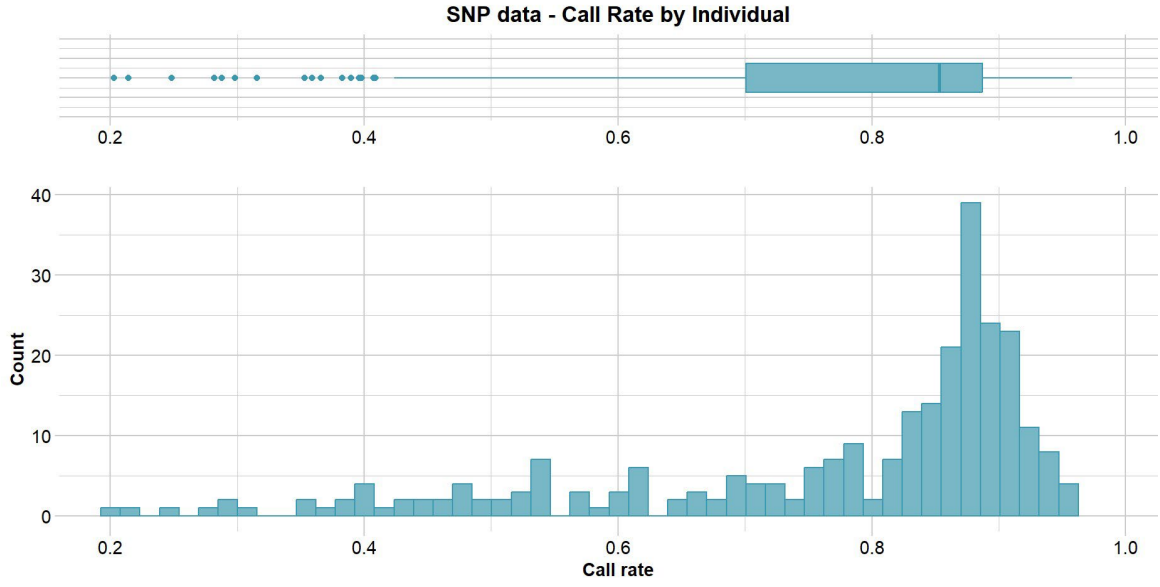

Figure 5-11 Individual call rates for SNP.

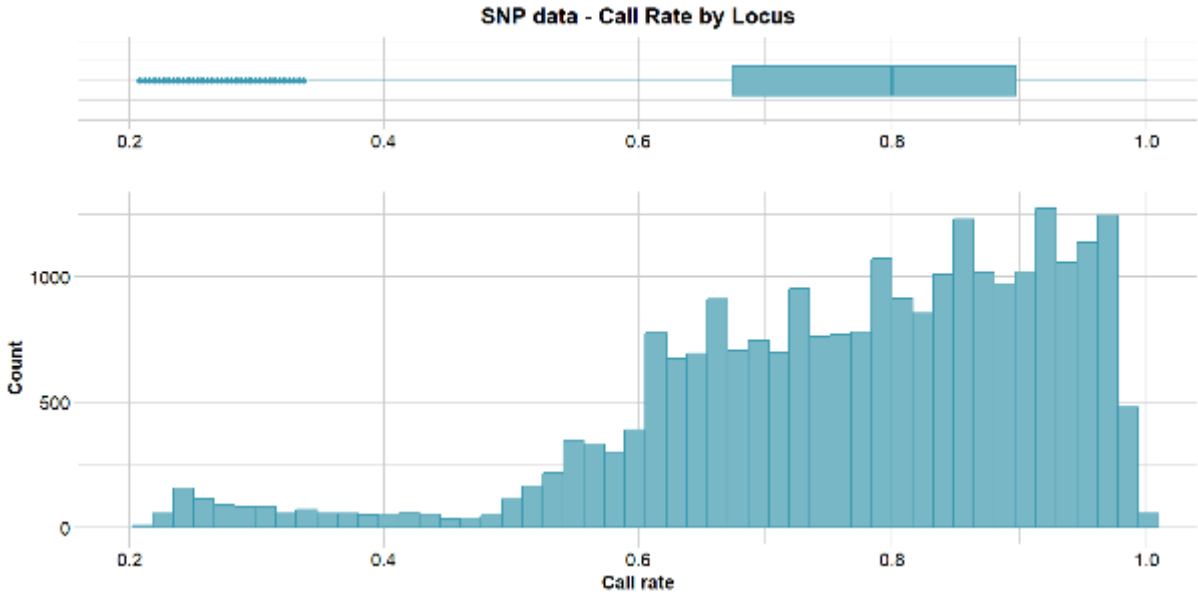

Figure 5-12 Locust call rates for SNP

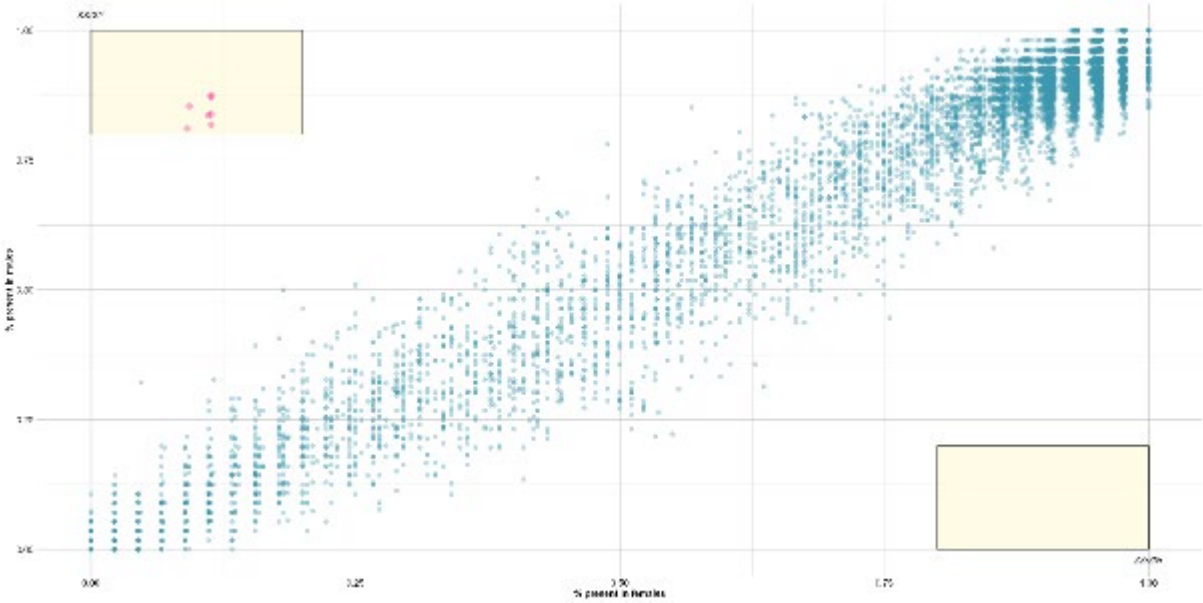

Figure 5-13 Screening and removal of sex-specific loci.

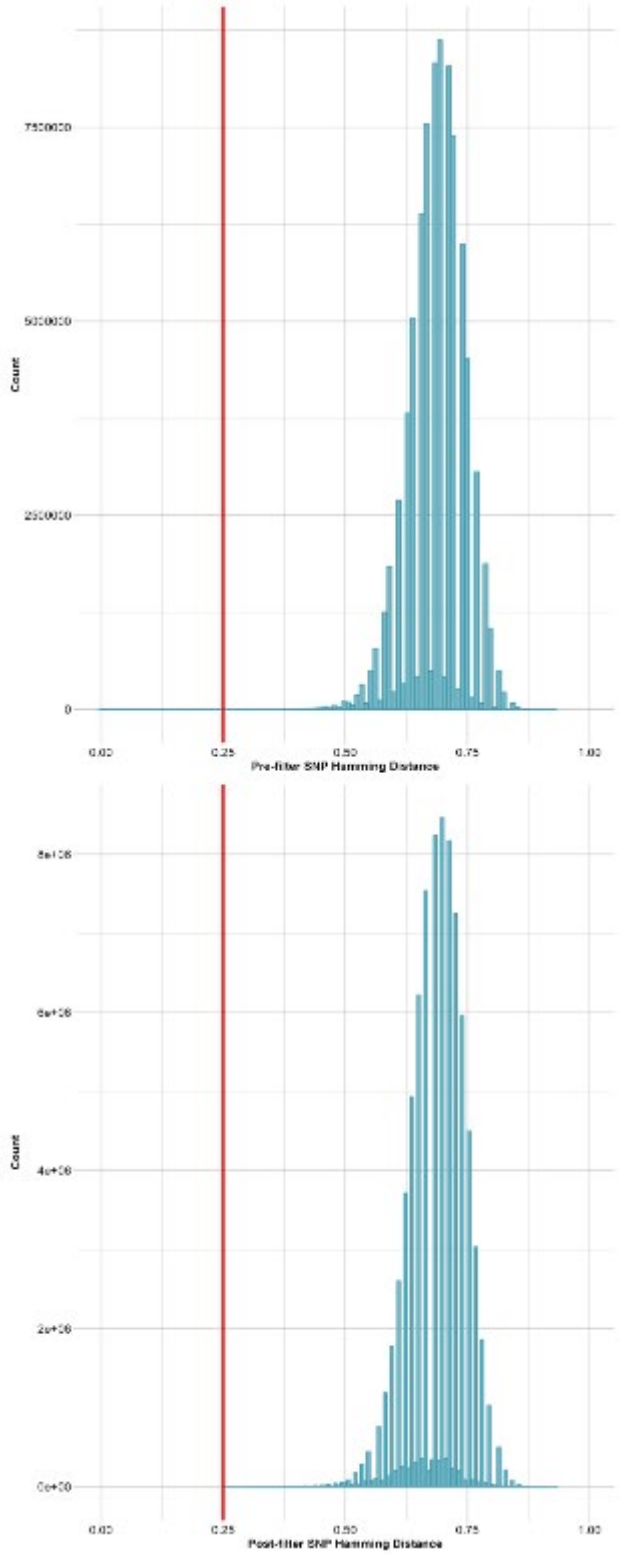

Figure 5-14 Hamming distance filtration. Pre filtration data (top) and filtered dataset (bottom). Filtering threshold=0.25

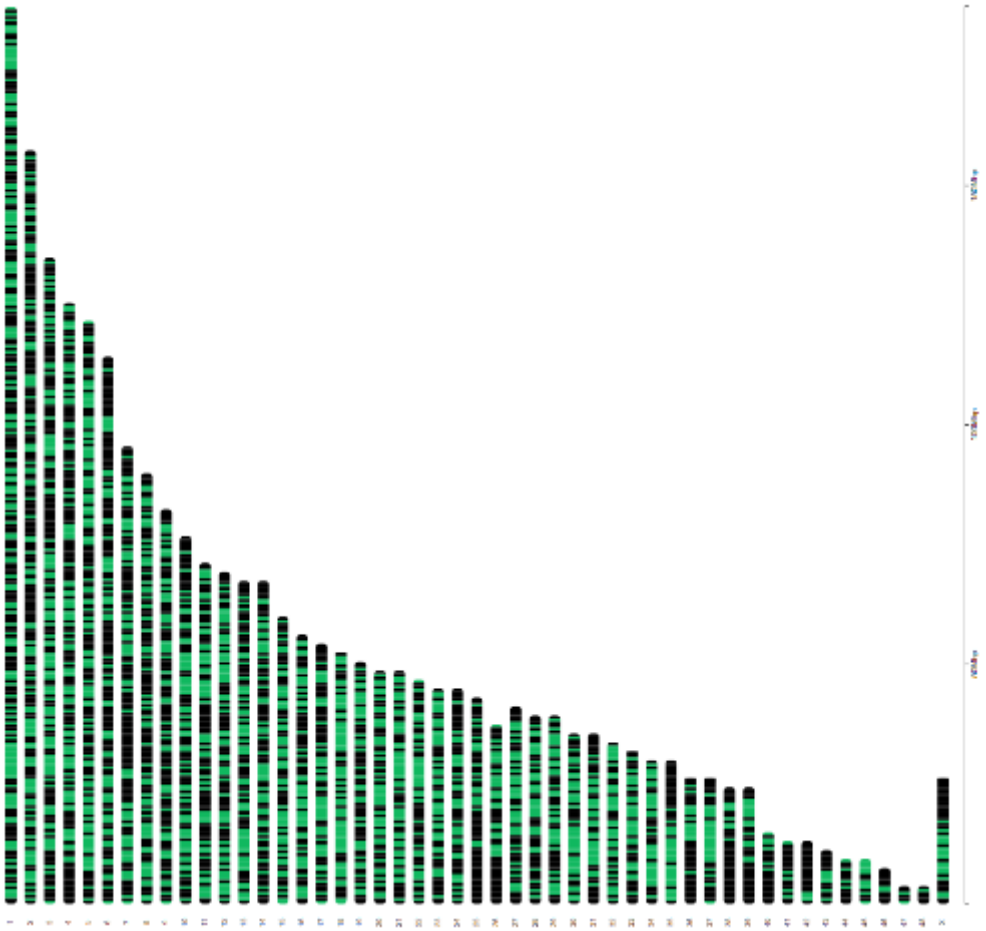

Figure 5-15 Distribution of the filtered 4662 SNPS (black bar) on 1 to 48 plus sex chromosome X of the reference genome *Raja brachyura* (GCA_963514005.1) The number on x axis indicates chromosome number.

Diversity and population structure

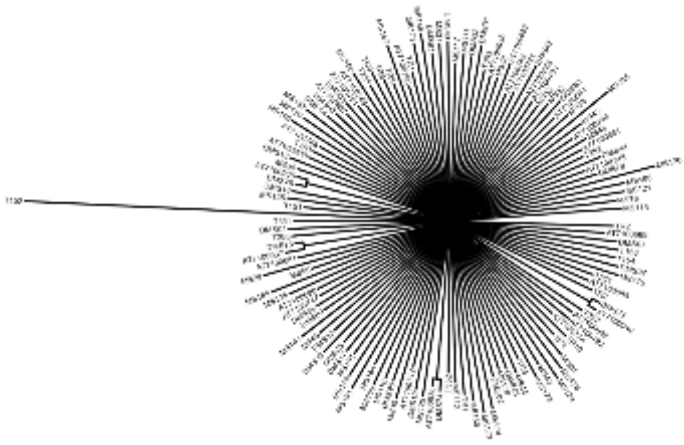

Figure 5-16 Phylogenetic tree showing no distinct clustering based on DACP.

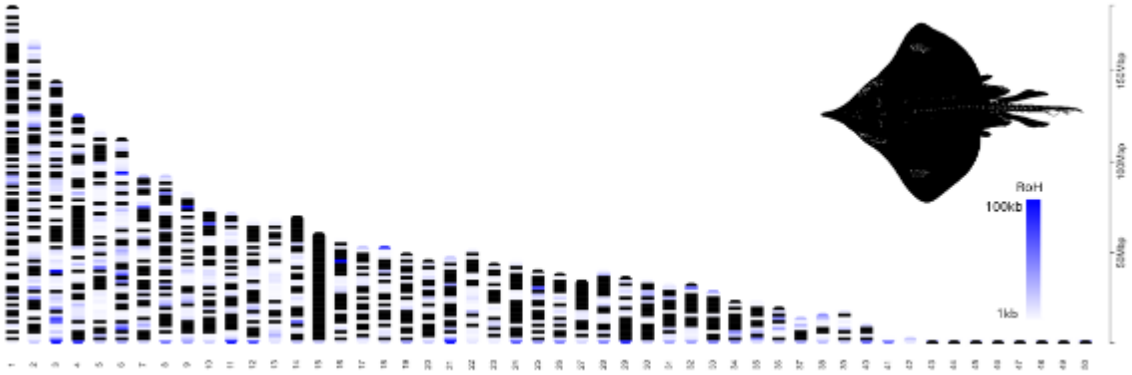

Figure 5-17 Position of run of homozygosity (RoH) fragments detected in a Maugean skate sampled in Long Bay, Macquarie Harbour in 2019 using bcftools RoH.

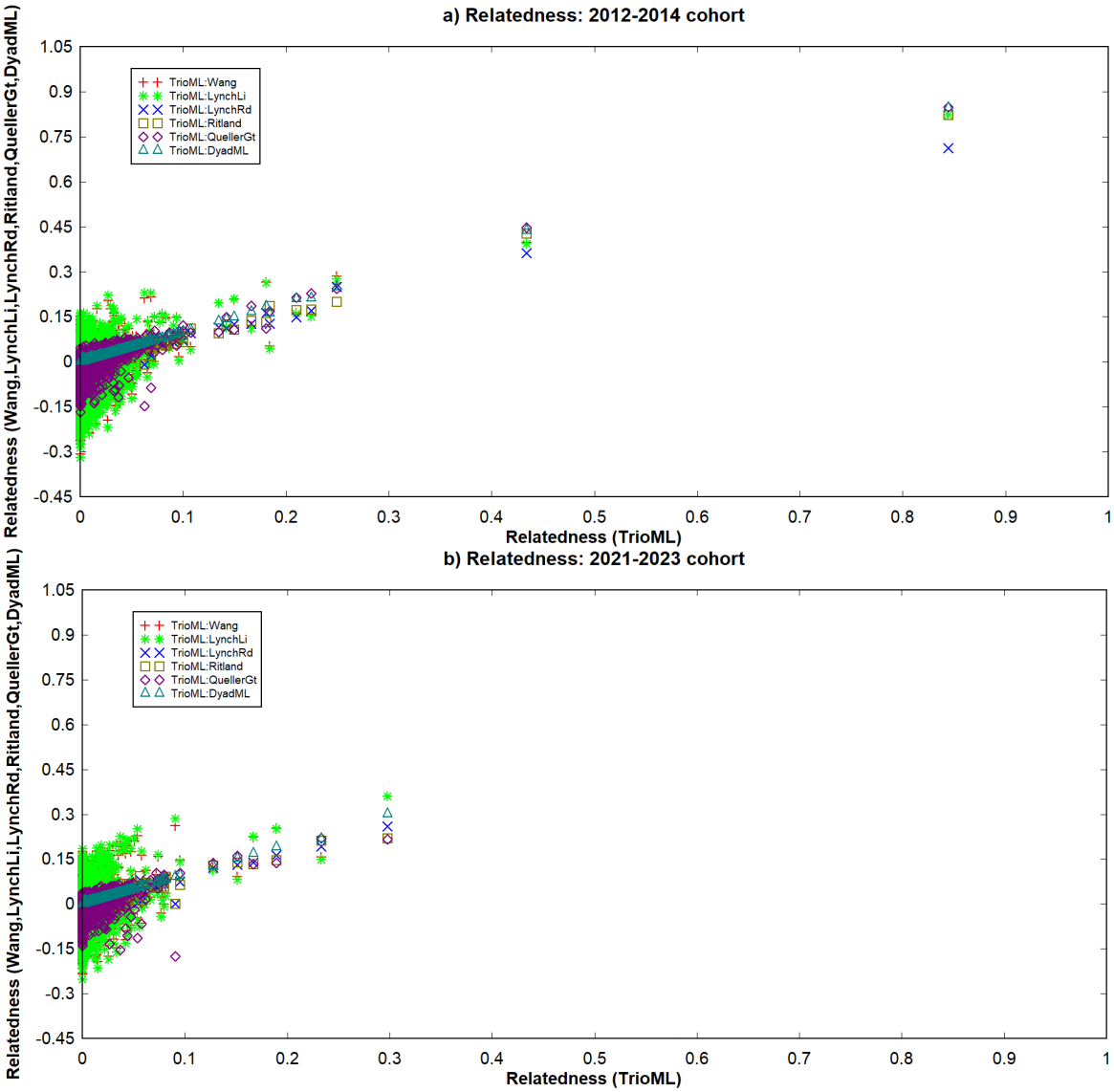

Figure 5-18 Pairwise relatedness of 162 Maugean skates representing a) 2012-2014 (n = 90) and b) 2021 to 2023 cohort (n = 72). The relatedness scores were analysed from the filtered DArT SNPs using seven relatedness estimators implemented in COANCESTRY, and the scores of any two estimators were scatter plotted for comparison.

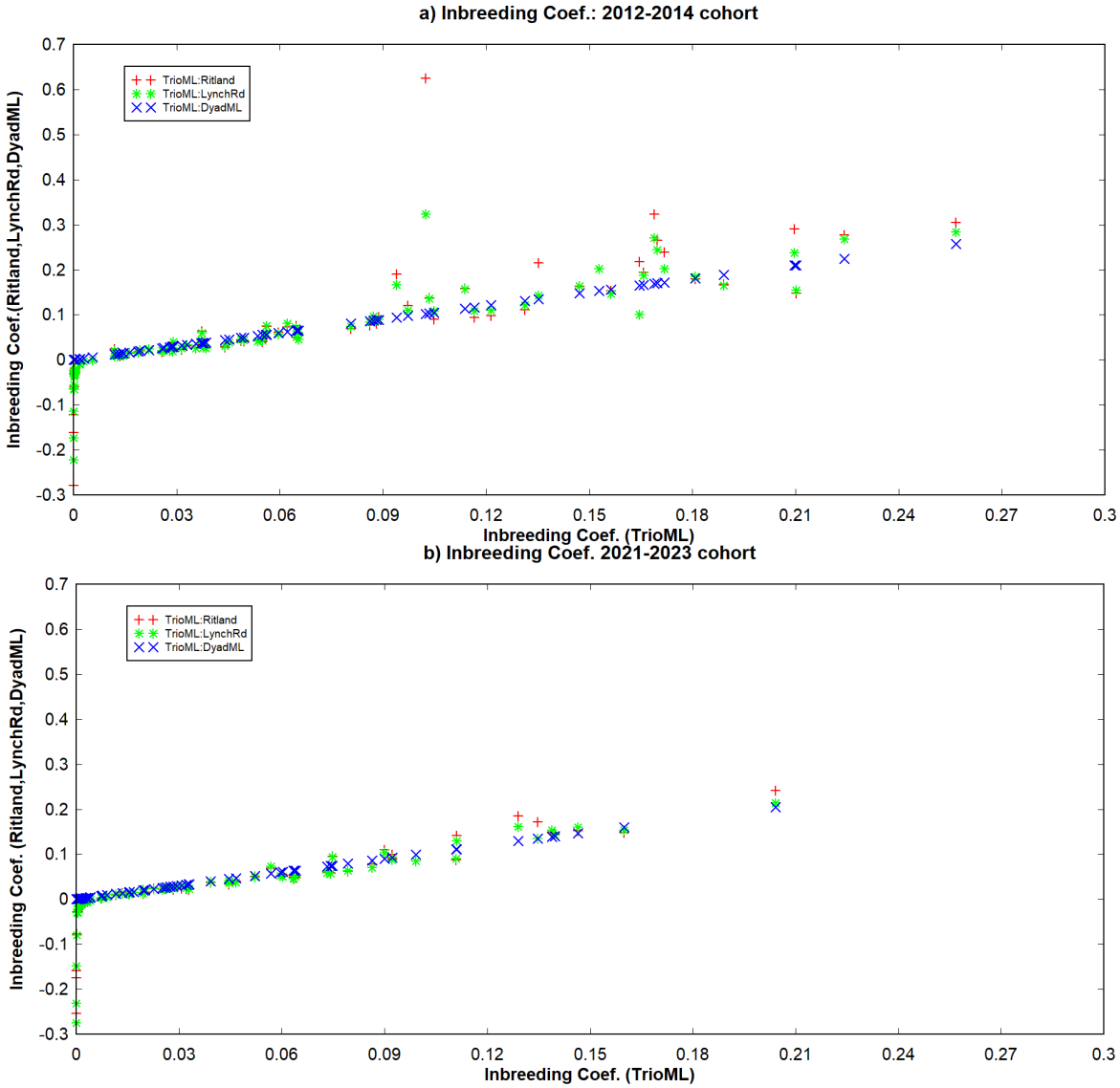

Figure 5-19 Individual inbreeding coefficient for 162 Maugean skates representing a) 2012-2014 (n = 90) and b) 2021 to 2023 cohort (n = 72). The coefficients were analysed from the filtered DArT SNPs using four inbreeding estimators implemented in COANCESTRY, and the coefficients of any two estimators were scatter plotted for comparison.

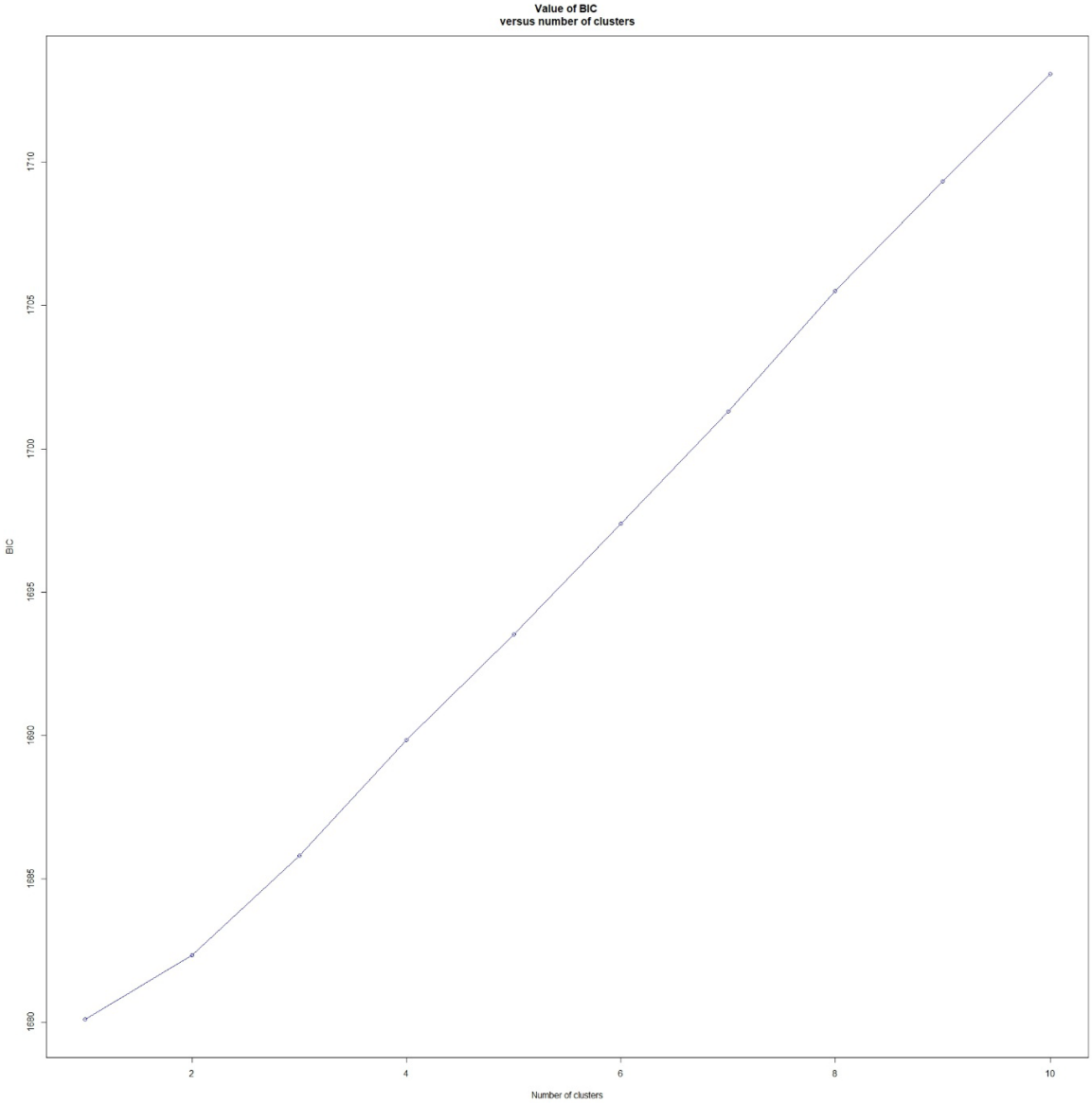

Figure 5-20 Discriminant Analysis of Principal Components (DAPC) showing no genetic clustering among wild Maugean skate individuals (n = 162).

Table 5-2 Relatedness metrics for the 2012-2014 cohort

n=2556	TrioML	Wang	LynchLi	LynchRd	Ritland	QuellerGt	DyadML
Mean	0.00736	-0.02217	-0.02991	-0.01421	-0.01457	-0.01503	0.00750
Variance	0.00022	0.00422	0.00473	0.00057	0.00060	0.00125	0.00022
Correlation C...	TrioML	Wang	LynchLi	LynchRd	Ritland	QuellerGt	DyadML
TrioML	1.00000						
Wang	0.36466	1.00000					
LynchLi	0.35332	0.99768	1.00000				
LynchRd	0.78136	0.43840	0.42048	1.00000			
Ritland	0.76805	0.46606	0.44720	0.99507	1.00000		
QuellerGt	0.53982	0.21176	0.17021	0.72987	0.72853	1.00000	
DyadML	0.99922	0.36330	0.35194	0.78432	0.77071	0.54044	1.00000

Table 5-3 Relatedness metrics for the cohort 2021-2023

n=4005	TrioML	Wang	LynchLi	LynchRd	Ritland	QuellerGt	DyadML
Mean	0.00858	-0.04201	-0.05065	-0.01138	-0.01209	-0.01180	0.00875
Variance	0.00045	0.00485	0.00532	0.00070	0.00079	0.00140	0.00045
Correlation C...	TrioML	Wang	LynchLi	LynchRd	Ritland	QuellerGt	DyadML
TrioML	1.00000						
Wang	0.41538	1.00000					
LynchLi	0.40308	0.99817	1.00000				
LynchRd	0.84638	0.49150	0.47699	1.00000			
Ritland	0.85401	0.53131	0.51604	0.98933	1.00000		
QuellerGt	0.69123	0.38298	0.35450	0.80183	0.80782	1.00000	
DyadML	0.99937	0.41491	0.40260	0.84833	0.85545	0.69086	1.00000

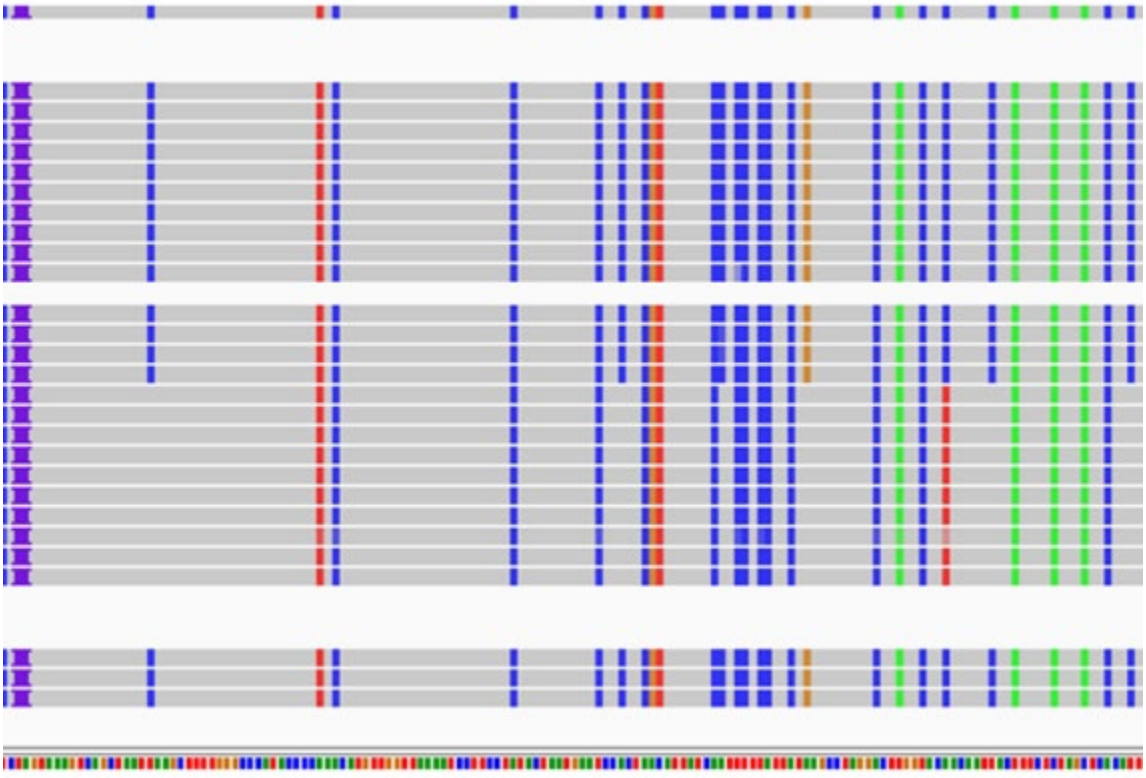

Figure 5-21 Example of single nucleotide polymorphisms (SNPs) detected in mito-genome of a female Maugean skate captured in Macquarie Harbour (individual DSM19).

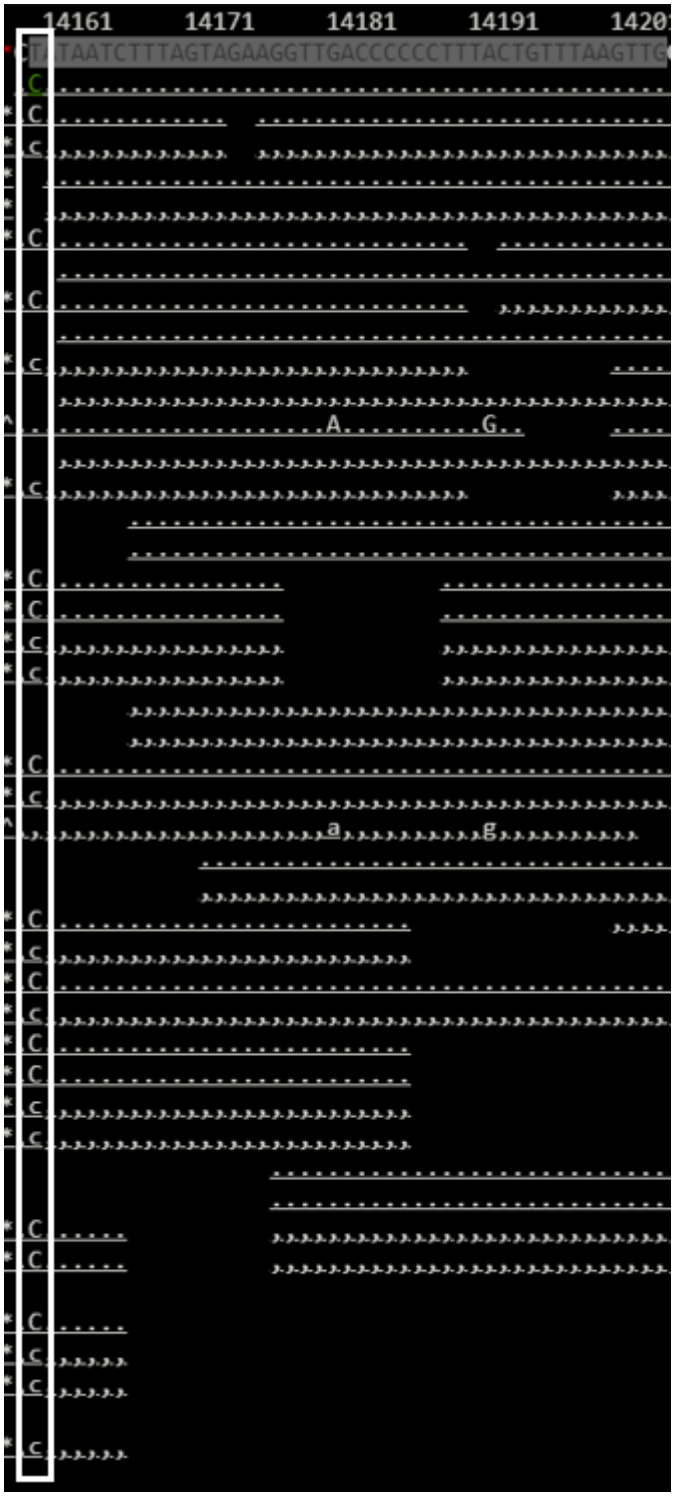

Figure 5-22 Example of a variant sequence detected from an alignment of Bathurst Harbour Maugean skate short reads against reference mito-genome of Macquarie Harbour skate. This is a region of sequence coding of NADH-ubiquinone oxidoreductase chain 1 (ND1) protein.

CONTACT

Name David Moreno or Jayson Semmens

Email: david.moreno@utas.edu.au; jayson.semmens@utas.edu.au

This project is supported with funding
from the Australian Government under the
National Environmental Science Program.